Birendra Kumar Shrestha

Regulation of autophagy during *Mycobacterium avium* infection in primary human macrophages

Master's thesis

Trondheim, June 2013

Norwegian University of Science and Technology

Faculty of Medicine

Centre of Molecular Inflammation Research and

Department of Cancer Research and Molecular Medicine

NTNU – Trondheim
Norwegian University of
Science and Technology

Acknowledgement

I would like to express the deepest appreciation to my supervisor, Dr. Trude Helen Flo, for her valuable comments, remarks, and motivation through the learning phase of my master thesis. Without her guidance and persistent help this project would not have been possible.

Furthermore, I would like to thank Dr. Jane Awtesoh Awuh for providing continuous theoretical and practical insight about the project. I like to thank Anne Marstad for her contribution during the entire project work. A special thanks to Dr. Øyvind Halaas for introducing me to the world of confocal microscopy and Dr. Markus Haug for helping me out during flow cytometry experiment.

I am highly indebted to all the members of Department of Cancer Research and Molecular Medicine, Faculty of Medicine, NTNU and like to extend my sincere thanks to all of them.

Finally, I would like to express my love and gratitude towards my family for their understanding and endless love throughout my study.

Birendra Kumar Shrestha

Trondheim, June 2013

Abstract

The main aim of this project was to study the induction and regulation of autophagy during *Mycobacterium avium* infection in primary human macrophages. Specifically, we wanted to elucidate the role of Toll-like receptors (TLRs) 2, TLR9 and Stimulator of interferon gene (STING) in induction of autophagy during *M. avium* infection, and to define if oxidative stress sensor, Kelch-like ECH-associated protein 1 (KEAP1) plays a role in regulation of autophagy.

We first established an immunofluorescence autophagy assay for quantifying endogenous LC3 II punctate in primary human macrophages using confocal microscopy and an alternative human embryonic kidney cells 293 (HEK293) reporter cells assay for monitoring autophagy flux by measuring the rate of degradation of green fluorescence protein (GFP) p62.

M. avium infection induced autophagy in human macrophages as early as four hours post infection. In contrast, *M. avium* infection failed to induce autophagy in HEK293 cell lines even after the introduction of functional TLR2 and TLR9. Stimulation of primary human macrophages with mycobacterial lipomannan (TLR2 ligand) or cyclic diguanylate monophosphate, cyclic-di-GMP (STING ligand) induced autophagy whereas deoxycytidine-deoxyguanosine oligodinucleotide, CpG ODN (TLR9 ligand) did not. Neutralization of TLR2 with TLR2 antibodies resulted in reduction of autophagy induced by either TLR2 ligand or *M. avium* infection. In addition, the level of autophagy was also reduced in TLR2 knockdown macrophages during *M. avium* infection, but no reduction was observed with TLR9 and STING knockdown. Thus, the results suggest that TLR2, but not TLR9 or STING, is involved in *M. avium* induced autophagy in primary human macrophages.

Unpublished results from our lab suggest a role for Keap1 in regulation of inflammation during *M. avium* infection in primary human macrophages. Keap1 has many interaction partners, including the autophagy receptor p62. In the present study, we found that Keap1 knockdown in macrophages resulted in increased levels of autophagy and decreased survival of the mycobacteria. These results suggest a role of Keap1 in the regulation of autophagy in *M. avium* infected primary human macrophages.

Abbreviations

- PRR: Pattern recognition receptor
- MyD88: Myeloid differentiation primary response protein
- TRAF6: Tissue necrosis factor (TNF) receptor-associated factor 6
- TLR: Toll like receptor
- DC-SIGN: Dendritic cell-specific intercellular adhesion molecule (ICAM)-3-grabbing non-integrin
- IL: Interleukin
- TRIF: Toll/IL-1 R (TIR) domain containing adapter-inducing interferon (IFN)-β
- LAM: Lipoarabinomannan
- LM: Lipomannan
- PIM: Phosphatidylinositol mannoside
- CpG ODN: Deoxycytidine-deoxyguanosine oligodinucleotide
- IFN-β: Interferon-β
- IP-10: IFN-inducible protein 10
- RANTES: Regulated on activation, normal T cell expressed and secreted
- MCP-1: Monocyte chemotactic protein-1
- ESAT6: Early secreted antigenic target protein 6
- STING. Stimulator of IFN genes
- TBK-1: TRAF family member-associated NF-kappa-B activator (TANK) binding kinase-1
- IRF3: Interferon regulatory factor 3
- ManLAM: Mannose-capped liparbinomannan
- ROS: Reactive oxygen species
- TNF α: Tissue necrosis factor α

- NLRs: Nucleotide binding oligomerization (NOD)-like receptors
- PAMP: Pathogen associated molecular pattern
- CARD: Caspase activation and recruitment domain
- BIR: Baculovirus inhibitors of apoptosis repeat domain
- ATG: Autophagy related genes
- LC3: Microtubule-associated protein 1A/1B-light chain 3
- ER: Endoplasmic reticulum
- mTOR: Mammalian target of rapamycin
- PI(3)K: Phosphatidylinositol-3-OH kinase
- ULK1: Unc-51-like kinase 1
- VPS34: Vascular protein sorting 34
- DFCP1: Double FYVE-containing protein 1
- WIPI: WD-repeat domain phospophoinositide-interacting family proteins
- PE: Phosphatidylethanolamine
- GABARAP: Gammaaminobutyrate receptor-associated protein
- GβL: G protein β-subunit like protein
- PRAS40: Proline rich Akt substrate of 40kDa
- SIN1: Stress activated map kinase (SAPK) interacting protein 1
- PROTOR: Protein observed with rictor
- PIP3: Phosphatidylinositol-3,4,5-trisphosphate
- PIP2: Phosphatidylinositol-4,5-bisphosphate
- TSC: Tuberous sclerosis complex
- DAG: Diacyl-glycerol
- PLC: Phospholipase C
- IP3: Inositol 1,4,5-triphosphate
- IPPase: inositol polyphosphate 1-phosphatase

- IMPase: Inositol monophosphatase
- 3MA: 3-Methyladenine
- LAP: LC3-associated phagocytosis
- NDP52: Nuclear dot protein 52
- UBA: Ubiquitin associated domain
- LIR: LC3 interacting region
- KIR: Keap 1 interacting region
- TBD: TRAF 6-binding domain
- KEAP1: Kelch-like ECH-associated protein 1
- Cyp27b1: 25-hydroxy cholecalciferol-1α-hydroxylase
- TetO2: Tetracycline operator sequence
- TetR: Tetracycline repressor protein
- PBMC: Peripheral blood mononuclear cells
- HEK293: Human embryonic kidney 293
- TE: Trypsin-Ethylenediaminetetraacetic acid
- FCS: Fetal calf serum
- DMEM: Dulbecco's modified eagle's medium
- PCR: Polymerase chain reaction
- β-ME: β-Mercarptoethanol
- MDM: Monocyte derived macrophage
- MOI: Multiplicity of infection
- PFA: Paraformaldehyde
- DMSO: Dimethyl sulfoxide
- ssRNA: Single stranded ribonucleic acid
- dsDNA: Double stranded deoxyribonucleic acid
- ELISA: Enzymes linked immunosorbent assay
- DAI: DNA-dependent activator of IFN-regulatory factors

- LMFIP1: Leucine-rich repeat (in Flightless I) interacting protein-1
- AIM2: Absent in melanoma 2
- IFI204: Interferon-inducible 204
- Cyclic-di-GMP: Cyclic diguanylate monophosphate
- DDX41: DEAD (Asp-Glu-Ala-Asp) box polypeptide 41
- MHC: Major histocompatibility complex
- FIP200: Focal adhesion kinase family interacting protein of 200 kD
- PKB: Protein kinase B
- PDK: Phosphoinositide-dependent kinase1
- AMPK: Adenosine monophosphate (AMP)-activated kinase
- Poly (I:C): Polyinosinic-polycytidylic acid
- Cyp27b1: 25-hydroxy cholecalciferol-1α-hydroxylase
- RISC: RNA inducing silencing complex

Contents

List of figure

List of table

1 Introduction

1.1 Mycobacteria

Mycobacterium tuberculosis are distinct rod-shaped bacteria; a causative agent of the communicable disease called tuberculosis. In the year 2011, WHO has estimated 8.7 million new cases (13% of which co infected with HIV), and 1.4 million death associated with this disease. (http://www.who.int/en/). There has been tremendous research in development of new anti-tuberculosis drugs and vaccines to minimize the number of cases of tuberculosis.

M. tuberculosis is transmitted by aerosol and primarily infects phagocytic cells of the lungs. An innate immune response against *M. tuberculosis* initiates with recruitment of neutrophils, macrophages, monocytes and dendritic cells to the site of infection. These immune cells are eventually infected by mycobacteria and leads to the formation of granuloma. This granuloma acts as cellular niche for bacterial replication[1].

The internalization of *M. tuberculosis* into the macrophage can occur via different types of receptors like mannose receptors, complement receptors, dendritic cell-specific intercellular adhesion molecule (ICAM)-3-grabbing non-integrin(DC-SIGN), and Fc receptors[2]. Once it is internalized, it resides within membrane bound vesicles called phagosomes, and prevents fusion of these phagosomes with lysosomes to form phagolysosomes. Inhibition of phagolysosomes formation avoids the antibacterial environment of the phagolysosomes. Such inhibition of phagolysosomes formation enhances the accessibility of host-derived nutrients, prevent antigen processing and presentation thereby inhibiting the activation of adaptive immunity[3].

The genus mycobacterium consists of both highly pathogenic species and non-pathogenic species. The medically significant species includes *M. tuberculosis, M. leprae, M. ulcerans and M. avium*. *M. avium* are usually isolated from the environment so large part of the population is bound to be in contact with the organism. It is a human pathogen that can cause infection in both immune-competent and immune-compromised individuals. Infection can be acquired both by respiratory and gastrointestinal routes. *M. avium* 104 strains have been extensively used for studying host immune response to mycobacteria because it is pathogenic to human, availability of genomic sequence, genetic stability and readily transfectable[4]. Better understanding of host immune response against mycobacteria leads to development of effective vaccine and drugs.

1.2 Innate immunity and mycobacterium infection

The innate immune response is initiated by recognition of various mycobacterial components via germ line coded pattern recognition receptors (PRRs). The TLRs are the most extensively studied PRRs. The TLR family consists of 12 members in human. These receptors are mainly expressed on the surface of all cells and on endocytics vesicle in immune cells. The TLRs known to recognize mycobacterial components are TLR2 in association with TLR1/TLR6, TLR4, TLR8 and TLR9[5, 6, 7, 8, 9].

TLR2 recognizes a variety of mycobacterial cell wall antigens such as lipoarabinomannan (LAM), lipomannan (LM), phosphatidylinositol mannoside (PIM), triacylated lipoprotein (TLR2/TLR1) and diacylated lipoprotein (TLR2/TLR6)[10]. The interaction between the mycobacterial component and TLR2 leads to initiation of signaling pathways that trigger the recruitment of adaptor protein called myeloid differentiation primary

response proteins (MyD88). Recruitment of MyD88 initiate the recruitment of protein like tissue necrosis factor (TNF) receptor-associated factor (TRAF) 6, TGFß-activated protein kinase 1 (TAK1), and mitogen-activated protein (MAP) kinase in the signaling cascade which in turn activates and translocate nuclear transcription factor (NF-kß)[11]. This eventually leads to transcription of genes related to innate immunity such as production of pro-inflammatory cytokines like TNF, IL-1, IL-12 chemokine and nitric oxide[12] (figure 1.2.1). In vivo studies in mice deficient in TLR2 showed contradictory results in susceptibility towards *M. tuberculosis* infection[13, 14]. However, one of the study using TLR2 knockout mice showed increased susceptibility to *M. tuberculosis* infection with reduced bacterial clearance and production of pro-inflammatory cytokines and unable to form mycobactericidal granuloma[14].

TLR4 is activated by heat shock proteins that are secreted by mycobacterium species[6]. TLR4 is also activated by lipopolysaccharides (LPS), and TLR4 uses both MyD88 dependent and MyD88 independent pathway. The recognition of LPS via TLR4 leads to recruitment of additional adaptor molecules called Toll/IL-1 R (TIR) domain containing adapter-inducing interferon (IFN)-β (TRIF) which mediates MyD88 independent pathway[15, 16]. The TRIF dependent TLR4 signaling pathway mediates secretion of pro-inflammatory cytokines, IFN-β and regulation of IFN-dependent genes such as IFN-inducible protein 10 (IP-10), regulated on activation, normal T cell expressed and secreted (RANTES), monocyte chemotactic protein-1 (MCP-1)[17].

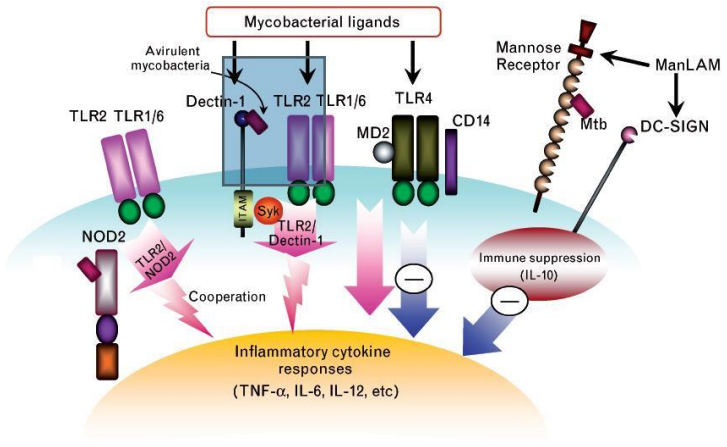

Figure 1.2.1. PRRs involved in mycobacterium infection

Recognition of mycobacterial ligands initiates the intracellular signaling leading to production of inflammatory cytokines as well as anti-inflammatory cytokines to prevent excessive inflammatory response. TLRs mainly initiate inflammatory response whereas non-TLR receptor like DC-SIGN induces anti-inflammatory response. Figure taken from[18]

TLR9 are activated by unmethylated CpG (deoxycytidine-deoxyguanosine) motifs present in bacterial DNA. In vivo study on mice suggests that TLR9 knockdown mice are more susceptible to *M. tuberculosis* infection as compared to wild one[7]. The role of TLR9 in innate immunity to mycobacterium infection was further supported by another study which showed that TLR9 deficient mice have higher bacterial burden than wild type mice indicating the role of TLR9 in controlling the mycobacterial infection[19].

The observation of immune stimulatory activity of microbial DNA in a cell lacking TLR9 lead to discovery of cytosolic DNA sensing pathway and its associated DNA recognition receptors[20]. There are at least six intracellular receptors that have been associated with DNA sensing pathway. These include DNA-dependent activator of interferon (IFN)-regulatory factors (DAI)[21], absent in melanoma 2 (AIM2)[22], leucine-rich repeat (in Flightless I) interacting protein-1 (Lmfip1)[23], RNA polymerase III (Pol III)[24],

aspartate-glutamate-any amino acid-aspartate/histidine (DExD/H)-box helicases (DHX9 and DHX36)[25] and IFN-inducible protein-16 (IFI16)[26].

The cytosolic DNA sensing pathways are activated when its receptors recognize DNA of *M. tuberculosis* and activation of such pathways initiate the production of type I interferon. The *M. tuberculosis* have a specialized secretion system called ESX-1 which produces virulent protein such as early secreted antigenic target protein 6 (ESAT-6) and this protein permeabilize phagosomes. The permeabilization of phagosomes leads to exposure of mycobacterium DNA to cytosol which are recognized by cytosolic DNA receptor such as DAI and IFI 16[21, 26]. Recognition of foreign DNA by cytosolic DNA receptors results in translocation of transmembrane protein STING from endoplasmic reticulum to Golgi apparatus[27]. STING further translocate from Golgi apparatus to cytoplasmic punctate structure where it co-localizes with TANK binding kinase-1 (TBK-1) and leads to TBK1 dependent phosphorylation of transcription factor IRF3 (interferon regulatory factor 3)[27]. The phosphorylation of such transcription factor results in production of type I IFN-β[27]. The STING, in addition to its role as an adaptor protein in cytosolic DNA sensor pathway, also has been reported as sensor of cyclic diguanylate monophosphate (cyclic-di-GMP) secreted by bacteria such as *Listeria monocytogenes*[28]. However, another study suggested that DDX41 (DEAD (Asp-Glu-Ala-Asp) box polypeptide 41) function as receptor for cyclic-di-GMP rather than STING and STING acts downstream of DDX41 receptor[29]. The production of type I IFN by STING-TBK1-IRF3 axis is co-related as a strategy adopted by *M. tuberculosis*[30] and *Listeria monocytogenes*[31] to promote infection.

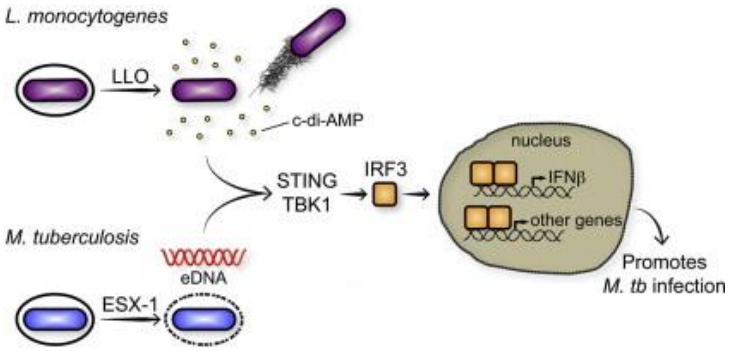

Figure 1.2.2. Activation of cytosolic DNA sensing pathway

M. tuberculosis and *Listeria monocytogenes* produce an ESAT-1 or listeriolysin O (LLO) protein respectively which permeabilize phagosomes. The permeabilization exposes extracellular DNA or cyclic-di-AMP on to the cytosol and is recognized by components of cytosolic DNA sensing pathway. The activation of such pathway results in production of type I interferons which are known to promote microbial infection. Figure taken from[30]

There are non-TLRs that are known to recognize mycobacterial ligands such as C-type lectin[32] and nucleotide oligomerization domain (NOD) like receptor[33].

C-type lectin, such as mannose receptors recognize mannose-capped liparbinomannan (ManLAM) and leads to production of anti-inflammatory cytokines IL-4 and IL-13 and inhibits the production of IL-12[32]. DC-SIGN, another C-type lectin receptor, is also involved in recognition of ManLAM, lipomannan and other ligands present in mycobacterium species. This receptor also plays a role in dendritic cell (DC) migration and DC-T-cell interaction[34]. A cohort study revealed that polymorphisms of *CD209*, a gene encoding DC-SIGN increases susceptible to mycobacterium infection[35]. Dectin-1, another C-type lectin receptor, is mainly expressed on macrophages, DCs, neutrophils and subset of T-cells. This receptor recognizes β-glucan found in fungal cell wall and on recognition of such ligand by these receptors trigger phagocytosis and subsequent production

of inflammatory cytokines and antimicrobial molecules such as reactive oxygen species (ROS) [36,37]. In addition to the role of production of inflammatory cytokines during fungal infection, dectin-1 also participates in autophagy pathway. The stimulation of macrophages with β-glucan results in recruitment of Microtubule-associated protein 1A/1B-light chain 3 II (LC3 II) to phagosomes suggesting direct involvement of dectin-1. The recruitment of LC3 II to phagosomes enhanced major histocompatibility complex (MHC) class II antigen presentation by recruiting MHC class II molecules to dectin-1 containing phagosomes[38]. The study of the role of dectin-1 during mycobacterial infection is extremely limited. Recently, a study showed that dectin-1 result in production of pro-inflammatory cytokines TNF when the macrophage are infected with a virulent strain of *M. avium* 724 but not with a virulent strains of *M. tuberculosis* H37Rv[39].

The NOD like receptor (NLR), a non-TLR cytoplasmic receptor recognizes various microbial products. NLR receptor consists of core domain called NOD domain. The C-terminal consists of leucine-rich repeats which are responsible for recognition of microbial components. The N-terminal consists of effector domain called CARD (caspase activation and recruitment domain), PYRIN or BIR (baculovirus inhibitors of apoptosis repeat domain)[40]. The CARD containing NLR such as NOD1 and NOD2 senses cytoplasmic presence of dipeptide γ-D-glutamyl-meso-diaminopimelic acid and muramyl dipeptide respectively[33]. The activation of NLR leads into two signaling pathways i.e. NF-kB pathway and inflammasome pathway. The functions of NOD2 during mycobacterial infection have been studied with NOD2 deficient mice and studies have demonstrated reduced production of pro-inflammatory cytokines and nitric oxide when infected with the virulent strain of *M. tuberculosis*[41].

1.3 Mechanism of autophagy

Autophagy is a general term for the degradation of cytoplasmic material, including soluble macromolecules and organelles within lysosomes[42]. It plays an essential role in various physiological and pathophysiological conditions such as starvation, clearance of intracellular proteins and organelles, development, anti-ageing, elimination of harmful microbes, cell death and tumor suppression[43].

There are at least three types of autophagy- macro-autophagy, micro-autophagy and chaperone-mediated autophagy. During autophagy, a portion of the cytoplasm is engulfed by an isolation membrane called phagophore which complete ligation results in the formation of double membrane structure known as autophagosome. These autophagosomes undergoes fusion with the lysosome and content of autophagosomes are degraded by lysosomal enzymes[43]. There are two major regulating pathway i.e. mTOR dependent and mTOR independent that control autophagy.

The mTOR is the mammalian orthologs of yeast protein kinase, target of rapamycin (TOR) which negatively regulates autophagy. Under nutrient condition, mTOR signaling pathway receive the signal from insulin or growth factor via Class I phosphatidylinositol-3-OH kinase (PI (3) K), which produce phosphatidylinositol-3,4,5-trisphosphate(PIP3) from the plasma membrane lipid phosphatidylinositol-4,5-bisphosphate(PIP2). The PIP3 recruits phosphoinositide-dependent kinase1 (PDK1) and Akt/PKB (Protein kinase B) to plasma membrane[44]. The Akt is activated via phosphorylation on two different sites. Upon activation of Akt, it in turn phosphorylates and inactivate tuberous sclerosis complex (TSC) 1/2. The inactivation of TSC 1/2 leads to activation of Rheb protein which subsequently activates mTORC1. The activation of mTORC1 leads to inhibition of autophagy[44].

Amino acid starvation or presence of rapamycin, results in inactivation of mTORC1[45, 46]. The inhibition of mTOR results in the translocation of mTOR substrate complex comprising ULK1/2 (Unc-51-like kinase 1/2), ATG13, focal adhesion kinase family interacting protein of 200 kD (FIP200) and ATG101 from the cytosol to ER[47]. This finally leads to recruitment of class III phosphatidylinositol-3-OH kinase (PI (3) K) complex consisting of VPS34 (Vascular protein sorting 34), VPS15, beclin 1 and ATG14 to the ER site[48]. The presence of 3-Methyl adenine (3MA) or wortmannin results in activation of mTOR dependent pathway via inhibition of this class III PI3K[49, 50]. The recruitment of this kinase complex results in the production of phosphatidylinositol-3-phosphate (PtdIns (3) P) which further recruits other Atg proteins such as double FYVE-containing protein 1 (DFCP1) and WD-repeat domain phosphoinositide-interacting (WIPI) family proteins[51]. The DFCP1 are mainly present in ER or Golgi bodies which translocate to autophagosomes formation site on PtdIns (3)P- dependent manner resulting in the formation of omega like structure called omegasome (figure 1.3.1)[52].

The next steps in formation of autophagosomes involve elongation of isolation membrane and completion of enclosure. Such process requires two ubiquitin like conjugates. The first one is Atg12-Atg5 conjugates which are produced by Atg7 and Atg10 enzymes. The Atg12-Atg5 conjugates oligomerize with Atg16 to form large multimeric complex[52]. The second is phosphatidylethanolamine (PE) conjugated Atg8 homologs-LC3. The C-terminal of Atg8/LC3 is cleaved by Atg4 protease to produce LC3 I with a C-terminal glycine residue. The cleaved LC3 I are conjugated to phosphatidylethanolamine (PE) by Atg7 and Atg3 enzymes. This lipidated form of LC3 II is attached to both outer and inner faces of

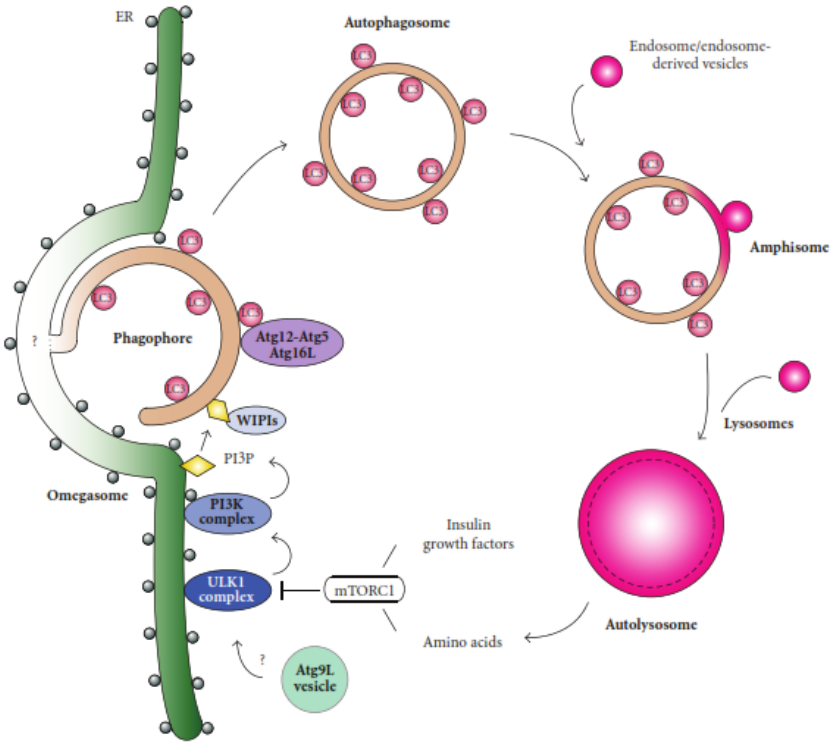

Figure 1.3.1. Role of Atg proteins in autophagosomes formation

The inhibition of mTOR results in activation and translocation of ULK1 complex to ER. The activation of ULK1 complex recruits PI3K complex. The activated PI3K complex results in production of PI3P and recruits Atg proteins such as WIPI and DFCP1. The WIPI proteins, ATG12-Atg5-Atg16L1 complex and LC3-phosphatidylethanolamine (PE) conjugate are essential in the elongation and closure of the isolation membrane. The complete closure of isolation membrane results in formation of autophagosomes and it later on fuses with lysosomes to form autophagolysosomes. Figure taken from[52]

phagophore. After completion of autophagosomes, Atg4 cleaves LC3 II from the outer surface of autophagosomes[52].

The LC3 proteins are grouped into three subfamilies. The first LC3 subfamily contains LC3A, LC3B, LC3B2 and LC3C. The second one is gammaaminobutyrate receptor-associated protein (GABARAP) subfamily

consisting GABARAP and GABARAP1. The third one is Golgi associated ATPase enhancer of 16kDa (GATE-16) protein[52].

The phosphoinositol signaling pathway is the major mTOR independent pathway that regulates autophagy in mammalian cells. The autophagy is negatively regulated by intracellular level of free inositol and inositol 1,4,5-triphosphate(IP_3)[53]. The phosphoinositol pathway is activated by G-protein coupled receptor mediated activation of phospholipase C (PLC). The enzymes phospholipase C hydrolyzes PIP_2 to form IP_3 and diacyl-glycerol (DAG). These IP_3 are degraded by two enzymes 5'-phosphatase and inositol polyphosphate 1-phosphatase (IPPase) to form inositol monophosphate (IP_1)[53].These IP_1 are further hydrolyzed by inositol monophosphatase (IMPase) into free inositol. The compound that reduces the level of intracellular inositol level induces autophagy[53].

1.4 Crosstalk between autophagy and innate immunity to defend against mycobacteria infection

Initially, autophagy was considered a non-selective bulk degradation process, but with increasing evidence defined autophagy as a highly selective process. The damaged organelles are selectively degraded by autophagy and cargo specific name have been given to such type of selective autophagy. For example, selective autophagy for ER are called reticulophagy or ERphagy, peroxisomes are called pexophagy, mitochondria are called mitophagy, pathogen are called xenophagy[54].

Autophagic recognition of intracellular microbes is mediated by autophagic adaptors, called sequestosome I/p62-like receptors (SLRs). The best studied autophagy adaptors are p62, NBR1 and nuclear dot protein 52 (NDP52). These autophagic adaptors bind ubiquitinated microbes through their ubiquitin associated (UBA) domain and to LC3 via their LC3 interacting region (LIR) motif and leads to autophagic degradation of ubiquitinated intracellular microbes (figure 1.5.3)[55].

The studies have shown a crosstalk between the receptors of innate immune system and autophagy. The mechanism behind such crosstalk have been proposed by some studies where stimulation of TLR4 with its ligands was found to regulate autophagy via TRAF6 mediated ubiquitination of beclin 1[56]. The ubiquitination of beclin 1 reduces its binding with Bcl-2 and thereby induces autophagy. Besides, TLRs, other PRRs and its associated ligands were further studied in relation to autophagy.

The series of studies of TLRs and its ligand showed variation in induction of autophagy. The TLRs ligands for TLR2, TLR3, TLR4 and TLR7 have been found to induce autophagy[57, 58, 59]. The induction of autophagy with TLR7 ligands such as imiquimod or single stranded RNA in RAW 264.7 macrophages were found to enhance the elimination of *M. tuberculosis var. bovis* Bacilli Calmette-Guerin (BCG)[59]. In the same study, stimulation of TLR3 with its ligand, double stranded RNA or poly (I:C) (polyinosinic-polycytidylic acid) also resulted increase level of autophagy[59]. A study with LPS, a TLR4 ligand induced autophagy found to enhance mycobacterial co-localization with autophagosomes[58].

Recently, a study showed that mycobacterial lipoprotein LpqH, a TLR2 ligand, induces autophagy in human macrophages. The activation of TLR2

by lipoprotein tends to up regulate the expression of 25-hydroxy cholecalciferol-1α-hydroxylase (Cyp27b1), an enzyme which converts inactive provitamin D3 hormone into the active form. Such increased expression of Cyp27b1 was found to be essential for LpqH induced cathelicidin expression and autophagy (figure 1.4.1)[57].

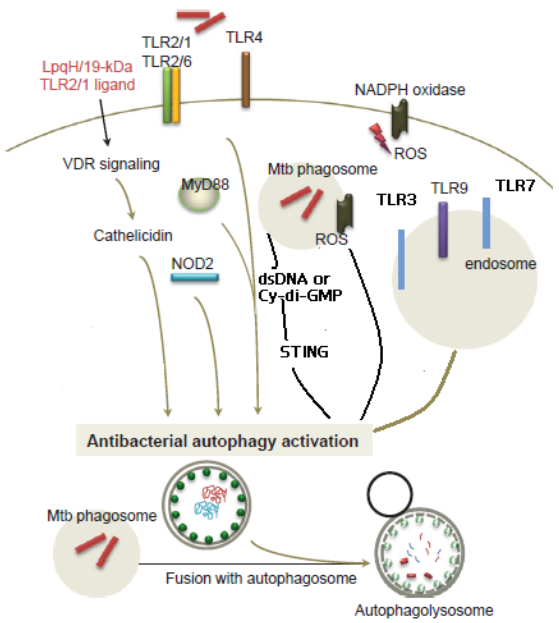

Figure 1.4.1. Crosslink between autophagy and innate immunity during mycobacterial infection

The TLR and non-TLR receptors are shown to induce autophagy after recognition of its specific ligands. Figure modified from[18]

Besides the activation of autophagy via TLRs signaling, TLRs also links autophagy pathway to phagocytosis. The latex beads in association with TLR ligands induce rapid recruitment of LC3 II to phagosomes[60]. For the recruitment of LC3 II to phagosomes, additional autophagy protein such as Atg5 and Atg7 were found to be essential. Similar to the process of autophagy, recruitment of LC3 II to phagosomes were preceded by

recruitment of beclin-1 and phosphoinositide 3-kinase activity[60]. The only difference between conventional autophagosomes and TLR induced LC3 II and autophagy protein recruitment was the absence of double membrane structure. The significance of such recruitment of LC3 IIto phagosomes was associated with enhanced phagosomes-lysosomes fusion[60]. This LC3 mediated enhanced phagocytosis is referred as LC3 associated phagocytosis (LAP). The LC3 associated phagocytosis was also demonstrated by a research group that investigated infection of RAW 264.7 macrophages with *M. marinum* containing functional ESX-1 secretion system[61].

Recent development revealed that STING, a transmembrane protein participate in autophagy. The induction of autophagy by intracellular bacteria depends upon cytosolic entry of their DNA and host STING adaptor protein[62]. The transfection of various double stranded DNA species, such as poly (dA:dT), poly (dT:dC) or plasmid DNA, and cyclic-di-GMP but no single stranded DNA, dsRNA or single stranded RNA was found to induce autophagy[62]. Such pathway was found to be involved in recognition of DNA of *M. tuberculosis*. The cytosolic entry of DNA depends upon the *M. tuberculosis* ESX-1 secretion systems which permeabilize phagosomal membrane. The permeabilization of phagosomal membrane exposes DNA on bacterial surface which are recognized by the component of cytosolic DNA sensing pathway and results in ubiquitination of *M. tuberculosis* via STING dependent manner[62]. The ubiquitinated *M. tuberculosis* is recognized by ubiquitin-LC3 binding autophagic receptors p62 and NDP52 and initiates autophagy by recruiting autophagic components by creating a phagophore around the bacterial. The activities of autophagic receptor p62 are dependent on protein kinase TBK1 which phosphorylate key serine residue present within UBA domain of p62[62].

In addition to TLRs, non-TLR such as NOD1 and NOD2 are found to be associated with induction of autophagy when such receptors are activated by mycobacterial muramyl dipeptide[63]. Recently, induction of autophagy via NOX2 NADPH-oxidase generated ROS resulted in enhanced elimination of *M. tuberculosis* which presents autophagy as strong therapeutic potential[64]. The current therapeutic drugs used for tuberculosis treatment are isoniazid or pyrazinamide which bactericidal activity is mediated via induction of autophagy through the production of reactive oxygen species[65]. Autophagy plays an essential role in elimination of mycobacterium and ability of *M. tuberculosis* survival in host may depend on alteration of autophagy. In addition to this, autophagy has been shown to enhance antigen presentation and thereby enhance efficacy of vaccines[66]. So, autophagy based tuberculosis therapy might be alternative strategy for tuberculosis treatment. There has been limited study about the role of autophagy during *M. avium* infection of primary human macrophages[67, 68]. Therefore, extensive studies to elucidate role of different autophagy associated receptors are essential for better understanding of role of autophagy during *M. avium* infection.

1.5 Kelch-like ECH-associated protein 1 (Keap1) and its association with autophagy

Structural analysis showed that Keap1 protein consists of four domains; N-terminal regions, BTB domain, intervening region and DC domain (figure 1.5.1). The DC domain contains six Kelch-repeat domain and C-terminal region. BTB domain and N-terminal region of intervening region (IVR) interact with Cul3 protein whereas DC domain interacts with Neh2 domain

of Nrf2[69]. The Keap1 plays an essential role in oxidative and electrophilic stress, inflammation, cancer and autophagy[70, 71, 72].

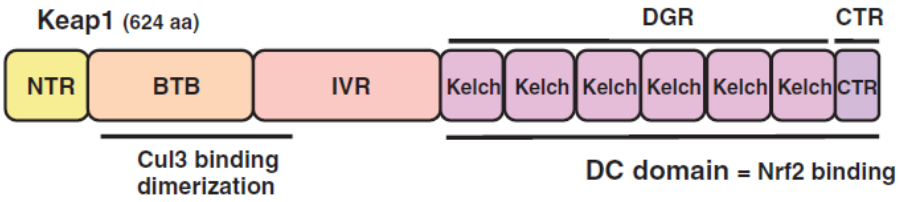

Figure 1.5.1. Structural and functional domain of Keap1

Keap1 consists of N-terminal region, BTB domain, Intervening region (IVR) and DC domain. DC domain interacts with Neh2 domain of Nrf2 whereas BTB domain and N-terminal region of IVR interact with Cul3-E3 ligase. Figure taken from[69]

Under electrophilic and oxidative stress, Keap1-Nrf2 (Nuclear like factor 2) system regulates the expression of cytoprotective genes. Keap1 acts as a stress sensor as well as an adaptor protein for Cullin 3 (Cul3)-based ubiquitin E3 ligase[73]. Under the normal unstressed condition, Keap1 binds to Nrf2 in the cytoplasm and promotes constitutive ubiquitination of Nrf2 via Cul3 ligase. The ubiquitinated Nrf2 are degraded by proteasome[73]. When cells are exposed to electrophilic and oxidative stress, reactive cysteine residues in Keap1 are covalently modified which leads to impairment of structural integrity of Keap1-Cul3 E3 ligase complex thereby diminishing the ubiquitination activity[74]. The diminished ubiquitination activity facilitates the stabilization of Nrf2 and translocation to nucleus. Nrf2 heterodimerize with small Maf protein then binds anti-oxidant/electrophile response element (ARE/EpRE) for transcription of target gene for cytoprotection[75] (figure 1.5.2).

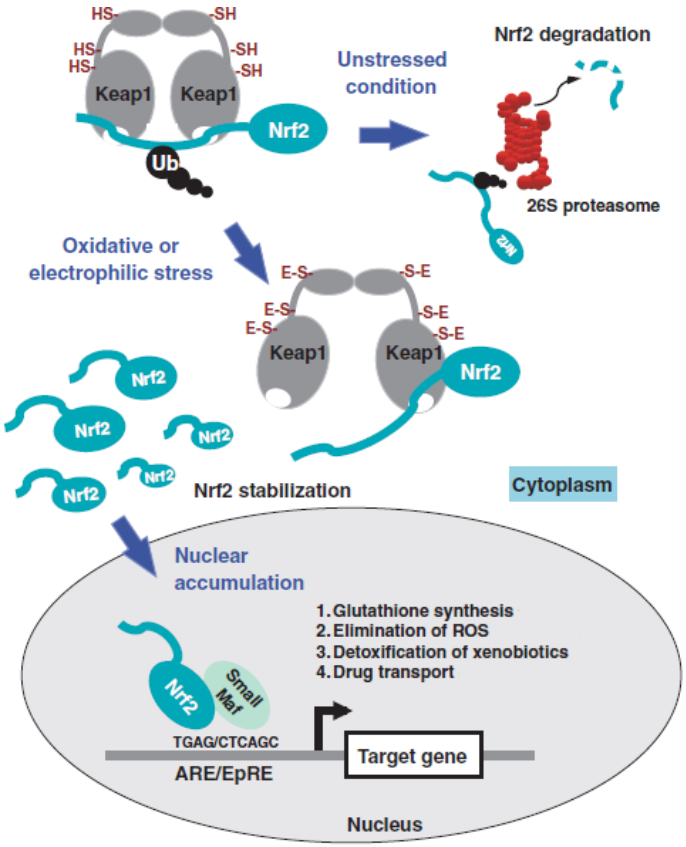

Figure 1.5.2. Keap1-Nrf2 pathway for sensing oxidative and electrophilic stress

In unstressed condition, Keap1 constitutively ubiquitinate Nrf2 via Cul3 ligase and ubiquitinated Nrf2 are degraded by proteasome[73]. Under oxidative and electrophilic stress, Keap1 are inactivated thereby stabilize Nrf2 and leads to accumulation and translocation of Nrf2 to nucleus[74]. In nucleus, Nrf2 undergoes heterodimerization with small Maf proteins and activates various cytoprotective genes by binding to ARE/EpRE[75]. Figure modified from[69]

The studies have shown that autophagic adaptor protein, p62 plays a role in oxidative and electrophilic stress by directly interacting with Keap1 (figure 1.5.3)[76]. The p62 share same Nrf2 binding site in Keap1 so p62 competes with Nrf2 for same binding site thereby disrupting the interaction between Keap1-Nrf2[76]. This disruption leads to abrogation of ability of Keap1 to facilitate ubiquitination and degradation of Nrf2 by Cullin3 ubiquitin ligase[76].

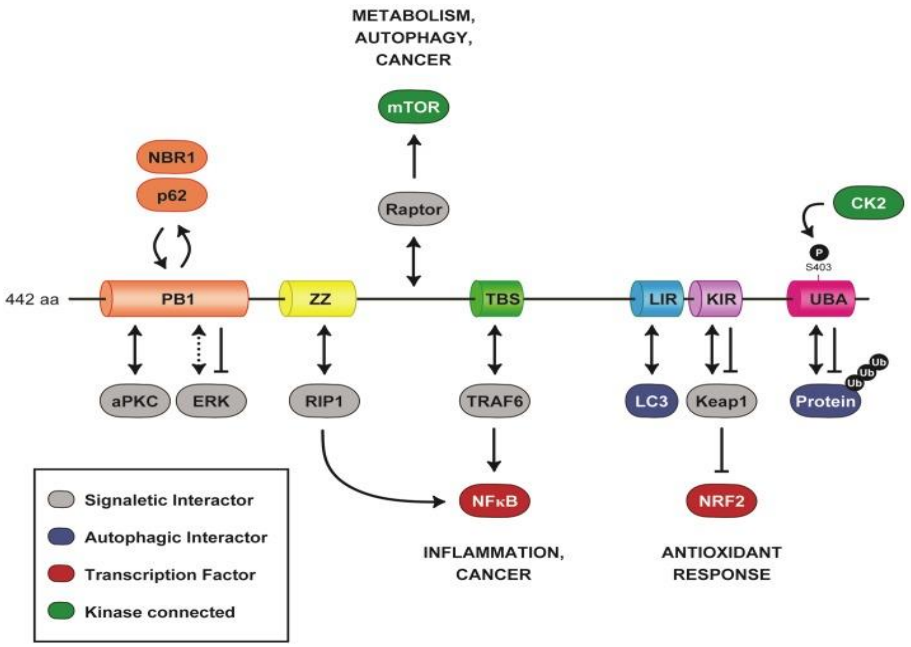

Figure 1.5.3. Structural and functional domains of p62

N-terminal Phox and Bpem1 (PB1) domain are responsible for self-oligomerization of p62 or hetero-dimerization with NBR1. The region between ZZ domain and TRAF6-binding domain (TBD) interacts with a protein called raptor which involved in activation of mTOR. The C-terminal consists of LIR and UBA which links p62 to autophagy**.** The domain in between LIR and UBA is Keap1-interaction region (KIR) which binds to Keap1 and stabilize NRF2 transcription factor thereby leading to expression of anti - oxidant protein. Figure taken from[77]

Recently, Keap1 was shown to have a role in selective autophagic pathway. Keap1 interacts indirectly with autophagic pathway via KIR region of p62. The interaction of Keap1 with p62 was found to be essential in removal of ubiquitin aggregates. The deletion of Keap1 resulted in accumulation of ubiquitin aggregates and defective activation of autophagy[71]. The perturbation of autophagy by knockdown of Atg7 gene in murine liver induced multiple tumors with inclusion bodies containing Keap1 and p62 indicating the role of Keap1 in tumorigenesis[72]. The studies of Keap1 are mainly focused on tumorigenesis but its role in relation to infection is yet to be defined.

2 Aim of the study

The main aim of this project was to established methods for quantification of autophagy in primary human macrophages and HEK293 cell lines and implementation of this method to elucidate the regulatory mechanism of autophagy during *M. avium* infection. To be specific, it includes:

1. Establishment of methods to quantify autophagy in primary human macrophages and HEK293 cell lines.
2. Examine if *M. avium* induces autophagy in primary human macrophages and HEK293 cell lines.
3. To study the role of TLR2, TLR9 and STING in induction of autophagy during *M. avium* infection.
4. Establish if Keap1 is involved in the regulation of autophagy during *M. avium* infection.

3 Material and Methods

3.1 Cells

3.1.1 Human primary macrophages

The human peripheral blood mononuclear cells (PBMCs) were isolated from buffy coat obtained from St. Olav hospital, blood bank department. The use of PBMC from healthy blood donor has been approved by the Regional committee from Medical and Health Research Ethics at NTNU.

The density gradient solution lymphoprep ™ (Axis shield PoC AS, Oslo, Norway) was used for the isolation of PBMCs from buffy coat. The 30 ml of buffy coat was diluted with 100ml of Dulbecco's phosphate buffer saline (DPBS, Sigma Aldrich, USA) then mixture was slowly deposited on 15 ml of density gradient solution present in 50ml falcon tubes.

The density gradient solution with buffy coat was centrifuged without brakes at 1800 rpm for 20 minutes at room temperature. After the centrifugation, PBMCs present at the interface between plasma-PBS and density gradient solution was carefully transferred along with some serum into new 50 ml falcon tubes but without drawing any lymphoprep solution as it is toxic to cells. The transferred PBMCs with serum were further centrifuged at 2000 rpm for 10 minutes at room temperature. The supernatant was removed, and remaining cell pellet was washed thrice with Hanks balanced salt solution (Sigma Aldrich, USA) by centrifugation at 800 rpm for 8 minutes. The cell count was done with coulter counter (Beckman coulter Inc., USA) then cells were diluted to $5X10^6$/ml in Roswell Park Memorial Institute medium (RPMI 1640, Sigma Aldrich, USA) medium with 5% human serum A^+ (blood bank, St. Olav Hospital, Trondheim, Norway). The appropriate amount of cell suspension (150µl)

was seeded only on center well of confocal dishes (MatTek corporation, Ashland, MA 01721, USA) and allowed monocytes to adhere for 1 hour. After the adherence, 5% human serum RPMI was replaced with 30% human serum RPMI medium for the differentiation of monocytes into macrophages for 3-5 days. Macrophages were maintained in 10% human serum throughout the assay.

3.1.2 Human Embryonic Kidney 293 (HEK293) cells

Human embryonic kidney 293 cells were cultured in Dulbecco's Modified Eagle's Medium (DMEM, BioWhittaker, USA) supplemented with 10% fetal calf serum (FCS, Sigma Aldrich, USA), 10mM Hepes (Invitrogen, USA) and 2nM glutamine (Sigma Aldrich, USA) at 37°C in 8% CO_2.

3.1.3 Maintenance of HEK293 GFP-p62 cells

3.1.3.1 Cryopreservation of HEK293 cells

The HEK293 cell lines were stored in freeze medium containing DMEM with sterile filtered 30% FCS and 10% Dimethyl sulfoxide (DMSO). The HEK293 cells were washed with warm PBS followed by detachment with 2 ml of pre-warmed Trypsin-Ethylenediaminetetraacetic acid (TE). The TE was neutralized with 5 ml of DMEM medium with 10% FCS then cells were transferred to 15 ml falcon tube. The cells were centrifuged for 5 minutes at 1500rpm. After centrifugation, supernatant were removed, and cell pellets were loosened by flicking it gently and suspended in freeze medium. The aliquot of about 1ml was pipetted in 1ml cryotube. The cryotube placed in Styrofoam box and incubated at -80°C overnight. Then, cryotube was transferred in liquid nitrogen storage tank on the next day with proper labeling and entry in the logbook.

3.1.3.2 Thawing of HEK293 cells

Before thawing of cells, all medium and reagent were warmed. The cryotube with HEK293 cells were placed in a screw-lid container containing water and floating device. The lid of cryotube were vent by loosening it slightly but not opened as it contaminate the cells. The screw-lid container was kept on water bath for thawing the cells. Then thawed cells were transferred in the tubes containing 5ml of warm medium. The cells were then centrifuged at 1500 rpm for 5 minutes and supernatant were removed and resuspended in 5 ml of 10% FCS, DMEM medium. Gently, cell pellets were pipetted up and down to prevent the clumping of cells so those single layers of cells is formed in culture flask. The cells counting were done according to countess protocol (Invitrogen, USA). For these cell lines, 2 $X10^6$ cells were added to T_{75} culture flask (Corning Incorporated, USA) containing 12 ml of DMEM with 10% FCS.

3.2 Measurement of LC3 II punctate via confocal microscopy

The LC3 protein plays an important role in the formation of phagophore during autophagy pathway and is characterized as autophagosomes marker. Therefore, LC3 is the most widely used for monitoring autophagy process. These proteins are synthesized as unprocessed form called proLC3 which later on undergo proteolytic cleavage at C terminus to form LC3 I form. This LC3I protein conjugates with phosphatidylethanolamine (PE) to form LC3 II[78].

Autophagic flux can be measured by determining the LC3 II turnover in the presence and absence of lysosomal or vacuolar degradation. The difference in the amount of LC3 II in the presence and absence of inhibitors would determine the state of autophagic flux. In general, if any intervention or certain drugs treatment on a cell results in higher level of

LC3 II in the presence of inhibitors than in the absence of inhibitors then it indicates some autophagic flux. But if intervention on cells has no difference in the level of LC3 II in the presence of inhibitors as compared to the absence of inhibitors than it indicates some blockage in autophagy pathway. There are inhibitors such as bafilomycin A1 and chloroquine that can be used in the assay. Bafilomycin A1, inhibitor of vacuolar-type H (+)-ATPase (V-ATPase) and Chloroquine, a lysosomotropic agent prevents the maturation of autophagosomes via inhibiting the acidification of lysosomes thereby impairs fusion between autophagosomes and lysosome[79].

Use of confocal microscopy for monitoring autophagy via using LC3 II as autophagic marker is sensitive and reliable method. For such method, either anti-LC3 antibody to detect endogenous protein or transfection of fusion gene that express LC3 protein tagged with fluorescent protein such as GFP (GFP-LC3) can be used for the assay.

The accurate method of quantification of level of autophagy via confocal microscopy is to count the numbers of LC3 II punctate per cell rather than counting the number of cells displaying punctate. As even in nutrient rich condition, cells have basal autophagy, so cells display some punctate. There are different ways of counting LC3 II punctate such as manually or using counting software like Bitplane Imaris and ImageJ which have been reported more accurate and reliable[79].

3.2.1 Optimization of immunofluorescence assay for LC3 II staining

Previously within our research group, detection of LC3 II punctate with different antibody was done. In which antibody from cell signaling technology, CST (LC3B (D11) XP Rabbit monoclonal antibody, USA) showed good specificity and low background fluorescence. In this project, further optimization was carried out with anti-LC3 II antibody from CST.

For optimization, MDMs were amino acid starved in Hanks balanced salt solution in the presence of 100 nM bafilomycin A1 for 2 hours. Amino acid starvation was used a positive control for autophagy. The induction of autophagy was analyzed by immunofluorescence assay based on LC3 II punctate count.

Basically, there are two methods in immunofluorescence assay, i.e. direct and indirect immunoassay. So, we compared both methods for the quantification of LC3 II dots. In addition to that, we also tried different fixative: 4% paraformaldehyde and methanol or 100% methanol only, and different time period for incubation of primary antibody i.e. overnight and 1 hour incubation.

In one of the protocols, cells were fixed with 4% paraformaldehyde placed on ice for 10 minutes followed by cell permeabilization with ice cold methanol for 20 minutes at -20°C. In another protocol, cell fixation and permeabilization was done with 100% methanol for 20 minutes at -20°C.

After fixation and cell permeabilization, cells were incubated in blocking buffer for 30 minutes at room temperature. The blocking buffer contained 2.5% bovine serum albumin (BSA A9647, Sigma Aldrich) and 20% human serum in PBS. The blocking step was followed by staining steps.

In direct staining method, cells were incubated with 5 µg/ml of Alexa546 tagged anti-LC3 II antibody overnight or 1 hour. Incubation with primary antibody was followed by three times washing with PBS. After washing, PBS was added to confocal dish then nuclear stain DRAQ5 was added before confocal imaging.

In indirect staining method, cells were incubated either overnight or 1 hour with 1:200 diluted anti-LC3 II rabbit monoclonal antibody. The staining

procedure was followed by three times washing with PBS and then incubation for 30 minutes with 1:1000 diluted alexa546 tagged goat anti-rabbit secondary antibody (Invitrogen, USA). Finally, PBS was added to confocal dish then nuclear stain DRAQ5 was added before confocal imaging.

After the analysis of images from these different staining and fixation method, we found no difference between fixation methods, staining methods and time of incubation for primary antibody i.e. overnight or 1 hours incubation (images on the appendix III). Immunofluorescence protocol of fixation with 4% PFA with cold methanol followed by indirect staining method with overnight incubation was chosen for the rest of the immunofluorescence assay.

During the immunofluorescence assay via indirect staining for LC3 II, various controls were used. Amino acid starvation of human primary macrophages for 2 hours was used as a positive control cells for LC3 II staining. Rabbit monoclonal IgG isotype control (CST, USA) was used to determine the specificity of primary rabbit monoclonal anti-LC3 II antibody. Unspecific binding of goat anti-rabbit alexa546 secondary antibody were checked in the absence of primary antibody. As bafilomycin A1 was prepared in DMSO, so the effect of DMSO was also checked to eliminate any background effect of DMSO on autophagy (images on appendix IV).

3.3 HEK293 GFP-p62 reporter cell system

HEK293 GFP-p62 reporter cell system is based on induced expression of fusion protein GFP-p62 followed by measurement of rate of degradation of fusion protein after the removal of inducer element. The rate of degradation

can be determined by flow cytometry, imaging or western blot, but flow cytometry produce the best quantitative measurement of autophagic flux[80].

The autophagic receptor p62 and NBR1 link the autophagic cargo to LC3/Atg8 protein located on the membrane of autophagosomes. During the process of lysosomal degradation of LC3, its interacting partner p62 or NBR1 are also degraded. So, reporter cell system that incorporates an idea of generating fusion protein of LC3 or its interacting protein with different fluorescent protein and subsequent degradation of these fluorescence fusion protein via autophagy process can provide an ideal reporter cell system for monitoring autophagic flux[81, 82].

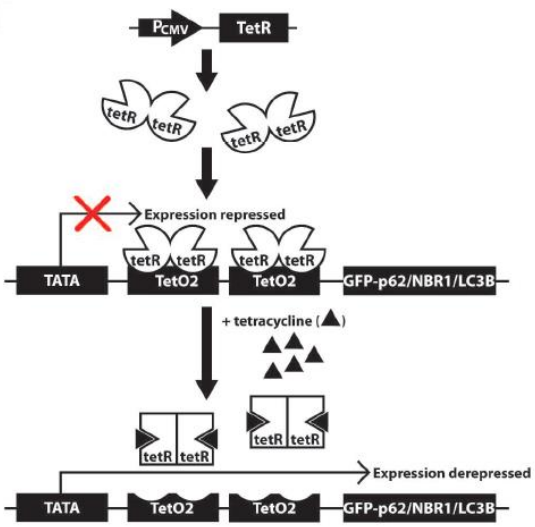

Figure 3.3.1: HEK293 Flp-ln TeREx expression system

TetR proteins are constitutively expressed, and it binds to tetracycline operator sequence TetO2 present upstream of GFP fusion reporter gene. Such binding inhibits the transcription of reporter gene, but the introduction of tetracycline in the cells system leads to binding of tetracycline to TetR protein thereby changing its structural confirmation and dissociating it from TetO2 sites. The dissociation of such repressor, leads to expression of reporter fusion protein. Figure taken from[80]

Implementing this principle, Flp-In T-Rex human embryonic kidney 293 cell lines have been generated with GFP-p62, GFP-NBR1 or GFP-LC3 II inserted into a single integrated FRT site in the genome (figure 3.3.1)[80]. These cell lines constitutively express tetracycline repressor protein (TetR) which binds to tetracycline operator sequences (TetO2) present on the upstream of GFP reporter fusion gene, and thereby inhibits the transcription of these fusion proteins. On the addition of tetracycline or its derivative drugs (doxycycline), it binds to the TetR protein and changes structural confirmation of this repressor protein. The change in confirmation leads to release of TetR repressor protein from TetO2 site thereby activating the expression of fusion protein gene. On this reporter cell system, GFP proteins were used as fusion partner for the convenient analysis with flow cytometry[80].

The autophagic flux are determined by inducing the expression of fusion protein of GFP-p62, GFP-NBR1 or GFP-LC3 II for 24 hours with inducer (doxycycline) followed by measurement of rate of degradation of these fusion proteins after the removal of inducer. For our study, HEK293 reporter cell system with GFP-p62 was used.

3.3.1 Optimization of HEK293 GFP-p62 reporter cell system

For the implementation of HEK293 GFP-p62 in our laboratory setting, optimization of the method was done. For the optimization, we monitor basal and starvation induced autophagy.

Flp-In T-Rex HEK293 cell lines (kindly provided by prof. Geir Bjørkøy, HIST, Trondheim, Norway) were seed on 12 well plates, a day before any intervention. The next day, the expression of GFP-p62 is induced with 1ng/ml of doxycycline (Sigma Aldrich, USA) for 24 hours. The inducer was removed via washing with warm PBS twice then warm DMEM with

10% FCS was added. The removal of inducer was followed by interventions such as amino acid starvation with Hanks balanced salt solution, amino acid starvation in presence of 3 MA (Sigma Aldrich, USA), and no intervention with incubation in nutrient rich DMEM medium with 10 % FCS for different time interval of 4,8,18 and 24 hours.

After the intervention, cells were harvested via trypsinization and resuspended in normal growth medium (DMEM) and kept on ice for an hour before analysis with flow cytometry (FACS LSRII, Becton Dickinson) was done. Cells were analyzed using blue laser for excitation of GFP and red laser for excitation of DsRed *M. avium*. The data was collected from a minimum of 10,000 single events per tube and mean GFP value was used for quantification. The mean fluorescence intensity after 24 hours of induction was set to one and relative loss of intensity (relative mean GFP fluorescence) in 10,000 cells at various time points after removal of inducer was estimated.

The amino acid starvation significantly increased the rate of degradation of GFP-p62 whereas the rate of basal autophagy was very low but detectable (Appendix VI).

3.4 Transfection assay

3.4.1 Principle

Transfection is a procedure that enables to introduce foreign nucleic acids into cells. The main objective behind transfection is to study the function of the gene or gene products, by either enhancing or inhibiting specific gene expression in cells, and also to produce recombinant protein[83]. The transfection can be carried out in cells either transiently or permanently. In stable or permanent transfection, foreign genetic materials are integrated

into the host genome and are expressed even after host cells replicate. In contrast to stable transfected gene, transiently transfected genes are not integrated into the host genome and are expressed for a limited period of time[83]. The transiently transfected gene could be lost by environmental factors and cell divisions, so choice of transfection method depends on the objective of experiments. There are several transfection methods, but ideal methods should have high transfection efficiency, minimal effects on normal physiology, low cell toxicity, easy to use, and reproducible. The method can be broadly classified into biological, chemical and physical mediated method. The biological methods include the use of biological vectors such as virus mediated transfection[84]. The chemical methods include the use of cationic polymer, calcium phosphate, cationic lipids, and cationic amino acids[85, 86]. The cationic lipid is the most popular method used for transfection. The physical method of transfection includes direct micro injection, biolistic particle delivery, electroporation and laser based transfection[87]. Electroporation is most widely used physical method of transfection.

RNA interference (RNAi) also called post translational gene silencing, is a biological process in which non-translated double stranded RNA (dsRNA) called small interfering RNA(siRNA) mediates sequence specific degradation of target messenger RNA (mRNA) thereby inhibiting the expression of target gene[88]. The long double stranded RNA are cleaved by dicer into produce small interfering RNA of 21-23 nucleotides long. These siRNA are loaded into multi-protein RNA inducing silencing complex (RISC). The duplex siRNA are unwound in strand specific manner which later binds with complimentary target mRNA for endonucleolytic cleavage[88]. Such biological processes are used as an experimental tool to knockdown specific genes of interest and to observe consequent changes of

phenotypes. For this purpose, chemically synthesized siRNA molecules that mimic dicer products are used to investigate gene function in mammalian cells. The method used to deliver siRNA is lipid/polymer mediated method and virus mediated method. In our study, we used lipid mediated delivery for siRNA based knock down.

3.4.2 Lipofection

It is a process of introducing genetic material into a cell by means of liposomes which can easily merge with the plasma membrane of cell as both are made up phospholipid bilayer. Generally, lipofection use cationic lipid to form aggregates with anionic genetic material. It results in net positive charge on this aggregates which are assumed to enhance the effectiveness of transfection through negatively charged lipid bilayer[89].

3.4.2.1 Lipofectamine RNAiMAX / Lipofectamine 2000 transfection

The lipofectamine RNAiMAX (Invitrogen, USA) was used for Keap1 TLR2, TLR9 and STING siRNA transfection whereas lipofectamine 2000 (Invitrogen, USA) was used for the transfection of cyclic-di-GMP (Biolog, C057, Germany). The monocyte derived macrophages (MDMs) were cultured on 35mm glass bottom γ-irradiated tissue cell dishes with RPMI medium without antibiotics. For siRNA mediated knockdown, human MDMs were transfected twice at 0 and 48 hours using the pool of Keap1 (16nm), TLR2 (20nM), TLR9 (20 nm) and STING (20nm) siRNA from Qiagen (detail in appendix I). AllStars Negative Control from Qiagen was used as non-target control siRNA (siNTC). The concentration of 8µg/ml of cyclic-di-GMP was transfected for 4 hours. The efficiency of geneknock down was evaluated using quantitative real-time PCR. For transfection, DNA-lipofectamine complexes were prepared as follows:

Tube 1: Opti-MEM medium (Invitrogen, USA) with lipofectamine RNAimax /lipofectamine 2000

Tube 2: Opti-MEM medium with Keap1/TLR2/TLR9/STING pool siRNA/ cyclic-di-GMP

The content in tube 1 and 2 were mixed gently and incubated for 5 minutes to allow the formation of DNA/cyclic-di-GMP-lipofectamine complex. The desire amount of the complex were added to the cells and mixed gently by rocking the dishes back and forth. The cells were incubated at 37°C in 5% CO2 incubator.

3.4.3 Gene juice transfection

Gene juice transfection reagent (Merck Millipore, USA) is composed of nontoxic cellular protein and a small amount of novel polyamine. It is different from lipid based transfection method. This method was used for the transfection of pcDNA3-TLR2/CD14/TLR9 plasmid. The wild type TLR2, TLR2-cherry and CD14 plasmid was kindly provided by Nadra Nilsen (Department of Cancer Research and Molecular Medicine, NTNU) and TLR9-Hemagglutin (HA) tagged plasmid was kindly provided by Harald Husebye (Department of Cancer Research and Molecular Medicine, NTNU). The transfection was performed when cells were 50-75% confluent. The protocol for transfection is described below.

Cells were plated in 12 well plate and 35 mm glass bottom γ-irradiated tissue cell dish and incubated at 37°C, 8% CO2 overnight.

For each well of 12 well plate and 35 mm confocal dish to be transfected, 50 µl of Opti-MEM medium for each well of 12 well plate and 100 µl for confocal dish was placed in sterile tube and 3µl per 1 µg DNA gene juice

transfection reagent was added to Opti-MEM medium. The mixture was vortexed thoroughly and incubated at room temperature for 5 minutes.

For each well, following concentration of plasmid was added to above Opti-MEM-gene juice mixture and mixed gently.

- 12 well plate:

  For TLR2 expression: 1µg pcDNA3-TLR2 and the 0,3µg pcDNA3-CD14 plasmid per well

  For TLR9 expression: 0,5µg TLR9-Hemagglutinin (HA) per well

- 35mm confocal dish:

  For TLR2 expression: 2µg TLR2-Cherry per well

  For TLR9 expression: 1µg TLR9-Hemagglutinin (HA) per well.

Incubation of gene juice/plasmid mixtures at room temperature for 10 minutes was carried out.

For each well of 12 well plate, 50 µl of mixtures and for confocal dish 100µl of mixtures were added drop wise over the entire surface of dishes and plates were gently rocked back and forth to distribute mixture evenly. The cells were incubated for 48 hours at 37°C, 8 % CO2.

3.5 Quantitative real time PCR

3.5.1 Principle

Quantitative real time PCR is a technique that has major advantages over standard PCR. It has a wide range of an application that includes analysis

of gene expression and regulation, determination of effects of variations in genetic composition, identification and quantification of microorganism and viruses.

PCR can only be used to estimate the amount of particular target DNA or RNA in a sample relative to either a standard or another sample that has been subjected to the same treatment. So, it has a very limited value as a quantitative tool. Real time PCR expands the utility of PCR for quantification through the use of fluorescent reporter molecules to the assay. The fluorescence intensity, which increases proportionally with each DNA molecules amplified, is measured during each cycle of PCR and plotted over time. As there is a direct correlation between the amount of PCR product in each cycle and the progression of a fluorescence amplification curve, an analysis of this curve enables calculation of the original starting quantity of target DNA or RNA.

In this study, TaqMan probe was used which is a hydrolysis probe. In such type of system, three oligonucleotides are used; forward primer, reverse primer and dual labeled non-extendable probe. Such a probe is labeled with a reporter dye on the 5'end and quencher dye on the 3'end and specifically binds to target region[90]. As long as a probe is intact, the fluorescence emission of the reporter dye is absorbed by the quenching dye. When the primers are extended by *Thermus aquaticus* DNA polymerase, the 5'-3' exonuclease activity of such DNA polymerase cleave and release reporter dye from probe[90]. The fluorescence intensity of reporter dye increases with amplification of target nucleic acid.

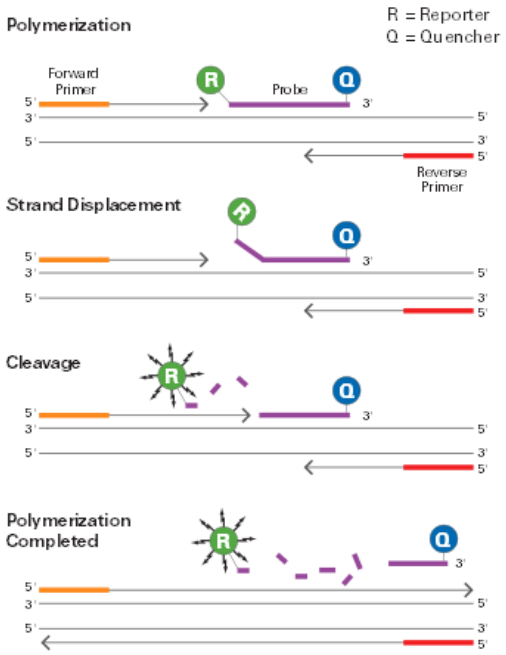

Figure 3.5.1. Principle of TaqMan probe

The three oligonucleotides bind specifically to target. The primers are extended by TaqMan DNA polymerase activity, such extension lead to displacement of fluorescence labeled probe. The 5'-3' nuclease activity of DNA polymerase results in degradation of the probe and subsequent release of reporter dye. Each amplification of target nucleic acid results in an increase in fluorescence intensity produced from cleaved reporter dye. Figure taken from applied biosystem website.

3.5.2 RNA isolation

The RNA isolation was performed using fully automated QIAcube (Qiagen) with Qiagen RNeasy Mini Kit. After preparation of cell lysate with treatment of RLT buffer/β-Mercaptoethanol (ME), the 350µl of cell lysate were transferred to 2ml Qiagen sample tube and loaded into QIAcube instrument. Such RLT buffer contains highly denaturing guanidine-thiocyanate which inactivates RNase. For the isolation of RNA,

Qiagen protocol for animal tissue and cells with DNase I digest were used. The principle behind using DNase I digest is to degrade DNA which is detected by TaqMan system. The samples are treated with ethanol which provides appropriate binding conditions. Subsequently ethanol treated sample are applied to RNease Mini spin column where the total RNA binds to the membrane and contaminants are washed away. Finally, RNAs are eluted in water.

3.5.3 Determination of nucleic acid concentration

The concentration of RNA on the sample was measured on a NanoDrop 1000 (thermo scientific, USA) spectrophotometer at 260nm.

3.5.4 Synthesis of cDNA from RNA via reverse transcription

The reverse transcription of RNA to cDNA was performed using High-Capacity Reverse Transcription kit from Applied Biosystems. The volumes per reaction in cDNA synthesis are mention on table 3.1

Table 3.1. The volume per reaction in cDNA synthesis

Reagent	Volume per reaction
2X RT buffer	10µl
20X RT enzymes	1 µl
RNA sample	9µl
Total volume	20µl

cDNA synthesis was carried out in low tube strips from Bio-Rad. The reverse transcription reaction was done in C1000™ thermal cycler (Bio-Rad, California, USA) with following programs:

Table 3.2. Reverse transcription reaction program on thermo cycler.

Temperature	Time
37°C	1 hour
95°C	5 minutes
4°C	Forever

3.5.5 Reaction Mixture preparation for RT-PCR analysis

The TaqMan® fast master mix (Quanta Biosciences, USA) and TaqMan® gene expression probe (Applied Biosystems, USA) were prepared in the following ways:

Table 3.3. RT-PCR reaction mixture volume

PCR reaction components	Volume per reaction
TaqMan® gene expression probe	1µl
TaqMan® fast master mix	10µl
Sample cDNA	9µl
Final volume	20µl

After the preparation of the above reaction mixture, it was then pipetted in duplicate wells into a 96 well reaction plate. The plates were sealed with adhesive strip and centrifuged briefly at 1500 rpm for 2 minutes in order to eliminate any air bubbles formed during pipetting. Finally, the plates were loaded into real time PCR instrument. The PCR reaction was performed in Applied Biosystems StepOnePlus real time PCR system with below cycling parameter.

Table 3.4. RT-PCR reaction program

Temperature	Time
50°C	2 minutes
95°C	20 seconds
95°C	1 seconds
60°C	20 seconds

The housekeeping gene Glyceraldehyde-3-Phosphate Dehydrogenase (GAPDH) was used as endogenous controls. Gene expression of the target sample was normalized to these endogenous control gene and to control (calibrator) using the formula $2^{-\Delta\Delta Ct}$, which yields sample relative quantification (RQ) values. The -ΔΔCt is equals to - ((ΔCt target)-(ΔCt calibrator)). The ΔCt is Ct of the target or calibrator subtracted from the Ct of endogenous control.

3.6 Immunofluorescence staining for TLR9

HEK293 cells were transiently transfected with TLR9 Hemagglutin (HA) tagged plasmid. For the detection of expression of TLR9, mouse monoclonal anti-HA antibody (Sigma Aldrich, H3663, USA) were used as primary antibody. The cells were fixed in the presence of 4% PFA for 10 minutes on ice followed by washing with PBS twice and permeabilization in ice cold methanol at -20°C for 20 minutes. After fixation and permeabilization, cells were washed twice with PBS and blocked with 2.5 % BSA for 30 minutes. Blocking steps were followed by incubation with 2 µg/ml of mouse anti-HA antibody for 1 hour. Finally, after washing with PBS twice, 1:1000 diluted goat anti-mouse alexa 546 tagged secondary antibodies (Invitrogen, USA) was incubated for 30 minutes. HEK293 cells without transient expression of TLR9 were used as negative control.

3.7 In vitro infection

Primary human monocytes were seeded in confocal dish and allowed to differentiate into macrophages before any intervention such as infection or gene knockdown was performed. The MDMs were infected with *M. avium* clone 104 expressing DsRed or Cyan Fluorescent Protein (CFP)[91]. The cells were infected at a multiplicity of infection (MOI) of 10. For in vitro infection assay, *M. avium* expressing DsRed or CFP were grown in complete 7H9 medium with 0.05% tween. The bacterial growth medium with *M. avium* was centrifuged at 10,000g for 2 minutes. The supernatant was removed, and bacterial cell pellets were washed twice with PBS by centrifugation at 10,000g for 2 minutes. After the final washing step, bacterial cells suspension were vortexed and sonicated with ultra-sonicator (Elma, GmBH) thrice for 30 seconds to remove any clumping of bacterial cells. Then bacterial optical density (O.D) was measured at 600nm with spectrophotometer (Spectronic genesys 20, thermo electron corporation,

USA). The O.D between 0.3-0.6 was used for the infection assay as it defines the exponential phase of bacteria. The O.D. at 600 nm was used to calculate the concentration of bacteria required to obtain MOI of 10. The O.D. of 1 = 4.5 X 10^8 bacterial cells/ml. In addition to determining the concentration of bacteria with spectrometer, serial dilution method for counting colony forming unit (CFU) was also done to determine actual viable bacterial count.

3.8 Stimulation of cells with lipomannan and CpG ODN

Primary human macrophages were stimulated with 100 ng/ml of lipomannan (Invivogen, USA) and 3µM of CpG ODN (Invivogen, USA) for 4 hours and 24 hours. The stimulation procedure was followed by 2 hours incubation in the presence of 100nm bafilomycin A1 (Sigma Aldrich, USA).

HEK293 cell lines were also stimulated with 100ng/ml of lipomannan and 3µM CpG ODN for 8 hours and 24 hours.

3.9 Neutralization of TLR2

For the neutralization of TLR2, primary human macrophages were pretreated with a mixture of anti-TLR2.1 and TLR2.3 antibody[92]. These antibodies were diluted in 10% human serum RPMI medium at a concentration of 10 µg/ml each. The mixture of each 10µg/ml of TLR antibodies were pipetted after removing the medium present in confocal dish containing human macrophages. The antibodies were incubated for 30 minutes at 37°C. Monoclonal IgG2a isotype antibody (Hycult Biotech, USA) was used as a negative control.

3.10 Enzymes linked immunosorbent assay (ELISA)

ELISA is a sensitive laboratory method used to detect the presence of antigen or antibody of interest in a wide variety of biological samples. These assays require an immunosorbent i.e. antigen or antibody immobilized on a solid surface such as wells of microtitre plates or membranes. Basically in ELISA, two antibodies that can bind to two different epitopes on the same antigen are required. One of the antibodies is immobilized on a microtitre well and is referred to as capture antibody. The basis for such immobilization is non-covalent bond resulted from hydrophobic interaction. Such immobilized antibody serve to specifically capture antigen of interest present in the sample and therefore referred capture antibody. These captured antigens are detected by biotin conjugated antibody followed by enzymes labeled avidin or streptavidin. On the addition of chromogenic substrate, results in production of colored produced which are measured by spectrophotometer.

For the detection of TNF-α and IP-10 commercial kits (R & D systems, USA) were used and protocols were adapted from the manufacturing company.

3.11 Confocal laser setting and image analysis

For the confocal imaging, cells were imaged using LSM 510 Zeiss microscope with plan apochromatic 63x/1.45 oil objective. The laser and filter setting used during the entire project are mentioned as follows.

Table 3.5. Confocal laser and filter setting

Fluorochrome	Laser	Filter	Pixels
Alexa 546	543	BP 565-615	512 X 512
CFP	458	BP 470-500	512 X 512
DRAQ 5	633	LP 650	512 X 512
Ds Red	633	LP 650	512 X 512

Bitplane Imaris software (Biplane, Zürich, Switzerland) was used for the analysis of Z stack images obtained from confocal microscopy. The spot detection wizard in Bitplane Imaris software was used for counting the LC3 II dots and LC3 II punctuates was counted per 100 cells. The threshold size of positive LC3 II dots was set as ≥1 µm in diameter and appropriate threshold sum intensity for LC3 II was set constant for each staining assay.

3.12 Statistical analysis

Statistical analysis of data was performed using GraphPad Prism software (GraphPad, San Diego, CA, USA). All data were analyzed using Student's t tests. For statistical analysis of data, experiments were performed at least three times and presented as the mean ± standard error of the mean (SEM). Difference was considered significant at $P<0.05$.

4 Results

4.1 *M. avium* induces autophagy in primary human macrophages that is constantly maintained during the time of infection.

A few studies have shown that mycobacteria can directly induce autophagy[61, 93]. To address if this is also the case with *M. avium* infection in macrophages, we used an immunofluorescence assay for the quantification of autophagy in primary human macrophages (establishment and optimization are described in methods with results shown in appendix I). Macrophages were infected with *M. avium* at MOI of 10 for 4 hours and excess bacteria were removed by washing. The autophagy was monitored at different time point of infection of 4 hours, 24 hours and 72 hours. Autophagic flux in each time point of infection was measured after 2 hours of incubation in 100nM bafilomycin A1. Macrophages infected with *M. avium* showed a significant increase in number of LC3 II dots as compared to uninfected cells indicating the ability of *M. avium* to induce autophagy by itself without the requirement of external inducer (figure 4.1.1). In addition, the rate of autophagy was found to be constantly maintained throughout the time period of infection as at each time of point infection the level of autophagy were similar. That means no significant difference in the level of autophagy at different time point.

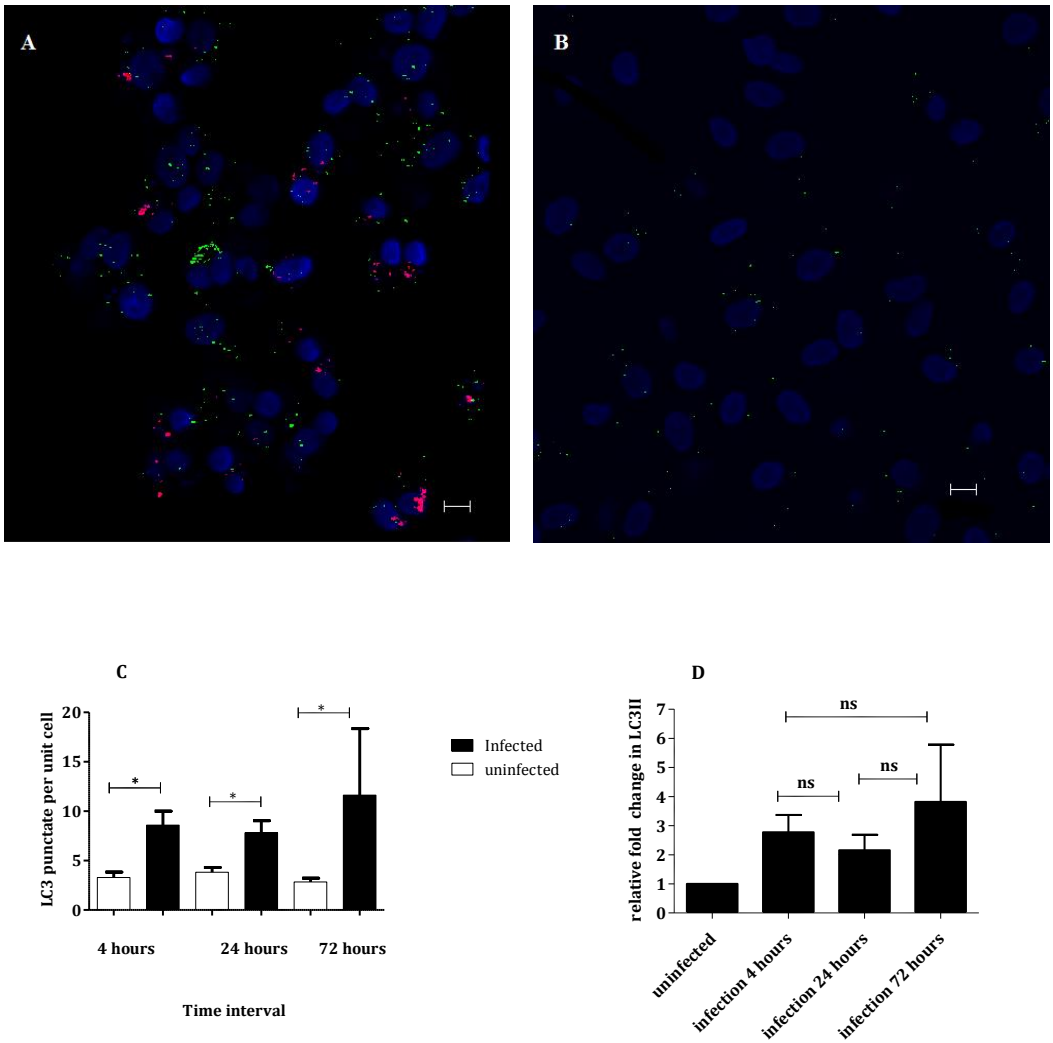

Figure 4.1.1. *M. avium* induces autophagy in primary human macrophages

Confocal image of macrophages infected with (A) CFP *M. avium* (red dots) for 4 hours and (B) macrophages without infection. The cells were imaged using Zeiss LSM 510 with scan zoom of 0.7 and scale bar=10µm. The LC3 II dots are represented as green dots and nuclei were stained blue with DRAQ5 (complete set of images in appendix IV) (C) Graphical representation of LC3 II dots counts measured after 4 hours, 24 hours and 72 hours post infection. (D)The relative fold change in LC3 II dots during different time point of infection in respect to uninfected one. The data are represented as mean ± SEM, data are representative of at least three independent experiment and p-value of <0.05 considered significant.

Furthermore, the induction of autophagy during *M. avium* infection was reduced in the presence of autophagy inhibitor, 3 MA confirming the process being an autophagy. For autophagy assay, amino acid starvation using Hanks balanced salt solution for 2 hours and amino acid starvation in presence of 10 mM 3 MA was used as a positive control. An amino acid starvation resulted in increased number of LC3 II punctate count, whereas starvation in the presence of 3 MA reduced LC3 II punctate count (figure 4.1.2 and confocal images on appendix IV).

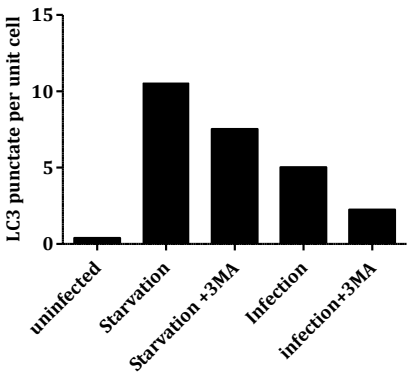

Figure 4.1.2. *M. avium* induced autophagy is reduced in presence of 3MA

The primary human macrophages were infected either with CFP- *M. avium* for 4 hours or infected in the presence of 10mM 3MA. For autophagy control, cells were amino acid starved in Hanks balanced salt solution or amino acid starved in the presence of 3MA for 2 hours. To elucidate the basal autophagy, cells with no intervention was included in the study. All these interventions were proceeded by incubation in 100nM bafilomycin A1 for 2 hours. The data represent single experiment.

4.2 *M. avium* infects HEK293 cell lines but does not induces autophagy

We next examined *M avium* induced autophagy using HEK293 GFP-p62 reporter cell system for monitoring autophagy flux[80]. The main objective of using GFP-p62 reporter cell system was to study autophagy in relation to *M avium* infection with different autophagic flux read out. To determine the level of autophagy, HEK293 GFP-p62 cells were infected for 4 hours and 24 hours and GFP-p62 degradation were measured via flow cytometry. Amino acid starvation in Hanks balanced salt solution and amino acid starvation in the presence of 3 MA were used as a positive inducer and inhibitors of autophagy respectively. As shown in figure 4.2.1, amino acid starvation showed remarkable rate of degradation of GFP-p62 as compared to basal autophagy at both 4 hours and 24 hours time point. Amino acid starvation induced autophagy was significantly reduced in the presence of 3 MA in both time point of 4 hours and 24 hours. Flow cytometry and confocal imaging showed that DsRed *M. avium* effectively infect the HEK293 cells after 4 hours of infection but *M. avium* infected HEK293 cell and uninfected HEK293 cells showed similar rate of GFP-p62 degradation at time point of 4 hours and 24 hours. So, it clearly indicates that *M. avium* does not induce autophagy on HEK293 cells.

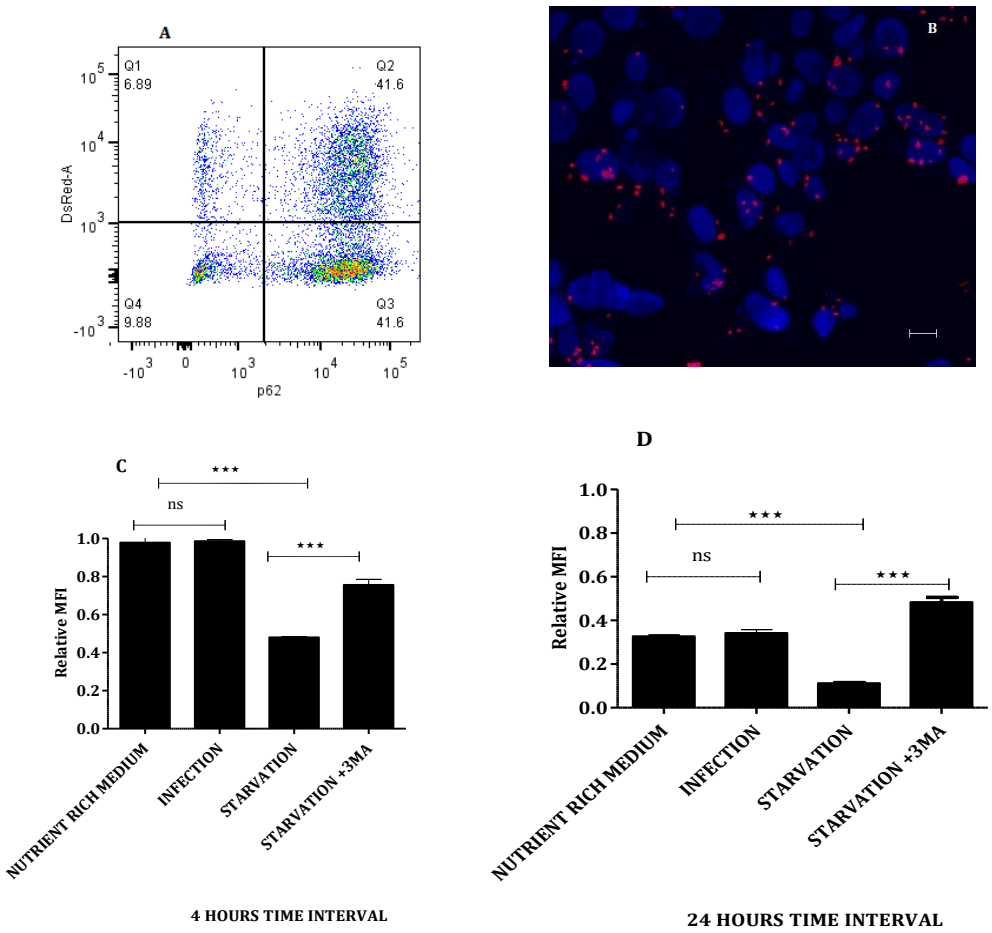

Figure 4.2.1. *M. avium* does not induce autophagy in HEK293 cells

(A) Flow cytometry analysis of HEK293 GFP-p62 cell line demonstrating Q4: double negative cells with no expression of GFP-p62 and no infection with DsRed *M. avium*, Q3: single positive cells expressing GFP-p62 only, Q2: double positive cells expressing GFP-p62 and being infected by DsRed *M. avium* and Q1: single positive cell that are being infected with DsRed *M. avium* but no expression of GFP-p62.(B) Confocal image of HEK293 cells infected with DsRed *M. avium* (red dots) for 4 hours. The nuclei were stained blue with DRAQ5 nuclear stain. The cells were imaged using Zeiss LSM 510 live with scan zoom of 0.7 and scale bar=10µm. Graphical representation of relative MFI when HEK293 cells were amino acid starved or amino acid starved in presence of 3MA or no starvation or infected with DsRed *M .avium* for (C) 4 hours and (D) 24 hours. The data are represented as mean ± SEM, data are representative of at least three independent experiment and p-value of <0.05 considered significant.

As *M. avium* did not induce autophagy in HEK293 cells, so in order to further confirm, we evaluated those results with LC3 II staining. The HEK293 GFP-p62 reporter cell system measures the p62 degradation, whereas the LC3 II staining quantifies the number of autophagosomes containing LC3 II. Amino acid starvation of HEK293 cells induced an increased number of LC3 II dots which was significantly reduced in the presence of 3 MA. The LC3 II staining of *M. avium* infected HEK293 cells did not show higher number of LC3 II dots as compared to uninfected; indicating that *M. avium* does not induces autophagy in HEK293 cells (figure 4.2.2 and confocal images on appendix VII).

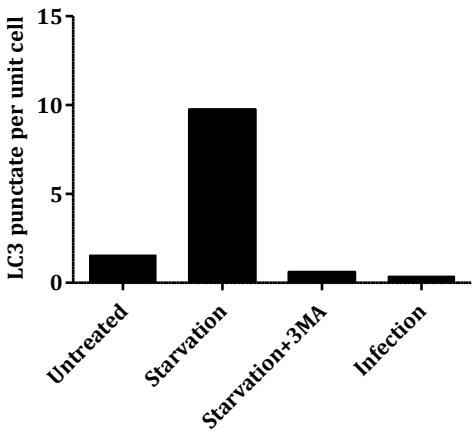

Figure 4.2.2. Comparison of monitoring autophagy via GFP-p62 degradation with LC3 II accumulation

The HEK293 cells were infected with CFP *M. avium* at MOI of 10 for 4 hours. For autophagic control, cells were incubated in amino acid free medium or amino acid free medium in the presence of 3 MA for 2 hours or nutrient rich DMEM medium with 10% FCS**.** Each intervention was proceeded by incubation in 100nM bafilomycin A1 for 2 hours. The data represent single experiment.

4.3 *M. avium* did not induce autophagy in HEK293 cells expressing TLR2

Several TLR ligands are shown to induce autophagy. As HEK293 cells lack several TLRs, including TLR2, TLR4 and TLR9, this could possibly explain why *M. avium* did not induce autophagy in the HEK293 GFP-p62 cells. To determine the role of TLR2 in recognition of *M. avium* and downstream induction of autophagy, TLR2 was transiently expressed in the HEK293 cells. As shown in the figure 4.3.1, TLR2 cherry was found to be expressed on the cell membrane of HEK293 cell lines. The functionality of TLR2 was determined by measuring production of TNF-α cytokines after stimulation with FSL-1, a potent synthetic ligand for TLR2. Stimulation of TLR2 expressing HEK293 with 50ng/ml FSL-1 for 8 hours, induced more than 2000 pg/ml TNF-α whereas HEK293 cell without TLR2 expression showed no detectable amount of TNF-α.

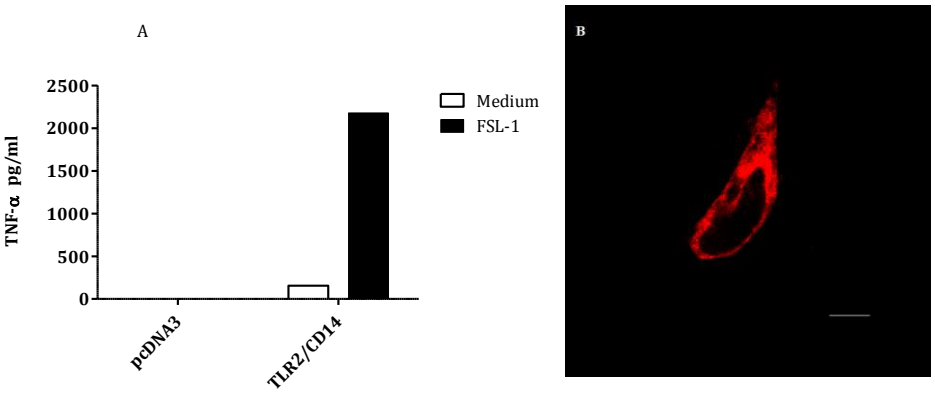

Figure 4.3.1. Confirmation of expression and functionality of TLR2

(A) HEK293 cells were transfected with wild type TLR2 (1µg/well of 12 well plate) and CD14 (0.3µ/well) for 48 hours. After the transfection of TLR2 in HEK293 cell lines, these cell lines were stimulated either with 50ng/ml of FSL-1 or left unstimulated (medium) for 8 hours and supernatant were harvested for the measurement of TNF-α via ELISA. (B) Confocal image of HEK293 expressing TLR2 cherry. HEK293 cell line was transfected with TLR2-cherry (2µg/dish) for 48 hours. The cells were imaged using Zeiss LSM 510 live with scan zoom of 2 and scale bar=10µm.

After the confirmation of expression and functionality of TLR2 on HEK293 cells, the role in autophagy were elucidated by infecting HEK293 expressing TLR2/CD14 and HEK293 cells with only vector plasmids pcDNA3 for 8 hours and 24 hours. The expression of GFP-p62 on HEK293 cells were induced with 1ng/ml doxycycline for 24 hours then removal of doxycycline via washing with PBS were followed by *M. avium* infection. As shown on the figure 4.3.2, there was no difference in the rate of degradation of GFP-p62 in between *M. avium* infected or uninfected HEK293 TLR2/CD14 expressing cells. So the results clearly indicate that *M. avium* does not induce autophagy in HEK293/TLR2/CD14 cells. The results were quite similar on both time interval of infection.

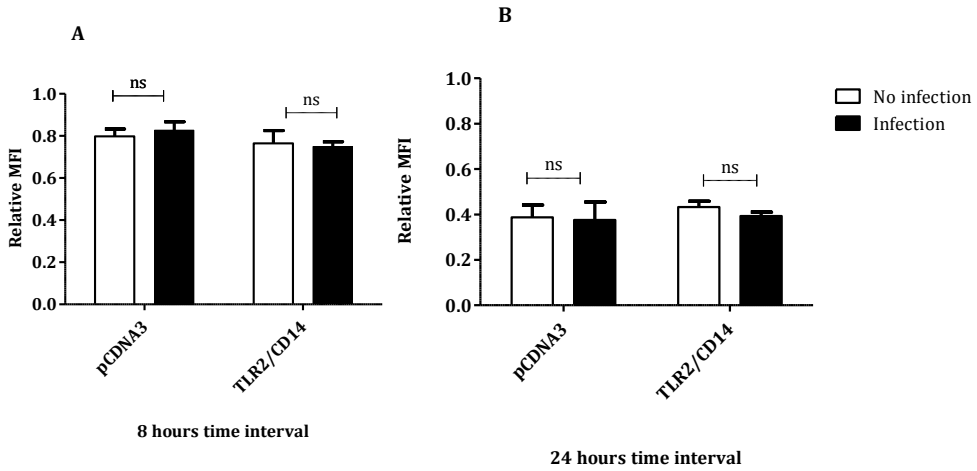

Figure 4.3.2. *M. avium* did not induce autophagy in HEK293 cells expressing human TLR2

Graphical representation of relative MFI of TLR2/CD14 or only pCDNA3 plasmid transfected HEK293 cells, infected with either DsRed *M. avium* at MOI 10 or uninfected for (A) 4 and (B) 24 hours. The data are represented as mean ± SEM, data are representative of at least three independent experiments and p-value of <0.05 are considered significance.

4.4 Lipomannan failed to induce autophagy in HEK293 cells expressing TLR2

Lipomannan is known TLR2 ligands. To answer the question whether TLR2 could at all induce autophagy in HEK293 cells, lipomannan was used for stimulating the cells. For this study, HEK293 cells with or without TLR2/CD14 was stimulated with 100 ng/ml of lipomannan for 8 hours and 24 hours. As shown in figure 4.4.1, effect of lipomannan in the rate of degradation of GFP-p62 was similar in lipomannan stimulated and unstimulated HEK293 TLR2/CD14 expressing cells. In both time point of stimulation for 8 hours and 24 hours, lipomannan does not induce autophagy.

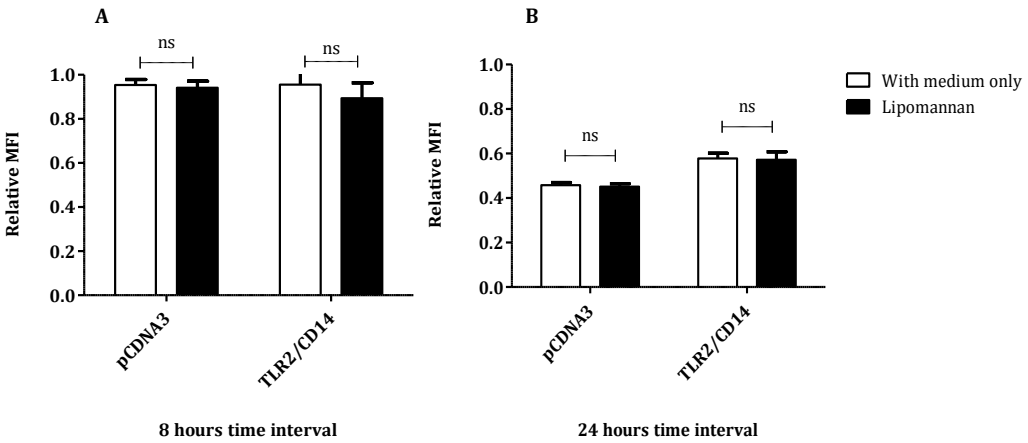

Figure 4.4.1. Lipomannan failed to induce autophagy in HEK293 cells expressing human TLR2

Graphical representation of relative MFI of HEK293 cells transiently expressing TLR2/CD14 stimulated with either 100 ng/ml of lipomannan or left unstimulated (medium) for (A) 8 hours and (B) 24 hours. The HEK293 with transient transfection of pcDNA3 plasmid were used as negative control. The data are represented as mean ± SEM, data are representative of at least three independent experiments and p-value of <0.05 are considered significance.

4.5 *M. avium* did not induce autophagy in HEK293 cells expressing TLR9

To explore if TLR9 could induce autophagy in HEK293 cells, TLR9-HA tagged was transiently expressed in HEK293 cells. As shown in figure 4.5.1, HEK293 cell lines were found to expresses the TLR9. The functionality of TLR9 was determined by measuring the production of IP-10 after stimulation with 3µM of CpG ODN for 8 hours. The ELISA results show about 1900 pg/ml of IP-10 production in TLR9 expressing HEK293 cells but no detectable induction of IP-10 in HEK293 cells without TLR9.

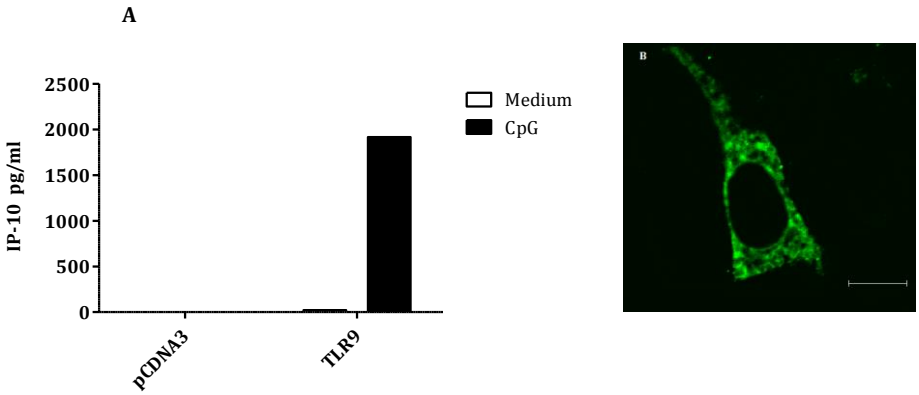

Figure 4.5.1. Confirmation of expression and functionality of TLR9

(A) HEK293 cells were transfected with TLR9-HA (0.5 µg/well of 12 well plate) for 48 hours. After the transfection of TLR9 in HEK293 cell lines, these cell lines were stimulated either with 3µM of CpG ODN or left unstimulated (medium) for 8 hours and supernatant were harvested for the measurement of IP-10 cytokines via ELISA. (B) Confocal image of HEK293 expressing TLR9-HA. HEK293 cell lines were transfected with TLR9-HA (1µg/dish) for 48 hours. The cells were imaged using Zeiss LSM 510 with scan zoom of 2 and scale bar=10µm.

After the transient expression of human TLR9, HEK293 cells were infected with DsRed *M. avium* for 8 hours and 24 hours. As shown figure 4.5.2, the rate of degradation of GFP-p62 in both uninfected and infected HEK293 TLR9 expressing cells was similar. It clearly indicates that

despite TLR9 are known to recognize foreign microbes DNA, were not associated with induction of autophagy in HEK293 cells.

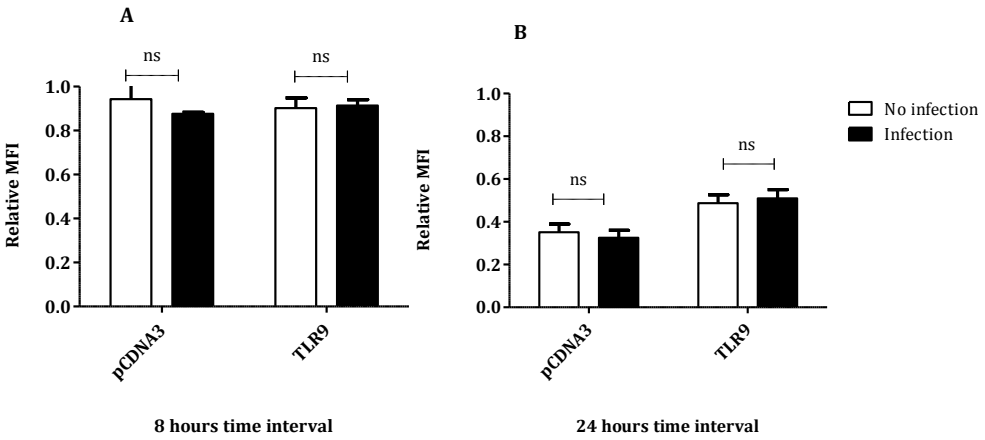

Figure 4.5.2. *M. avium* did not induce autophagy in HEK293 cells expressing human TLR9

Graphical representation of relative MFI of HEK293 cells transient expressing TLR9-HA, infected with either DsRed *M. avium* at MOI of 10 or uninfected for (A) 8 hours and (B) 24 hours. The HEK293 cells line with only pcDNA3 plasmid was used as negative control. The data are represented as mean ± SEM, data are representative of at least three independent experiments and p-value of <0.05 are considered significance.

4.6 CpG ODN failed to induce autophagy in HEK293 cells expressing TLR9

CpG ODN is a known TLR9 ligand. To further confirm, if TLR9 could induce autophagy in HEK293 cells, CpG ODN was used for the stimulation. HEK293 cells expressing TLR9 was stimulated with 3µM of CpG ODN for 8 hours and 24 hours. As shown in figure 4.6.1, CpG ODN stimulated and unstimulated HEK293 cells expressing TLR9 showed similar rate of GFP-p62 degradation indicating CpG ODN do not induce autophagy.

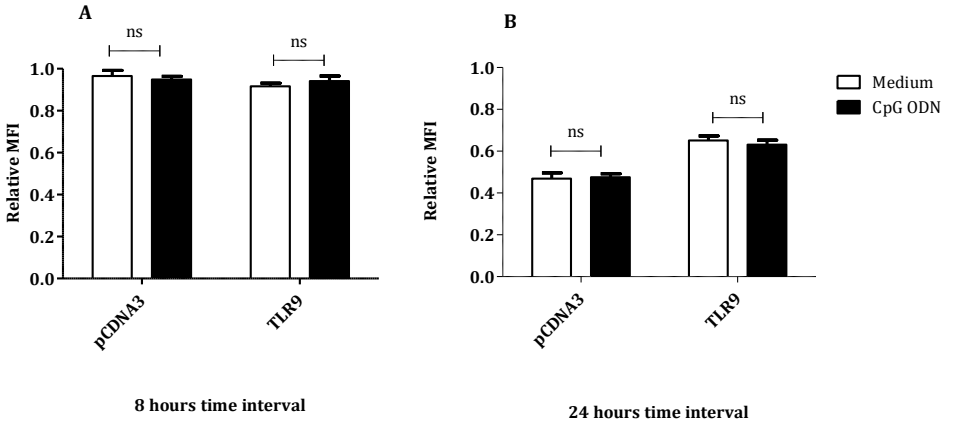

Figure 4.6.1. CpG ODN does not induce autophagy on TLR9-HA expressing cells.

Graphical representation of relative MFI of HEK293 cells transiently expressing TLR9-HA, stimulated with either 3µM CpG ODN or unstimulated (medium) for (A) 8 hours and (B) 24 hours. The HEK293 pcDNA3 plasmid transfected cells were used as a negative control. The data are represented as mean± SEM, data are representative of at least three independent experiments and p-value of <0.05 are considered significance.

4.7 Lipomannan induces autophagy in primary human macrophages

M. avium induced autophagy in primary human macrophages but not in HEK293 cells even when expressing relevant TLRs. To determine whether the induction of autophagy in primary human macrophages could be mediated via TLR2, 100 ng/ml of lipomannan was used for the stimulation for 4 hours and 24 hours followed by incubation with 100nM bafilomycin A1. As shown in figure 4.7.1, stimulation with lipomannan at 4 hours and 24 hours showed increased number of LC3 II punctate as compared to unstimulated cells.

To further confirm the induction of autophagy was mediated via TLR2, neutralizing antibody against TLR2 were used before the stimulation of macrophages with lipomannan. The induction of autophagy was reduced in

presence of neutralizing antibody at both 4 hours and 24 hours of stimulation.

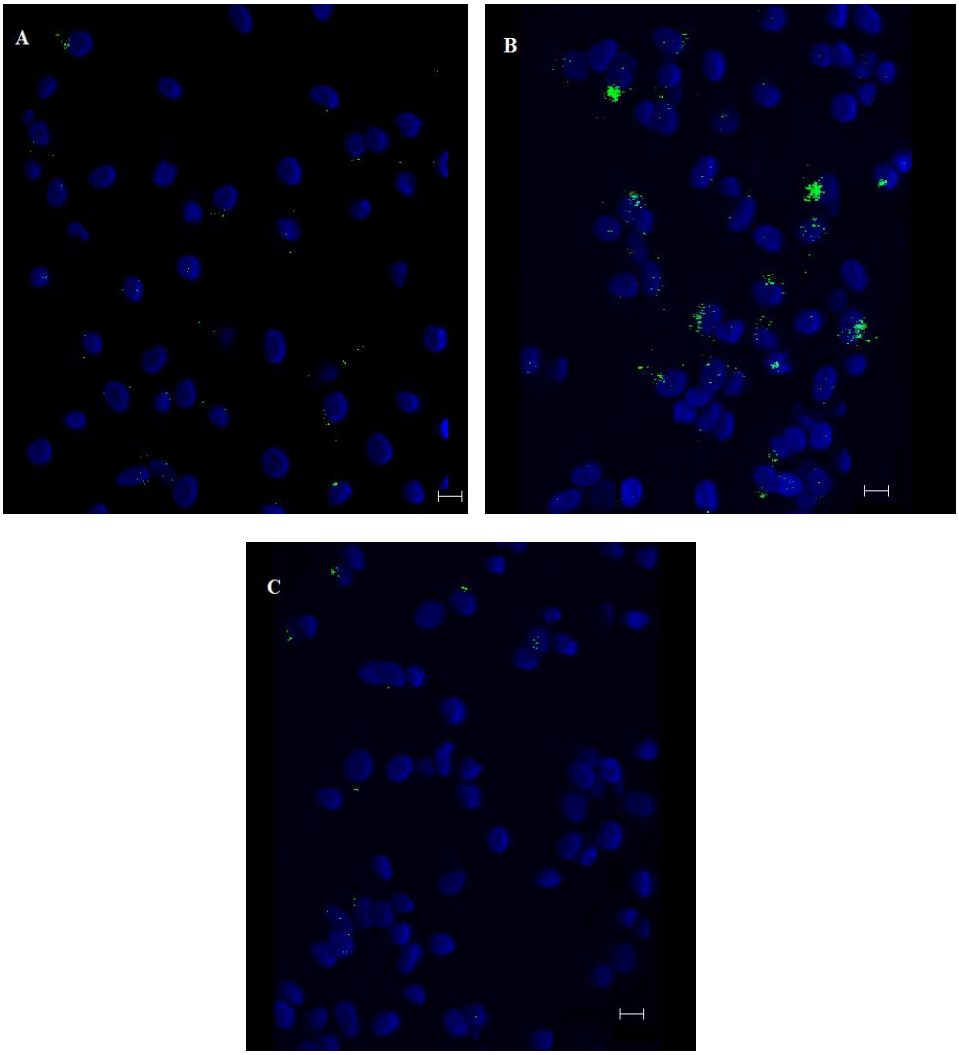

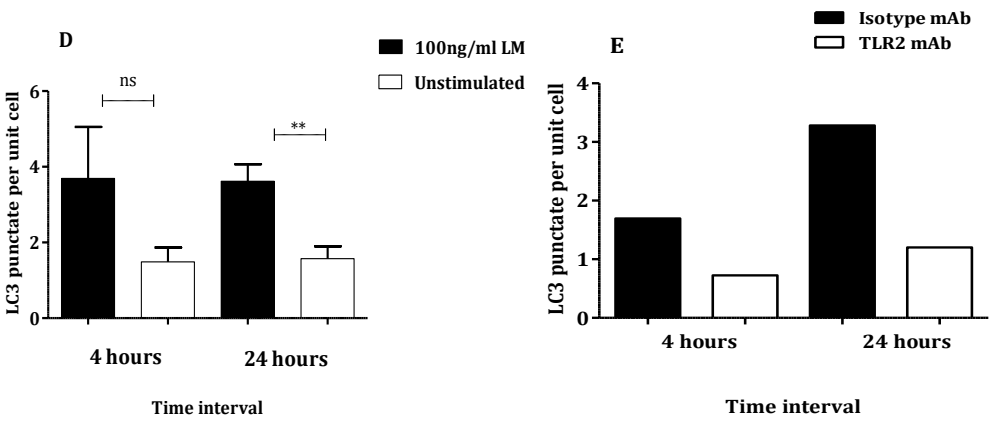

Figure 4.7.1. Lipomannan induces autophagy in primary human macrophages

Confocal images showing (A) MDMs without any stimulation, (B) MDMs pretreated with monoclonal isotype antibody followed by stimulation with 100ng/ml lipomannan for 24 hours, (C) MDMs pretreated with TLR2 monoclonal antibody followed by stimulation with 100 ng/ml lipomannan for 24 hours. The cells were imaged using Zeiss LSM 510 with scan zoom of 0.7 and scale bar=10µm. The LC3 II punctate are represented by green dots and nuclei were stained with DRAQ5 (complete set of images in appendix VIII & IX). Graphical representation of LC3 II dots counts when (D) MDMs were stimulated with 100ng/ml of lipomannan for 4 hours and 24 hours. The data are represented as mean ± SEM, data are representative of at least three independent experiments and p-value of <0.05 are considered significance. (E) MDMs stimulated with 100 ng /ml lipomannan for 4 hours and 24 hours after neutralization of TLR2 receptors with either TLR2 antibody or monoclonal isotype antibody. The data represent a single experiment.

4.8 CpG ODN failed to induce autophagy in primary human macrophages

To determine whether the induction of autophagy in primary human macrophages could also be mediated via TLR9, CpG ODN was used for the stimulation of macrophages for 4 hours and 24 hours. The LC3 II punctate counts were similar in CpG ODN stimulated and unstimulated macrophages at both time point of 4 hours and 24 hours indicating TLR9 might not play a role in induction of autophagy during *M. avium* infection

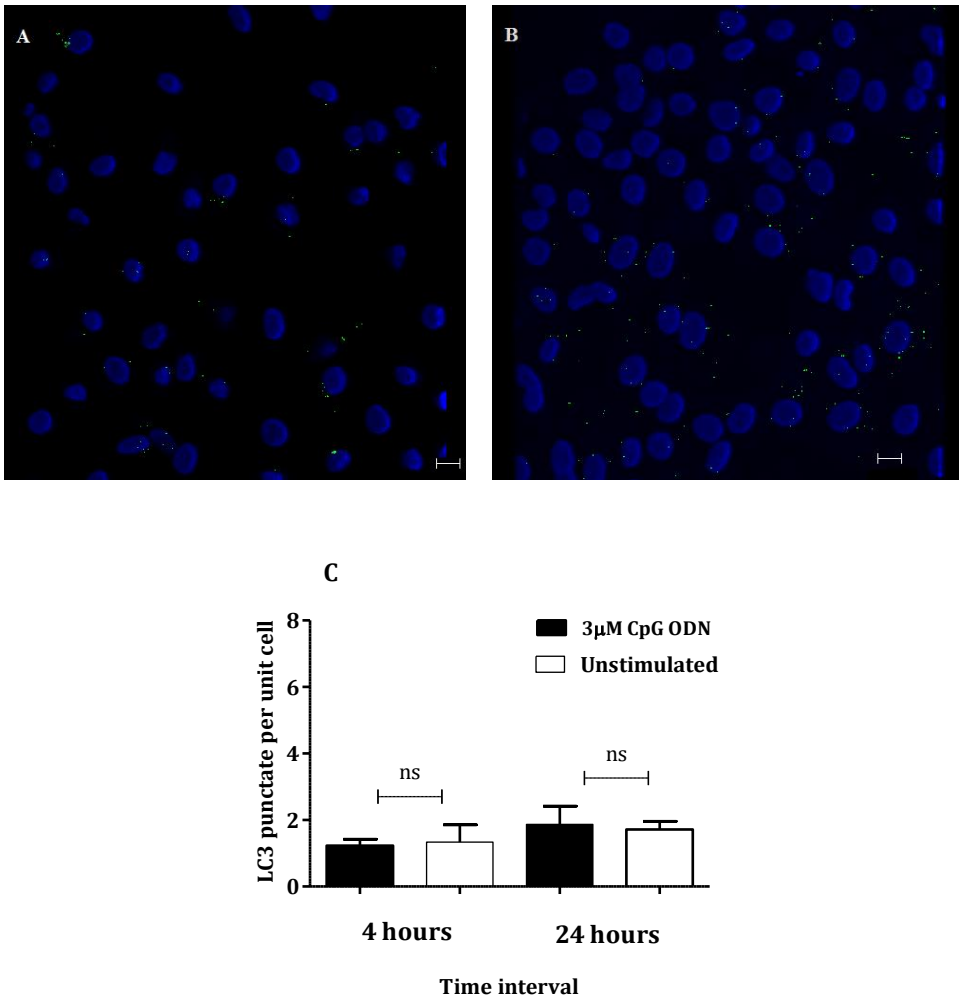

Figure 4.8.1.CpG ODN do not induces autophagy in primary human macrophages

Confocal images showing (A) MDMs without any stimulation, (B) MDMs stimulated with 3 µM CpG ODN for 24 hours. The cells were imaged using Zeiss LSM 510 with scan zoom of 0.7 and scale bar=10µm. The LC3 II punctate are represented by green dots and nuclei were stained with DRAQ5 (complete set of images in appendix X). Graphical representation of LC3 II dots counts when (C) MDMs were stimulated with 3µM of CpG ODN for 4 hours and 24 hours followed by incubation with 100nm bafilomycin A1 for 2 hours. The data are represented as mean ± SEM, data are representative of at least three independent experiments and p-value of <0.05 are considered significance.

4.9 Cyclic-di-GMP transfection induces autophagy in primary human macrophages

The cyclic-di-GMP is a secondary messenger molecule secreted by intracellular microbes inside host cells. A study has shown that cyclic-di-GMP initiates induction of autophagy via STING dependent manner[62]. To elucidate their role, 8µg/ml of cyclic-di-GMP was transfected in primary human macrophages. The confocal imaging of macrophages showed increased number of LC3 II dots in macrophages transfected with cyclic-di-GMP both for 4 hours and 24 hours post transfection as compared to macrophages transfected with only lipofectamine control.

To further confirm that induction of autophagy were STING dependent, macrophages were pretreated with STING siRNA. The knockdown was followed by transfection with cyclic-di-GMP. The knockdown of STING remarkably reduced the level of LC3 dots in both time interval of 4 and 24 hours as compared to non-target negative control (figure 4.9.1).

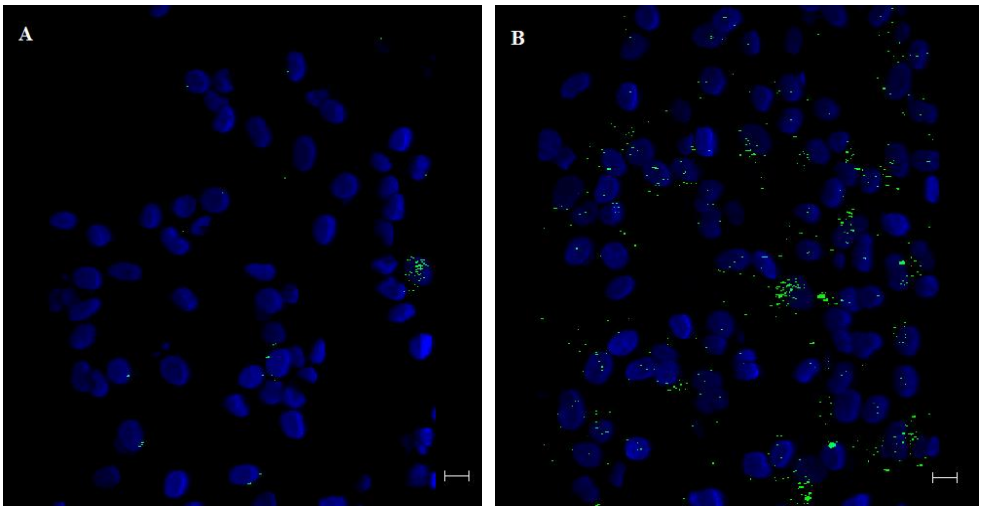

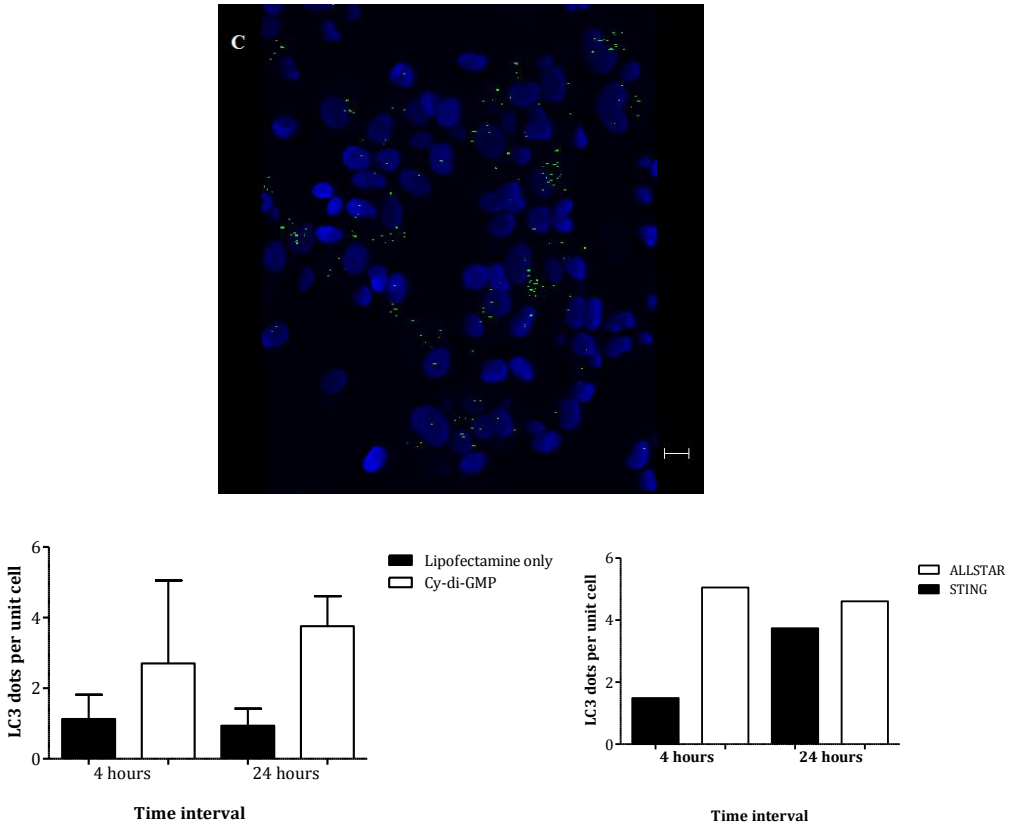

Figure 4.9.1. Cyclic-di-GMP induces autophagy

Confocal images showing (A) MDMs without any stimulation, (B) MDMs pretreated with AllStars siRNA followed by stimulation with 8µg/ml of cyclic-di-GMP for 24 hours (C) MDMs pretreated with STING siRNA followed by stimulation with 8µg/ml of cyclic-di-GMP for 24 hours. The cells were imaged using Zeiss LSM 510 with scan zoom of 0.7 and scale bar=10µm. The LC3 II punctate are represented by green dots and nuclei were stained with DRAQ5 (complete set of images in appendix XIII). Graphical representation of LC3 II dots counts when (D) MDMs were transfected with 8µg/ml of cyclic-di-GMP or lipofectamine only as a negative control for 4 hours and 24 hours. The transfections were followed by incubation with 100 nM of bafilomycin A1 for 2 hours. The data represent duplicate experiments. (E) MDMs pretreated with either STING siRNA or AllStars as a negative control. The siRNA treatments were followed by stimulation with 8µg/ml of cyclic-di-GMP for 4 hours and 24 hours. The LC3 II dots were counted after addition of 100ng/ml of bafilomycin A1 for 2 hours. The data represent single experiment.

4.10 *M. avium* induced autophagy was reduced in presence of TLR2 neutralizing antibody and pre-treatment with TLR2 siRNA

To finally determine the role of TLR2, TLR9 and STING in *M. avium* infection induced autophagy; MDMs were knocked down with respective siRNA treatment. The efficiency of knockdown was lower in TLR9 (mean 40% knockdown) as compared to TLR2 (mean 85.1% knockdown) and STING (mean 76 % knockdown). The knockdown of TLR2 receptors reduced the level of autophagy in *M. avium* infected MDMs for 4 hours and 24 hours. No such effect was seen with both TLR9 and STING knockdown MDMs.

To further elucidate that *M. avium* induced autophagy was mediated via TLR2, macrophages were pretreated with neutralizing antibody against TLR2 before infection assay. The neutralization of TLR2 receptor reduced LC3 II punctate counts in both time point of 4 hours and 24 hours of infection.

Finally, our result shows that TLR2 and STING, but not TLR9 could induce autophagy in primary human macrophages. However, only TLR2 seemed to be involved in induction of autophagy by infection with *M. avium.*

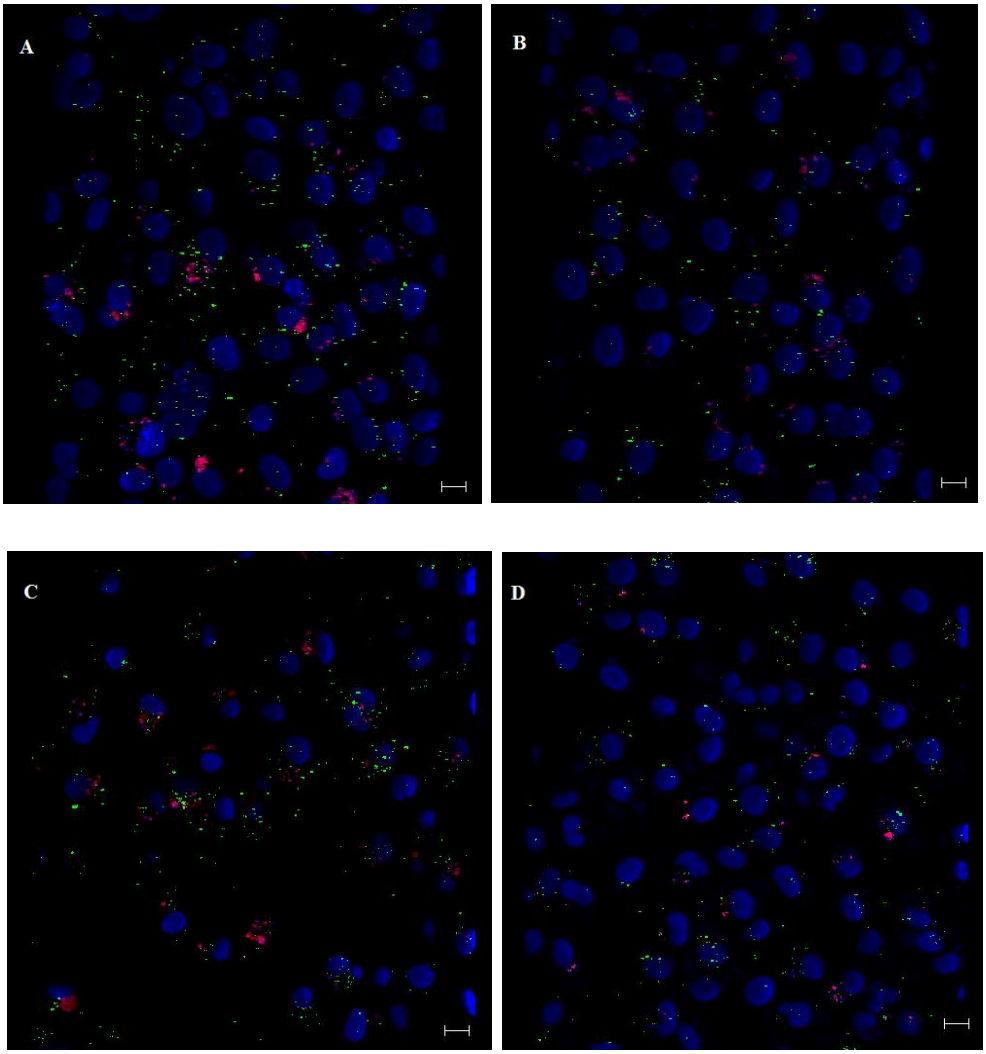
A
B
C
D

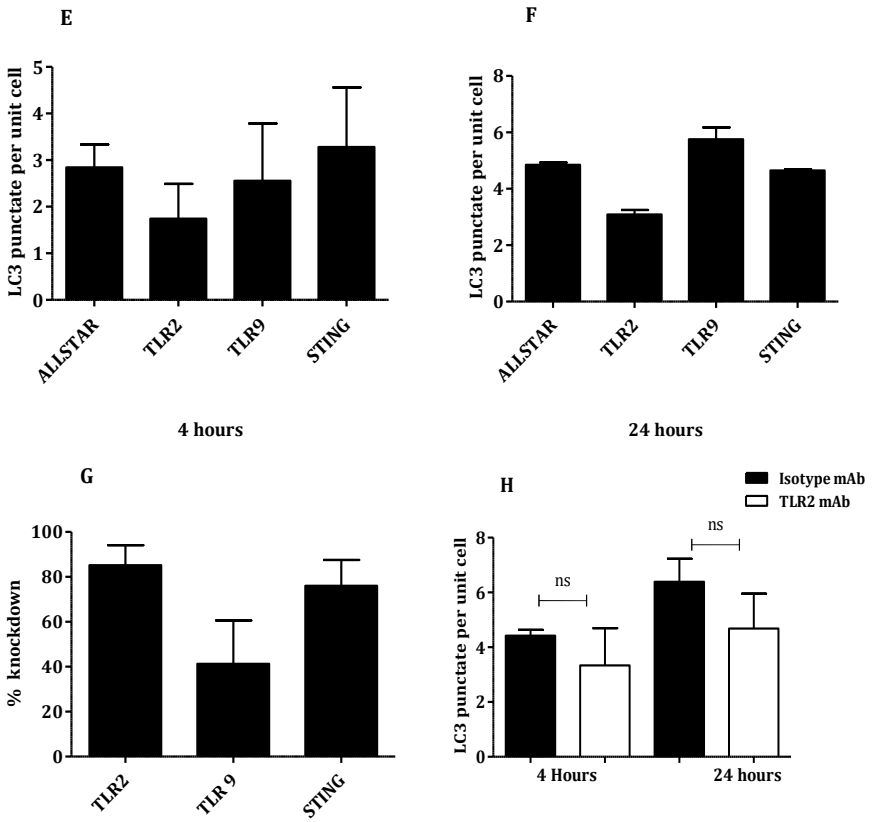

Figure 4.10.1. *M. avium* induces autophagy via TLR2

Confocal images of (A) MDMs pretreated with AllStars siRNA as a negative control followed by infection with CFP *M. avium* for 24 hours, (B) MDMs pretreated with TLR2 siRNA followed by infection with CFP *M. avium* for 24 hours, (C) MDMs infected with CFP *M .avium* for 24 hours after neutralization of TLR2 receptors with monoclonal isotype antibody, (D) MDMs infected with CFP *M. avium* for 24 hours after neutralization of TLR2 with TLR2 antibody. The cells were imaged using Zeiss LSM 510 with scan zoom of 0.7 and scale bar=10µm. The LC3 II punctate are represented by green dots, CFP *M. avium* by red dots and nuclei were stained with DRAQ5 (complete set of images in appendix XI & XII). Graphical representation of LC3 II dots counts when MDMs were pretreated with TLR2, TLR9, STING siRNA and AllStars as negative non-target control followed by CFP *M. avium* infection for (E) 4 hours and (F) 24 hours. The LC3 BII dots quantification were done after incubation with 100nm bafilomycin A1. (G) The knockdown efficiency of TLR2, TLR9 and STING measured via relative quantification of mRNA. The data represent duplicate experiment. (H) The TLR2 were blocked with antiTLR2.1 and TLR2.3 monoclonal antibody followed by infection with CFP *M. avium* for 4 and 24 hours. The data are represented as mean ± SEM, data are representative of at least three independent experiments and p-value of <0.05 are considered significance.

4.11 Keap1 might negatively regulates autophagy during *M. avium* infection but no regulation during basal autophagy

There has been several studies regarding the role of Keap1 as an oxidative and electrophilic sensor, but less is known about its role in autophagy during infection. Therefore, to investigate its role in autophagy during *M avium* infection in MDMs, Keap1 was transiently knocked down in MDMs by siRNA treatment. The Keap1 knockdown of 40% or more was chosen as a cutoff to answer the biological question about the role of Keap1 during *M. avium* induced autophagy.

Keap1 knockdown resulted in increased LC3 II dots in 24 hours and 72 hours post infection, but the difference was only significant for 24 hours post infection. There was no effect of Keap1 knockdown on early infection of 4 hours.

As Keap1 knockdown showed a significant effect on autophagy in MDMs infected with *M. avium*, we next tested the effect of Keap1 knockdown on basal autophagy. As shown in figure 4.11.1, the effect of Keap1 knockdown has no significant difference in LC3 II punctate over a different period of time.

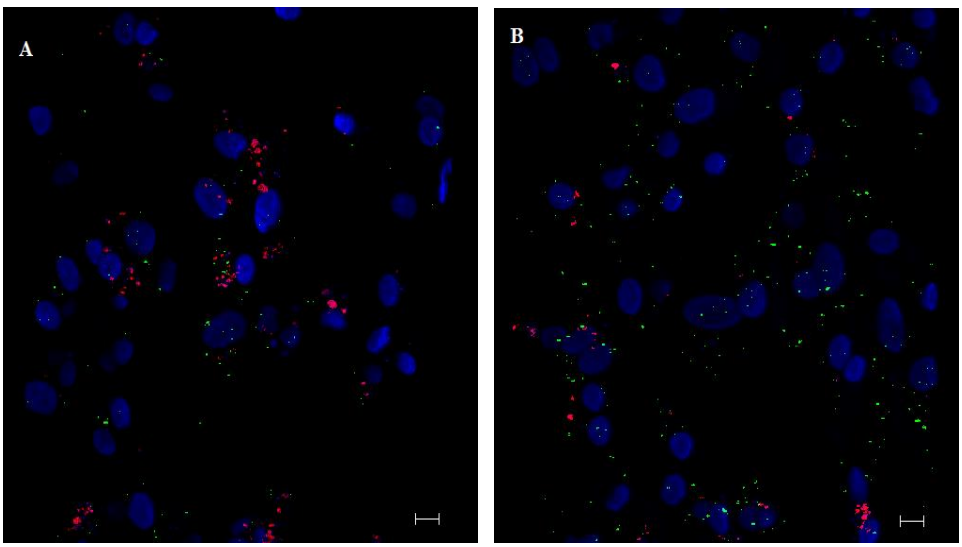

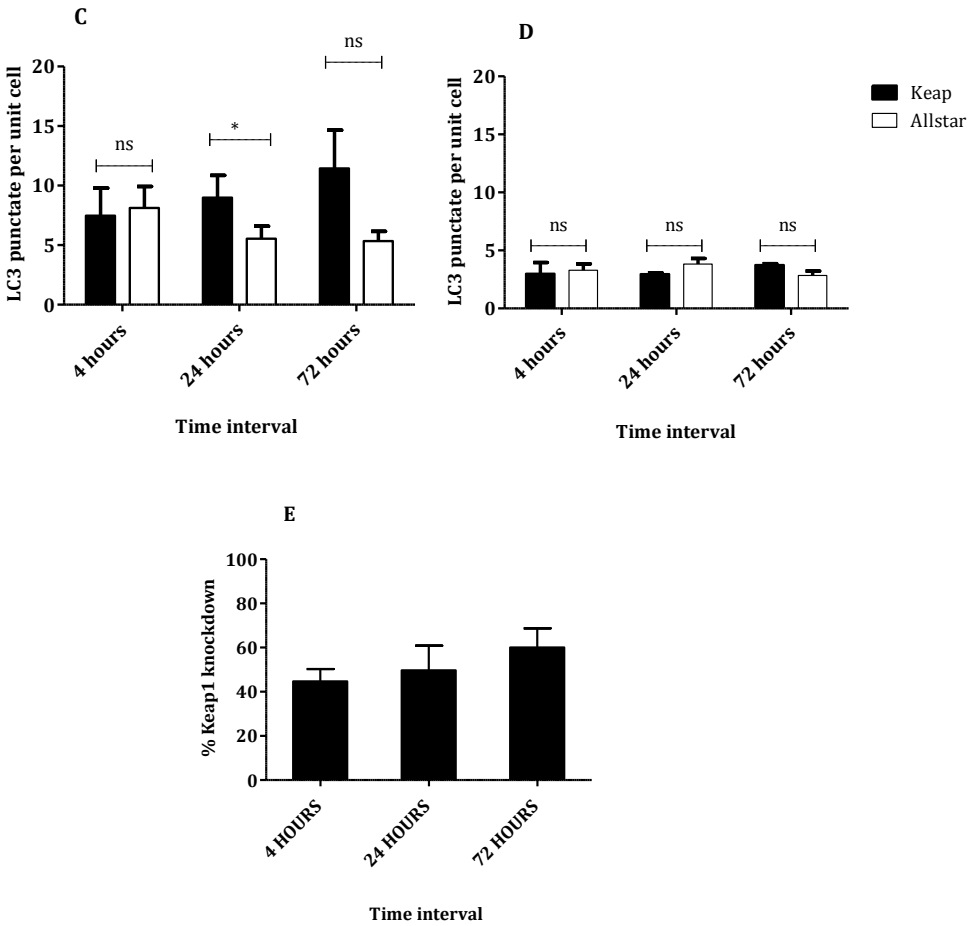

Figure 4.11.1. : Keap1 might negatively regulate autophagy during infection but not basal autophagy

Confocal images of MDMs infected with CFP *M. avium* for 24 hours after treatment with (A) AllStars siRNA as a negative control, (B) MDMs infected with CFP *M. avium* for 24 hours after siRNA knockdown of Keap1. The cells were imaged using Zeiss LSM 510 with scan zoom of 0.7 and scale bar=10µm. The LC3 II punctate are represented by green dots, CFP *M. avium* by red dots and nuclei were stained with DRAQ5 (complete set of images in appendix XIV). Graphical representation of LC3 II dots counts when (C) human primary macrophages were transfected with Keap1 siRNA and AllStars siRNA as non-target negative control, followed by infection with CFP-*M .avium* infection for 4 hours, 24 hours and 72 hours. After each time point of infection, incubation with 100 nM bafilomycin A1 for 2 hours was proceeded. (D) MDMs transfected with AllStars and Keap1 siRNA and autophagy measured at 4, 24 and 72 hours without infection. (E) The knockdown efficiency of Keap1 at the each time point. The data are represented as mean ± SEM, data are representative of at least three independent experiments and p-value of <0.05 are considered significance.

4.12 Keap1 knockdown in human macrophage decreases the survival of *M. avium*

The autophagy pathway is known to enhance the killing of bacterial pathogens. As our study showed that Keap1 might negatively autophagy pathway, so we tried to investigate whether such regulation might have any effect on the survival of *M. avium* in primary human macrophages. For this purpose, Keap1 proteins were knocked down in macrophages prior to *M. avium* infection. The survival of *M. avium* during infection was determined via measuring luciferase activity over 72 hours of infection. The luciferase assay showed equal number of bacteria after 4 hours of post infection indicating equal intake of bacteria during earlier infection whereas 24 hours post infection in keap1 knockdown macrophage showed slight lower number of bacterial count as compared to non-targeted siRNA treated cells (figure 4.12.1). The luciferase assay measured after 72 hours infection showed significant decreased number of bacterial in Keap1 knockdown macrophages indicating Keap1 knockdown decreases survival of *M. avium*. The luciferase survival assay was performed by Jane A. Awuh and Ngoc Phuc C. Do.

Our results indicate that knockdown of Keap1 increases the level of autophagy and increased level of autophagy seems to decrease the survival of *M. avium* in macrophages.

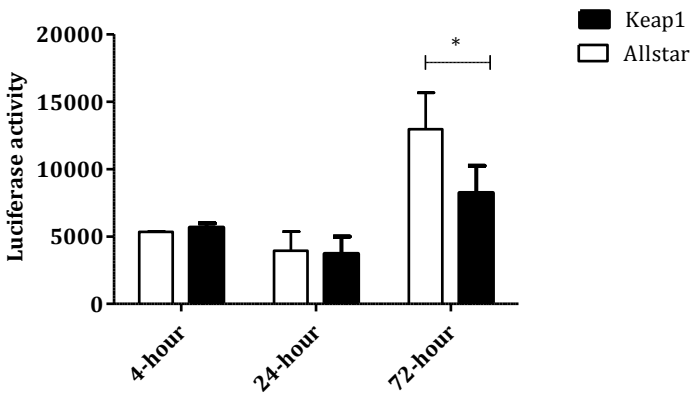

Figure 4.12.1. Keap1 knockdown decreases mycobacterial survival

MDMs were either pretreated with Keap1 siRNA or AllStars followed by infection with firefly luciferase expressing *M. avium* over a period of 72 hours. The luciferase activity was measured at 4, 24 and 72 hours time point. The data are represented as mean ± SEM, data are representative of at least three independent experiments and p-value of <0.05 are considered significance.

5 Discussion

Mycobacterium species are potent intracellular bacteria which evades host immune defense mainly by arresting phagosomal maturation and persisting inside host cells[94]. To counteract such bacterial immune evasion strategy, host immune system has evolved defense mechanisms like autophagy. The activation of autophagy results in increased maturation of phagosomes and overcome mycobacterial induced phagolysosomes biogenesis block[93].

Understanding autophagy during mycobacterial infection helps us to understand the molecular basis of host defense against mycobacteria. So, in order to study the autophagy, we first established the method for monitoring the autophagy in primary human macrophages and later on, in HEK293 cell lines. The immunofluorescence assay for quantification of endogenous LC3 II proteins as punctate counts was established. Besides, endogenous LC3 II quantification, there are methods that quantify exogenous LC3 II such as measurement of GFP-LC3 after stable or transient transfection of fusion gene. There are advantages of quantifying endogenous LC3 proteins over GFP-LC3 as it avoid the need of transfection or generation of transgenic organism and also avoid artifact resulting from overexpression of such transfected gene[79]. The establishment of method for monitoring autophagy in primary human macrophages adds more significance as it is the primary host for mycobacterium.

After the establishment of method for quantification of autophagy, the main aim of the study was to answer whether *M. avium* induces autophagy in primary human macrophages. In our study, *M. avium* infection of macrophages showed significant increase in level of autophagy indicated by increase in number of LC3 II punctate counts. The induction of

autophagy was found to be constantly maintained throughout the period of infection. A study has shown similar increase in level of autophagy when human primary macrophages were infected with *M. tuberculosis*[93]. Another study in RAW 264.7 macrophages also showed increased level of autophagy when it is infected with *M. marinum*[61] *or M. tuberculosis*[62]. Our study shows for the first time, induction of autophagy by *M. avium*. The major difference with respect to other studies is the requirement of ESX-1 system to elicit autophagy as *M. avium* strains 104 used in our study does not have such secretory system[95].

Furthermore, in addition to association of LC3 II to autophagy, LC3 II is also found to be associated with membrane of non-autophagic structure. A study has shown that LC3 are recruited to bacteria containing phagosomes and process being referred as LAP[60]. In our study we quantified the level of autophagy in presence of inhibitors of autophagolysosomal fusion and it represent the measurement of degradation of LC3 II embedded in inner membrane of autophagosomes. In LAP, LC3 II are embedded only on the outer membrane of single membrane structure which are later on eventually released to cytosol via cleavage of PE from LC3 II by Atg4 protein[78]. So, in LAP there is no degradation of LC3 II. In addition to this, induction of autophagy during *M. avium* infection was reduced in the presence of autophagy inhibitor 3MA indicating further that process measured is autophagy.

It is better to use two different methods for answering the biological question. So, we established and optimized a HEK293 reporter cell system to quantify the autophagic flux. The reporter cell system was able to determine level of autophagy in both amino acid starvation induced autophagy as well as basal autophagy as mentioned in previous study[80]. In

our study, p62 adaptor protein for monitoring autophagy have been cautiously used as p62 are known to modulate Nrf2 anti-oxidant pathway through Keap1 and influences its own endogenous expression via Nrf2[76].

In contrast to primary human macrophages, infection of HEK293 cell lines with *M. avium* did not induce autophagy. So, we tried to elucidate the difference in autophagy between these cells. The HEK293 reporter cell lines measures the degradation of GFP-p62 whereas immunofluorescence assay determine the level of endogenous LC3 II protein as punctate. The differences in method were compared with quantification of endogenous LC3 II protein in HEK293 cells which also showed no induction of autophagy when infected with *M. avium*. These results shifted to focus on other difference between HEK293 cells and primary human macrophage. HEK293 cells lack several TLRs such as TLR2 and TLR9 known to recognize mycobacterium and expression of such TLRs in HEK293 was implemented to answer the difference. The HEK293 cells expressing functional TLR2 and TLR9 also failed to induce autophagy when infected with *M. avium* as well as when stimulated with its respective ligands. The results indicates that *M. avium* do not induce autophagy in HEK293 cells system.

To elucidate the mechanism of induction of autophagy in primary human macrophages during *M. avium* infection different TLRs and non-TLRs that are known to induce autophagy in other studies were evaluated.

Our study showed that induction of autophagy in macrophages during *M. avium* infection was mediated via TLR2. The stimulation of macrophages with lipomannan showed increased level of autophagy and such increased level of autophagy were reduced in presence of TLR2 neutralizing antibody. Furthermore, siRNA knockdown of TLR2 also resulted in

reduction of autophagy during *M. avium* infection. Our results are in perfect agreement with a study showing the induction of autophagy in human macrophages when stimulated with mycobacterium lipoprotein LpqH, a known TLR2 ligand. However, a study in RAW 264.7 macrophages did not induce autophagy when stimulated with TLR2 ligands such as Pam_3CSK_4 and Pam_2CSK_4[59]. None of these studies investigated infection with live mycobacterial infection.

Our results showed that TLR9 does not involve in the induction of autophagy during *M. avium* infection. As siRNA knockdown of TLR9 showed no reduction in level of autophagy as well as stimulation with TLR9 ligand CpG ODN also failed to induce autophagy. Similar, results were published in a study showing no induction of autophagy when RAW 264.7 macrophages were stimulated with CpG ODN.

The mandatory requirement of certain virulence factors has been suggested for the induction of autophagy during mycobacterium infection. One of such virulence factors being ESX-1 system that is primarily present in *M. tuberculosis, M. marinum and M smegmatis* species[95]. In our study, we used *M. avium* strains 104 which do not contain such secretory system but it does contain other secretory system such as ESX-2, ESX-3, ESX-4, and ESX-5[95]. The ESAT6 secretory protein produced by ESX-1 secretory system have been shown to be essential for the permeabilization of phagosomes and thereby recognition of escaped microbes by cytosolic DNA sensing pathway[62]. These pathways were found to be associated with the induction of autophagy. Such pathways are dependent upon an adaptor protein called STING[62]. In our study, we used *M. avium* for the infection assay and it is not known whether *M. avium* or its DNA escape from phagosomes and enter to cytosol by using other secretory system that it

possess. To rule out any role of STING in the *M. avium* induced autophagy, we knockdown the STING adaptor proteins with siRNA technique. Macrophages with and without STING knockdown showed no difference in the level of autophagy during *M. avium* infection indicating no role of STING in the *M. avium* induced autophagy. Moreover, our study support previous studies about the role of STING to elicit autophagy on stimulation of macrophages with cyclic-di-GMP indicating STING do induce autophagy but not in *M. avium* induced autophagy[62].

The studies have shown Keap1 facilitates removal of ubiquitinated protein via autophagy by interacting with p62[71]. In addition to this, our research group found that Keap1 and LC3 II are recruited and associated with *M. avium* phagosomes (Jane A. Awuh, unpublished). The Keap1 knockdown macrophages showed significance increase level of autophagy when infected with *M. avium*. The concurrent study in our research group, Keap1 knockdown macrophages also showed increased level of TBK1 during *M avium* infection (Jane A. Awuh, unpublished) indicating Keap1 might negatively regulate the level of TBK1. Recently, TBK1 have been associated with phosphorylation of autophagic adaptor protein p62 at UBA domain site enhancing binding to polyubiquitin chain present in substrate cargo and thereby positively regulating the autophagy pathway[62]. So, Keap1 might negatively regulate autophagy via TBK1 pathway. In contrast to negative regulation of autophagy during infection, Keap1 was found to have no regulatory effect on the basal autophagy. Such contrasting result might be due to very low level of basal autophagy.

In this study, Keap1 knockdown was associated with an increased level of autophagy during *M. avium* infection. In addition to this up regulation of autophagy, a parallel study in our research group showed that Keap1

knockdown were also associated with increased inflammatory cytokines production. Such dual mechanism of Keap1 for increasing inflammatory cytokines production and up regulation of autophagy might resulted in decreased survival of *M. avium* in human macrophages as shown by our study from *M. avium* luciferase survival assay. Besides this study, other study also shows that autophagy is associated with increased anti-mycobacterial activity and anti-inflammatory to subsidized the damaged from increased inflammation.[96]

6 Conclusion and future perspectives

Little is known about the induction and regulation of autophagy during infection with *M. avium.* In this study we aimed to establish method for quantification of autophagy to monitor autophagy and its regulatory mechanism during *M. avium* infection. In present study, we found that *M. avium* induces autophagy in primary human macrophages but failed to do so in HEK293 cell lines. The induction of autophagy in macrophages during *M. avium* infection might be mediated via TLR2. The oxidative and electrophilic sensor, Keap1 might negatively regulate *M. avium* induced autophagy and thereby results in decrease bacterial survival.

The study related to TLR2 mediated autophagy induction during *M. avium* infection needs to be further investigated and verified. The method used in this study is based on quantification of endogenous LC3 II via confocal microscopy. The confirmation of study with other autophagy quantification methods might further contribute to better understanding about the regulations of autophagy during *M. avium* infection.

7 References

1. Davis JM, Ramakrishnan L. The Role of the Granuloma in Expansion and Dissemination of Early Tuberculous Infection. *Cell* 2009, **136**(1)**:** 37-49.

2. Ernst JD. Macrophage Receptors for Mycobacterium tuberculosis. *Infection and Immunity* 1998, **66**(4)**:** 1277-1281.

3. Russell DG. Who puts the tubercle in tuberculosis? *Nat Rev Micro* 2007, **5**(1)**:** 39-47.

4. Cole S, Brosch R, Parkhill J, Garnier T, Churcher C, Harris D, *et al.* Deciphering the biology of Mycobacterium tuberculosis from the complete genome sequence. *Nature* 1998, **393:** 537 - 544.

5. Means TK, Wang S, Lien E, Yoshimura A, Golenbock DT, Fenton MJ. Human toll-like receptors mediate cellular activation by Mycobacterium tuberculosis. *Journal of immunology (Baltimore, Md : 1950)* 1999, **163**(7)**:** 3920-3927.

6. Bulut Y, Michelsen KS, Hayrapetian L, Naiki Y, Spallek R, Singh M, *et al.* Mycobacterium tuberculosis heat shock proteins use diverse Toll-like receptor pathways to activate pro-inflammatory signals. *The Journal of biological chemistry* 2005, **280**(22)**:** 20961-20967.

7. Bafica A, Scanga CA, Feng CG, Leifer C, Cheever A, Sher A. TLR9 regulates Th1 responses and cooperates with TLR2 in mediating optimal resistance to Mycobacterium tuberculosis. *The Journal of experimental medicine* 2005, **202**(12)**:** 1715-1724.

8. Means TK, Jones BW, Schromm AB, Shurtleff BA, Smith JA, Keane J, *et al.* Differential effects of a Toll-like receptor antagonist on Mycobacterium tuberculosis-induced macrophage responses. *Journal of immunology (Baltimore, Md : 1950)* 2001, **166**(6)**:** 4074-4082.

9. Davila S, Hibberd ML, Hari Dass R, Wong HEE, Sahiratmadja E, Bonnard C, *et al.* Genetic Association and Expression Studies Indicate a Role of Toll-Like Receptor 8 in Pulmonary Tuberculosis. *PLoS Genet* 2008, **4**(10)**:** e1000218.

10. Kleinnijenhuis J, Oosting M, Joosten LA, Netea MG, Van Crevel R. Innate immune recognition of Mycobacterium tuberculosis. *Clinical & developmental immunology* 2011, **2011:** 405310.

11. Akira S, Takeda K. Toll-like receptor signalling. *Nat Rev Immunol* 2004, **4**(7)**:** 499-511.

12. Ryffel B, Fremond C, Jacobs M, Parida S, Botha T, Schnyder B, *et al.* Innate immunity to mycobacterial infection in mice: Critical role for toll-like receptors. *Tuberculosis* 2005, **85**(5–6)**:** 395-405.

13. Wards B, de Lisle G, Collins D. An esat6 knockout mutant of Mycobacterium bovis produced by homologous recombination will contribute to the development of a live tuberculosis vaccine. *Tuber Lung Dis* 2000, **80:** 185 - 189.

14. Drennan MB, Nicolle D, Quesniaux VJ, Jacobs M, Allie N, Mpagi J, *et al.* Toll-like receptor 2-deficient mice succumb to Mycobacterium tuberculosis infection. *The American journal of pathology* 2004, **164**(1)**:** 49-57.

15. Mahairas G, Sabo P, Hickey M, Singh D, Stover C. Molecular analysis of genetic differences between Mycobacterium bovis BCG and virulent M. bovis. *J Bacteriol* 1996, **178:** 1274 - 1282.

16. Philipp W, Nair S, Guglielmi G, Lagranderie M, Gicquel B, Cole S. Physical mapping of Mycobacterium bovis BCG pasteur reveals differences from the genome map of Mycobacterium tuberculosis H37Rv and from M. bovis. *Microbiology* 1996, **142:** 3135 - 3145.

17. Yamamoto M, Sato S, Hemmi H, Hoshino K, Kaisho T, Sanjo H, *et al.* Role of Adaptor TRIF in the MyD88-Independent Toll-Like Receptor Signaling Pathway. *Science* 2003, **301**(5633)**:** 640-643.

18. Jo EK. Mycobacterial interaction with innate receptors: TLRs, C-type lectins, and NLRs. *Current opinion in infectious diseases* 2008, **21**(3)**:** 279-286.

19. Fratti RA, Backer JM, Gruenberg J, Corvera S, Deretic V. Role of phosphatidylinositol 3-kinase and Rab5 effectors in phagosomal

biogenesis and mycobacterial phagosome maturation arrest. *The Journal of cell biology* 2001, **154**(3)**:** 631-644.

20. Brosch R, Gordon S, Billault A, Garnier T, Eiglmeier K, Soravito C, *et al.* Use of a Mycobacterium tuberculosis H37Rv bacterial artificial chromosome library for genome mapping, sequencing, and comparative genomics. *Infect Immun* 1998, **66:** 2221 - 2229.

21. Takaoka A, Wang Z, Choi MK, Yanai H, Negishi H, Ban T, *et al.* DAI (DLM-1/ZBP1) is a cytosolic DNA sensor and an activator of innate immune response. *Nature* 2007, **448**(7152)**:** 501-505.

22. Brosch R, Philipp W, Stavropoulos E, Colston M, Cole S, Gordon S. Genomic analysis reveals variation between Mycobacterium tuberculosis H37Rv and the attenuated M. tuberculosis H37Ra strain. *Infect Immun* 1999, **67:** 5768 - 5774.

23. Gordon S, Brosch R, Billault A, Garnier T, Eiglmeier K, Cole S. Identification of variable regions in the genomes of tubercle bacilli using bacterial artificial chromosome arrays. *Mol Microbiol* 1999, **32:** 643 - 655.

24. Brosch R, Gordon S, Buchrieser C, Pym A, Garnier T, Cole S. Comparative genomics uncovers large tandem chromosomal duplications in Mycobacterium bovis BCG Pasteur. *Yeast* 2000, **17:** 111 - 123.

25. Behr M, Wilson M, Gill W, Salamon H, Schoolnik G, Rane S, *et al.* Comparative genomics of BCG vaccines by whole-genome DNA microarray. *Science* 1999, **284:** 1520 - 1523.

26. Unterholzner L, Keating SE, Baran M, Horan KA, Jensen SB, Sharma S, *et al.* IFI16 is an innate immune sensor for intracellular DNA. *Nat Immunol* 2010, **11**(11)**:** 997-1004.

27. Ishikawa H, Ma Z, Barber GN. STING regulates intracellular DNA-mediated, type I interferon-dependent innate immunity. *Nature* 2009, **461**(7265)**:** 788-792.

28. Burdette DL, Monroe KM, Sotelo-Troha K, Iwig JS, Eckert B, Hyodo M, *et al.* STING is a direct innate immune sensor of cyclic di-GMP. *Nature* 2011, **478**(7370)**:** 515-518.

29. Zumarraga M, Bigi F, Alito A, Romano M, Cataldi A. A 12.7 kb fragment of the Mycobacterium tuberculosis genome is not present in Mycobacterium bovis. *Microbiology* 1999, **145:** 893 - 897.

30. Manzanillo PS, Shiloh MU, Portnoy DA, Cox JS. Mycobacterium tuberculosis activates the DNA-dependent cytosolic surveillance pathway within macrophages. *Cell host & microbe* 2012, **11**(5)**:** 469-480.

31. McCaffrey RL, Fawcett P, O'Riordan M, Lee KD, Havell EA, Brown PO, *et al.* A specific gene expression program triggered by Gram-positive bacteria in the cytosol. *Proceedings of the National Academy of Sciences of the United States of America* 2004, **101**(31)**:** 11386-11391.

32. Nigou J, Zelle-Rieser C, Gilleron M, Thurnher M, Puzo G. Mannosylated lipoarabinomannans inhibit IL-12 production by human dendritic cells: evidence for a negative signal delivered through the mannose receptor. *Journal of immunology (Baltimore, Md : 1950)* 2001, **166**(12)**:** 7477-7485.

33. Chamaillard M, Hashimoto M, Horie Y, Masumoto J, Qiu S, Saab L, *et al.* An essential role for NOD1 in host recognition of bacterial peptidoglycan containing diaminopimelic acid. *Nat Immunol* 2003, **4**(7)**:** 702-707.

34. Geijtenbeek TB, Krooshoop DJ, Bleijs DA, van Vliet SJ, van Duijnhoven GC, Grabovsky V, *et al.* DC-SIGN-ICAM-2 interaction mediates dendritic cell trafficking. *Nat Immunol* 2000, **1**(4)**:** 353-357.

35. Barreiro LB, Neyrolles O, Babb CL, Tailleux L, Quach H, McElreavey K, *et al.* Promoter Variation in the DC-SIGN–Encoding Gene CD209 is Associated with Tuberculosis. *PLoS Med* 2006, **3**(2)**:** e20.

36. Herre J, Gordon S, Brown GD. Dectin-1 and its role in the recognition of beta-glucans by macrophages. *Molecular immunology* 2004, **40**(12)**:** 869-876.

37. Brown GD, Herre J, Williams DL, Willment JA, Marshall AS, Gordon S. Dectin-1 mediates the biological effects of beta-glucans. *The Journal of experimental medicine* 2003, **197**(9)**:** 1119-1124.

38. Ma J, Becker C, Lowell CA, Underhill DM. Dectin-1-triggered recruitment of light chain 3 protein to phagosomes facilitates major histocompatibility complex class II presentation of fungal-derived antigens. *The Journal of biological chemistry* 2012, **287**(41)**:** 34149-34156.

39. Yadav M, Schorey JS. The beta-glucan receptor dectin-1 functions together with TLR2 to mediate macrophage activation by mycobacteria. *Blood* 2006, **108**(9)**:** 3168-3175.

40. Proell M, Riedl SJ, Fritz JH, Rojas AM, Schwarzenbacher R. The Nod-like receptor (NLR) family: a tale of similarities and differences. *PloS one* 2008, **3**(4)**:** e2119.

41. Gandotra S, Jang S, Murray PJ, Salgame P, Ehrt S. Nucleotide-binding oligomerization domain protein 2-deficient mice control infection with Mycobacterium tuberculosis. *Infect Immun* 2007, **75**(11)**:** 5127-5134.

42. Mizushima N, Yoshimori T, Levine B. Methods in mammalian autophagy research. *Cell* 2010, **140**(3)**:** 313-326.

43. Mizushima N. The pleiotropic role of autophagy: from protein metabolism to bactericide. *Cell death and differentiation* 2005, **12 Suppl 2:** 1535-1541.

44. Cantley LC. The phosphoinositide 3-kinase pathway. *Science* 2002, **296**(5573)**:** 1655-1657.

45. Seglen PO, Gordon PB. Amino acid control of autophagic sequestration and protein degradation in isolated rat hepatocytes. *The Journal of cell biology* 1984, **99**(2)**:** 435-444.

46. Kim DH, Sarbassov DD, Ali SM, King JE, Latek RR, Erdjument-Bromage H, *et al.* mTOR interacts with raptor to form a nutrient-sensitive complex that signals to the cell growth machinery. *Cell* 2002, **110**(2)**:** 163-175.

47. Mizushima N. The role of the Atg1/ULK1 complex in autophagy regulation. *Current opinion in cell biology* 2010, **22**(2)**:** 132-139.

48. Itakura E, Mizushima N. Characterization of autophagosome formation site by a hierarchical analysis of mammalian Atg proteins. *Autophagy* 2010, **6**(6)**:** 764-776.

49. Seglen PO, Gordon PB. 3-Methyladenine: specific inhibitor of autophagic/lysosomal protein degradation in isolated rat hepatocytes. *Proceedings of the National Academy of Sciences of the United States of America* 1982, **79**(6)**:** 1889-1892.

50. Blommaart EF, Krause U, Schellens JP, Vreeling-Sindelarova H, Meijer AJ. The phosphatidylinositol 3-kinase inhibitors wortmannin and LY294002 inhibit autophagy in isolated rat hepatocytes. *European journal of biochemistry / FEBS* 1997, **243**(1-2)**:** 240-246.

51. Axe EL, Walker SA, Manifava M, Chandra P, Roderick HL, Habermann A, *et al.* Autophagosome formation from membrane compartments enriched in phosphatidylinositol 3-phosphate and dynamically connected to the endoplasmic reticulum. *The Journal of cell biology* 2008, **182**(4)**:** 685-701.

52. Reggiori F, Komatsu M, Finley K, Simonsen A. Selective types of autophagy. *International journal of cell biology* 2012, **2012:** 156272.

53. Andersen P, Andersen A, Sorensen A, Nagai S. Recall of long-lived immunity to Mycobacterium tuberculosis infection in mice. *Journal of immunology (Baltimore, Md : 1950)* 1995, **154:** 3359 - 3372.

54. Klionsky DJ, Cuervo AM, Dunn WA, Jr., Levine B, van der Klei I, Seglen PO. How shall I eat thee? *Autophagy* 2007, **3**(5)**:** 413-416.

55. Zheng YT, Shahnazari S, Brech A, Lamark T, Johansen T, Brumell JH. The adaptor protein p62/SQSTM1 targets invading bacteria to the autophagy pathway. *Journal of immunology (Baltimore, Md : 1950)* 2009, **183**(9)**:** 5909-5916.

56. Shi C-S, Kehrl JH. TRAF6 and A20 Regulate Lysine 63-Linked Ubiquitination of Beclin-1 to Control TLR4-Induced Autophagy. *Science Signaling* 2010, **3**(123)**:** ra42.

57. Shin DM, Yuk JM, Lee HM, Lee SH, Son JW, Harding CV, *et al.* Mycobacterial lipoprotein activates autophagy via TLR2/1/CD14 and a functional vitamin D receptor signalling. *Cellular microbiology* 2010, **12**(11)**:** 1648-1665.

58. Xu Y, Jagannath C, Liu X-D, Sharafkhaneh A, Kolodziejska KE, Eissa NT. Toll-like Receptor 4 Is a Sensor for Autophagy Associated with Innate Immunity. *Immunity* 2007, **27**(1)**:** 135-144.

59. Delgado MA, Elmaoued RA, Davis AS, Kyei G, Deretic V. Toll-like receptors control autophagy. *The EMBO journal* 2008, **27**(7)**:** 1110-1121.

60. Sanjuan MA, Dillon CP, Tait SW, Moshiach S, Dorsey F, Connell S, *et al.* Toll-like receptor signalling in macrophages links the autophagy pathway to phagocytosis. *Nature* 2007, **450**(7173)**:** 1253-1257.

61. Lerena MC, Colombo MI. Mycobacterium marinum induces a marked LC3 recruitment to its containing phagosome that depends on a functional ESX-1 secretion system. *Cellular microbiology* 2011, **13**(6)**:** 814-835.

62. Watson RO, Manzanillo PS, Cox JS. Extracellular M. tuberculosis DNA targets bacteria for autophagy by activating the host DNA-sensing pathway. *Cell* 2012, **150**(4)**:** 803-815.

63. Travassos LH, Carneiro LAM, Ramjeet M, Hussey S, Kim Y-G, Magalhaes JG, *et al.* Nod1 and Nod2 direct autophagy by recruiting ATG16L1 to the plasma membrane at the site of bacterial entry. *Nat Immunol* 2010, **11**(1)**:** 55-62.

64. Shin D-M, Jeon B-Y, Lee H-M, Jin HS, Yuk J-M, Song C-H, *et al.* Mycobacterium tuberculosis Eis Regulates Autophagy, Inflammation, and Cell Death through Redox-dependent Signaling. *PLoS Pathog* 2010, **6**(12)**:** e1001230.

65. Kim JJ, Lee HM, Shin DM, Kim W, Yuk JM, Jin HS, *et al.* Host cell autophagy activated by antibiotics is required for their effective antimycobacterial drug action. *Cell host & microbe* 2012, **11**(5)**:** 457-468.

66. Jagannath C, Bakhru P. Rapamycin-induced enhancement of vaccine efficacy in mice. *Methods in molecular biology (Clifton, NJ)* 2012, **821:** 295-303.

67. Early J, Fischer K, Bermudez LE. Mycobacterium avium uses apoptotic macrophages as tools for spreading. *Microbial pathogenesis* 2011, **50**(2)**:** 132-139.

68. de Chastellier C, Thilo L. Cholesterol depletion in Mycobacterium avium-infected macrophages overcomes the block in phagosome maturation and leads to the reversible sequestration of viable mycobacteria in phagolysosome-derived autophagic vacuoles. *Cellular microbiology* 2006, **8**(2)**:** 242-256.

69. Taguchi K, Motohashi H, Yamamoto M. Molecular mechanisms of the Keap1-Nrf2 pathway in stress response and cancer evolution. *Genes to cells : devoted to molecular & cellular mechanisms* 2011, **16**(2)**:** 123-140.

70. Carvalho NB, Oliveira FS, Duraes FV, de Almeida LA, Florido M, Prata LO, *et al.* Toll-like receptor 9 is required for full host resistance to Mycobacterium avium infection but plays no role in induction of Th1 responses. *Infect Immun* 2011, **79**(4)**:** 1638-1646.

71. Fan W, Tang Z, Chen D, Moughon D, Ding X, Chen S, *et al.* Keap1 facilitates p62-mediated ubiquitin aggregate clearance via autophagy. *Autophagy* 2010, **6**(5)**:** 614-621.

72. Komatsu M, Kurokawa H, Waguri S, Taguchi K, Kobayashi A, Ichimura Y, *et al.* The selective autophagy substrate p62 activates the stress responsive transcription factor Nrf2 through inactivation of Keap1. *Nature cell biology* 2010, **12**(3)**:** 213-223.

73. Kobayashi M, Yamamoto M. Molecular mechanisms activating the Nrf2-Keap1 pathway of antioxidant gene regulation. *Antioxidants & redox signaling* 2005, **7**(3-4)**:** 385-394.

74. Kobayashi A, Kang MI, Watai Y, Tong KI, Shibata T, Uchida K, *et al.* Oxidative and electrophilic stresses activate Nrf2 through inhibition of ubiquitination activity of Keap1. *Molecular and cellular biology* 2006, **26**(1)**:** 221-229.

75. Itoh K, Chiba T, Takahashi S, Ishii T, Igarashi K, Katoh Y, *et al.* An Nrf2/small Maf heterodimer mediates the induction of phase II detoxifying enzyme genes through antioxidant response elements. *Biochemical and biophysical research communications* 1997, **236**(2)**:** 313-322.

76. Jain A, Lamark T, Sjottem E, Larsen KB, Awuh JA, Overvatn A, *et al.* p62/SQSTM1 is a target gene for transcription factor NRF2 and creates a positive feedback loop by inducing antioxidant response element-driven gene transcription. *The Journal of biological chemistry* 2010, **285**(29)**:** 22576-22591.

77. Puissant A, Fenouille N, Auberger P. When autophagy meets cancer through p62/SQSTM1. *American journal of cancer research* 2012, **2**(4)**:** 397-413.

78. Yang Z, Klionsky DJ. Mammalian autophagy: core molecular machinery and signaling regulation. *Current opinion in cell biology* 2010, **22**(2)**:** 124-131.

79. Klionsky DJ, Abdalla FC, Abeliovich H, Abraham RT, Acevedo-Arozena A, Adeli K, *et al.* Guidelines for the use and interpretation of assays for monitoring autophagy. *Autophagy* 2012, **8**(4)**:** 445-544.

80. Larsen KB, Lamark T, Overvatn A, Harneshaug I, Johansen T, Bjorkoy G. A reporter cell system to monitor autophagy based on p62/SQSTM1. *Autophagy* 2010, **6**(6)**:** 784-793.

81. Farkas T, Høyer-Hansen M, Jäättelä M. Identification of novel autophagy regulators by a luciferase-based assay for the kinetics of autophagic flux. *Autophagy* 2009, **5**(7)**:** 1018-1025.

82. Shvets E, Fass E, Elazar Z. Utilizing flow cytometry to monitor autophagy in living mammalian cells. *Autophagy* 2008, **4**(5)**:** 621-628.

83. Recillas-Targa F. Multiple strategies for gene transfer, expression, knockdown, and chromatin influence in mammalian cell lines and transgenic animals. *Molecular biotechnology* 2006, **34**(3)**:** 337-354.

84. Pfeifer A, Verma IM. Gene therapy: promises and problems. *Annual review of genomics and human genetics* 2001, **2:** 177-211.

85. Schenborn E, Goiffon V. DEAE-Dextran Transfection of Mammalian Cultured Cells. In: Tymms M (ed). *Transcription Factor Protocols*, vol. 130. Humana Press, 2000, pp 147-153.

86. Holmen SL, Vanbrocklin MW, Eversole RR, Stapleton SR, Ginsberg LC. Efficient lipid-mediated transfection of DNA into primary rat hepatocytes. *In vitro cellular & developmental biology Animal* 1995, **31**(5)**:** 347-351.

87. Mehier-Humbert S, Guy RH. Physical methods for gene transfer: improving the kinetics of gene delivery into cells. *Advanced drug delivery reviews* 2005, **57**(5)**:** 733-753.

88. Hammond SM. Dicing and slicing: The core machinery of the RNA interference pathway. *FEBS Letters* 2005, **579**(26)**:** 5822-5829.

89. Felgner PL, Gadek TR, Holm M, Roman R, Chan HW, Wenz M, *et al.* Lipofection: a highly efficient, lipid-mediated DNA-transfection procedure. *Proceedings of the National Academy of Sciences of the United States of America* 1987, **84**(21)**:** 7413-7417.

90. Arya M, Shergill IS, Williamson M, Gommersall L, Arya N, Patel HR. Basic principles of real-time quantitative PCR. *Expert review of molecular diagnostics* 2005, **5**(2)**:** 209-219.

91. Halaas Ø, Steigedal M, Haug M, Awuh JA, Ryan L, Brech A, *et al.* Intracellular Mycobacterium avium intersect transferrin in the Rab11(+) recycling endocytic pathway and avoid lipocalin 2 trafficking to the lysosomal pathway. *The Journal of infectious diseases* 2010, **201**(5)**:** 783-792.

92. Flo TH, Halaas Ø, Lien E, Ryan L, Teti G, Golenbock DT, *et al.* Human toll-like receptor 2 mediates monocyte activation by Listeria monocytogenes, but not by group B streptococci or

lipopolysaccharide. *Journal of immunology (Baltimore, Md : 1950)* 2000, **164**(4)**:** 2064-2069.

93. Petruccioli E, Romagnoli A, Corazzari M, Coccia EM, Butera O, Delogu G, *et al.* Specific T cells restore the autophagic flux inhibited by Mycobacterium tuberculosis in human primary macrophages. *The Journal of infectious diseases* 2012, **205**(9)**:** 1425-1435.

94. Gutierrez MG, Master SS, Singh SB, Taylor GA, Colombo MI, Deretic V. Autophagy is a defense mechanism inhibiting BCG and Mycobacterium tuberculosis survival in infected macrophages. *Cell* 2004, **119**(6)**:** 753-766.

95. Gey van Pittius N, Gamieldien J, Hide W, Brown G, Siezen R, Beyers A. The ESAT-6 gene cluster of Mycobacterium tuberculosis and other high G+C Gram-positive bacteria. *Genome Biology* 2001, **2**(10)**:** research0044.0041 - research0044.0018.

96. Castillo EF, Dekonenko A, Arko-Mensah J, Mandell MA, Dupont N, Jiang S, *et al.* Autophagy protects against active tuberculosis by suppressing bacterial burden and inflammation. *Proceedings of the National Academy of Sciences of the United States of America* 2012, **109**(46)**:** E3168-3176.

8 Appendices

Appendix I: siRNA sequences

a. Keap1 siRNA sequence

Name	Catalog no.	Sequence
Hs_KEAP1_2	SI00451675	CCGGGAGTACATCTACATGCA
Hs_KEAP1_5	SI03246439	CCAGGATGCCTCAGTGTTAAA
Hs_KEAP1_6	SI04155424	CAGCTGTCACCATGTGATTTA
Hs_KEAP1_7	SI04267886	CTCCAGCGCCCTGGACTGTTA

b. TLR2 siRNA sequence

Name	Catalog no.	Sequence
Hs_TLR2_1	SI00050051	CTGGGCAGTCTTGAACATTTA
Hs_ TLR2_2	SI00050022	CAGGTAAAGTGGAAACGTTAA
Hs_ TLR2_3	SI00050029	AACATTTAGACTTATCCTATA
Hs_ TLR2_4	SI00050036	CCGCAACTCAAAGAACTTTAT

c. TLR9 siRNA sequence

Name	Catalog no.	Sequence
Hs_TLR9_1	SI00118279	CGGCAACTGTTATTACAAGAA
Hs_ TLR9_5	SI02642612	CACTCAATAAATGCTACCGAA
Hs_ TLR9_7	SI03108504	TACCAACATCCTGATGCTAGA
Hs_ TLR9_8	SI03118612	TGCCTTCGTGGTCTTCGACAA

d. STING siRNA sequence

Name	Catalog no.	Sequence
Hs_TMEM_1	SI04132170	CCGGGAGTACATCTACATGCA
Hs_ TMEM_2	SI04263189	ATGGGCTGGCATGGTCATATT
Hs_ TMEM_3	SI04287626	CAACATTCGCTTCCTGGATAA
Hs_ TMEM_4	SI04357696	CCGGATTCGAACTTACAATCA

Appendix II: DuoSet ELISA development kits

a. Human TNFα DuoSet ELISA development kits

Capture antibody concentration: 720 µg/ml of mouse anti-human TNF-α reconstituted in PBS. The stock concentration diluted to working concentration of 4 µg/ml in PBS.

Detection antibody concentration: 90 µg/ml of biotinylated goat anti-human TNF-α reconstituted in PBS. The stock concentration diluted to 500 ng/ml of working concentration in reagent diluent.

Standard concentration: 370 ng/ml of recombinant human TNF-α reconstituted in reagent diluent. The stock concentration diluted to working concentration of 1000 pg/ml.

Streptavidin-HRP: 1 ml of streptavidin conjugated to horseradish-peroxidase. The working concentration of 1:200 dilution prepared in reagent diluent.

Substrate solution: 1:1 mixture of substrate reagent A (H_2O_2) substrate B (tetramethylbenzidine) prepared before addition to plate.

b. Human IP-10 DuoSet ELISA development Kits

Capture antibody concentration: 360 µg/ml of mouse anti-human IP-10 reconstituted in PBS. The stock concentration diluted to working concentration of 2 µg/ml in PBS.

Detection antibody concentration: 9 µg/ml of biotinylated goat anti-human IP-10 reconstituted in PBS. The stock concentration diluted to working concentration of 50 ng/ml in reagent diluent.

Standard concentration: 90 ng/ml of recombinant human IP-10 reconstituted in reagent diluent. The stock concentration diluted to working concentration of 2000 pg/ml in reagent diluent.

Streptavidin-HRP: 1 ml of streptavidin conjugated to horseradish-peroxidase. The working concentration of 1:200 dilution prepared in reagent diluent.

Substrate solution: 1:1 mixture of substrate reagent A (H_2O_2) substrate B (tetramethylbenzidine) prepared before addition to plate.

Appendix III: Optimization of immunofluorescence assay for LC3 II

a. Indirect staining method:

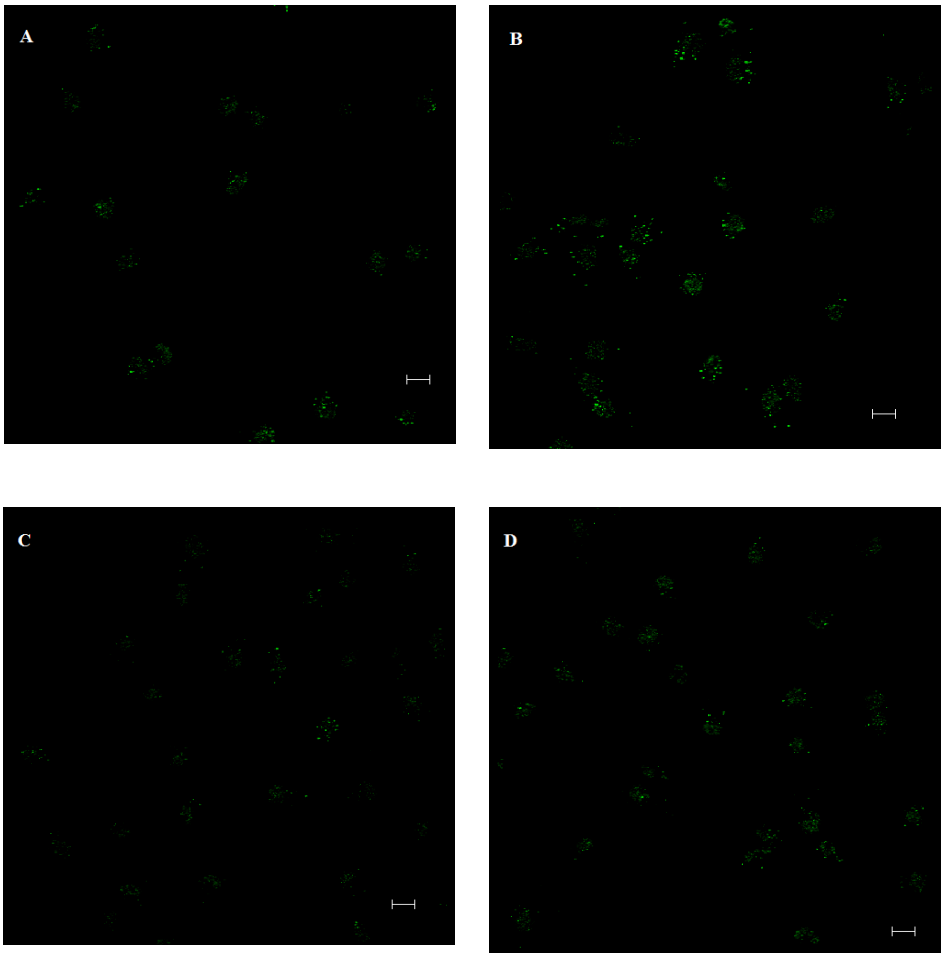

Confocal images of (A) MDMs fixed with 4% PFA followed by staining with primary antibody for 1 hour, (B) MDMs fixed with 4% PFA followed by staining with primary antibody for overnight, (C) MDMs fixed with 100 % methanol followed by staining with primary antibody for 1 hour, (C) MDMs fixed with 100% methanol followed by staining with primary antibody for overnight. The cells were imaged using Zeiss LSM 510 with scan zoom of 0.7 and scale bar=10µm. The LC3 II punctate are represented by green dots.

b. Direct staining method:

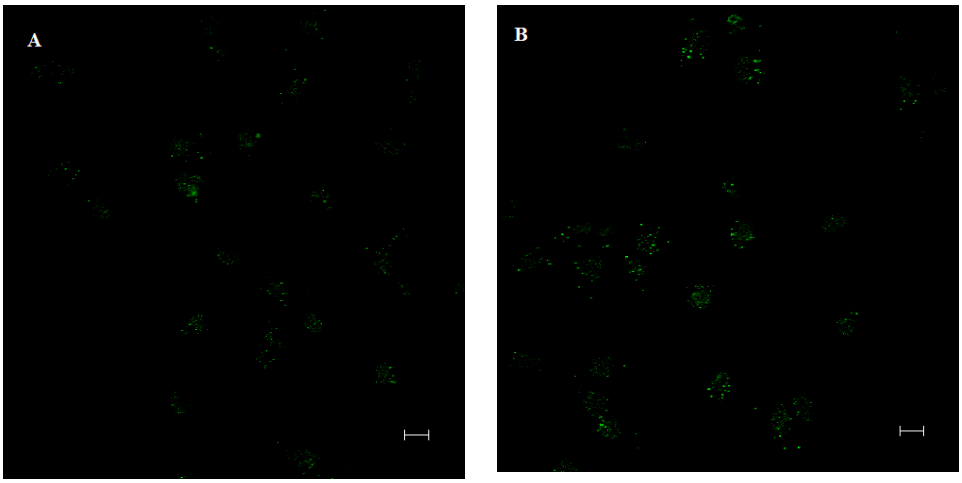

Confocal images of (A) MDMs fixed with 4 % PFA followed by direct staining, (B) MDMs fixed with 100% methanol followed by direct staining. The cells were imaged using Zeiss LSM 510 with scan zoom of 0.7 and scale bar=10µm. The LC3 II punctate are represented by green dots.

c. Immunofluorescence LC3 controls:

Controls for optimization of LC3 punctate immunofluorescence staining

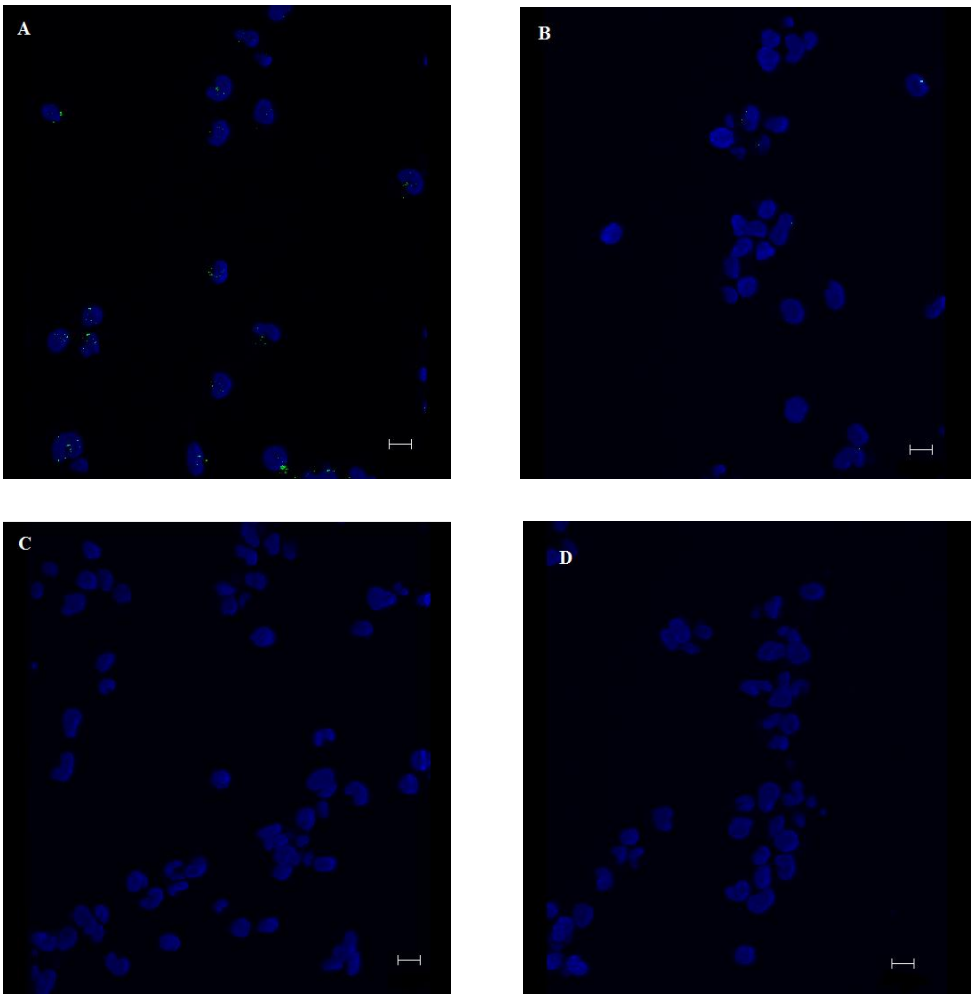

Confocal images of (A) Indirect staining of unstarved MDMs, (B) indirect staining of MDMs treated with DMSO, (C) starved MDMs stained with rabbit monoclonal isotype antibody instead of LC3 II antibody, (D) starved MDMs stained with alexa-546 tagged secondary anti-rabbit monoclonal antibody but no prior primary LC3 II antibody staining. The cells were imaged using Zeiss LSM 510 with scan zoom of 0.7 and scale bar=10µm. The LC3 II punctate are represented by green dots and nuclei were stained blue with DRAQ5.

Appendix IV: *M. avium* induces autophagy in primary human macrophages

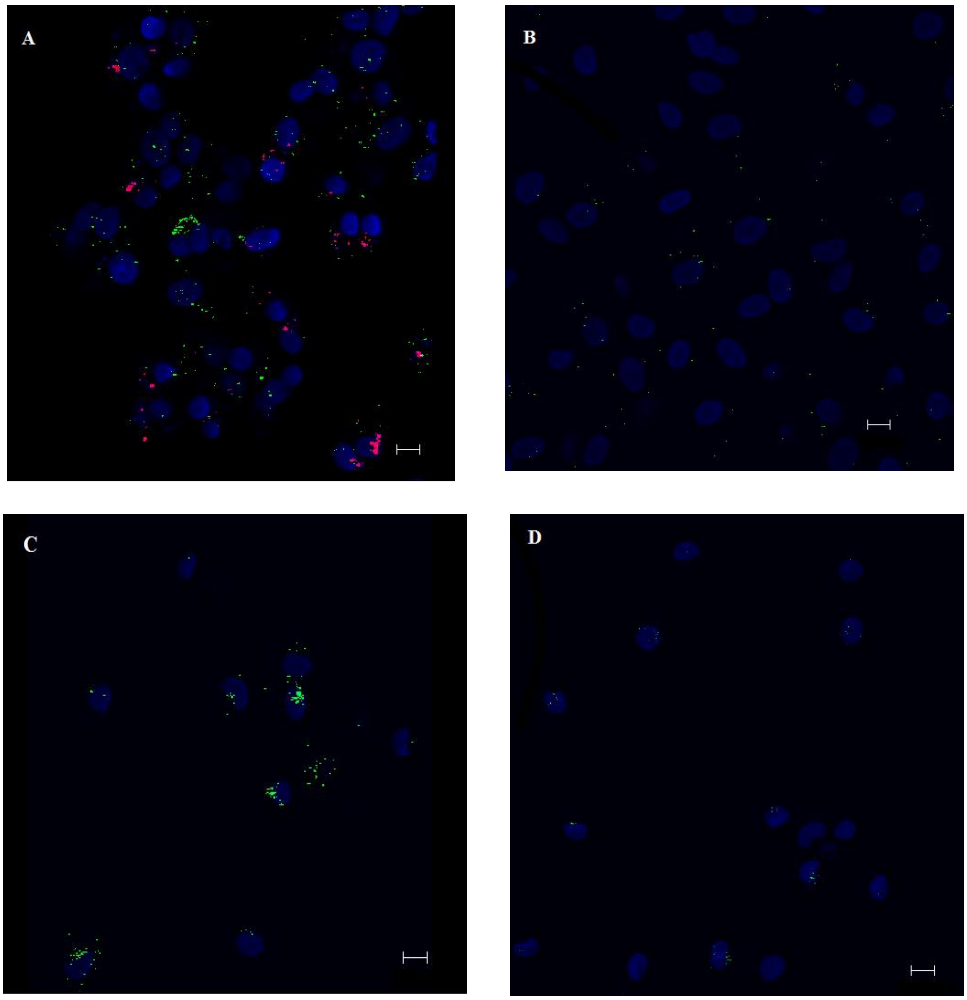

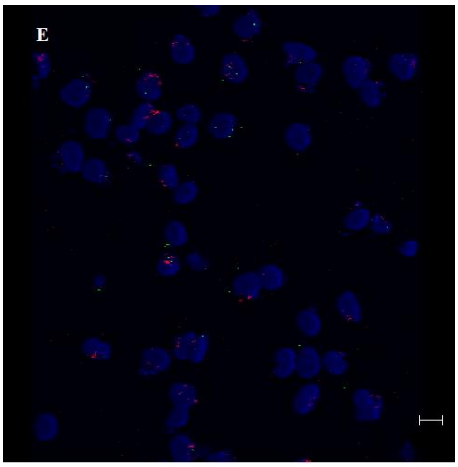

Confocal images of (A) untreated MDMs, (B) MDMs infected with CFP-*M. avium* (red dots) for 4 hours, (C) Amino acid starvation of MDMs for 2 hours, (D Amino acid starvation of MDMs in presence of 3 MA, (E) MDMs infected with *M. avium* in presence of 3 MA. The cells were imaged using Zeiss LSM 510 with scan zoom of 0.7 and scale bar=10µm. The LC3II punctate are represented by green dots and nuclei were stained blue with DRAQ5.

Appendix V: Autophagy is constantly maintained during period of infection.

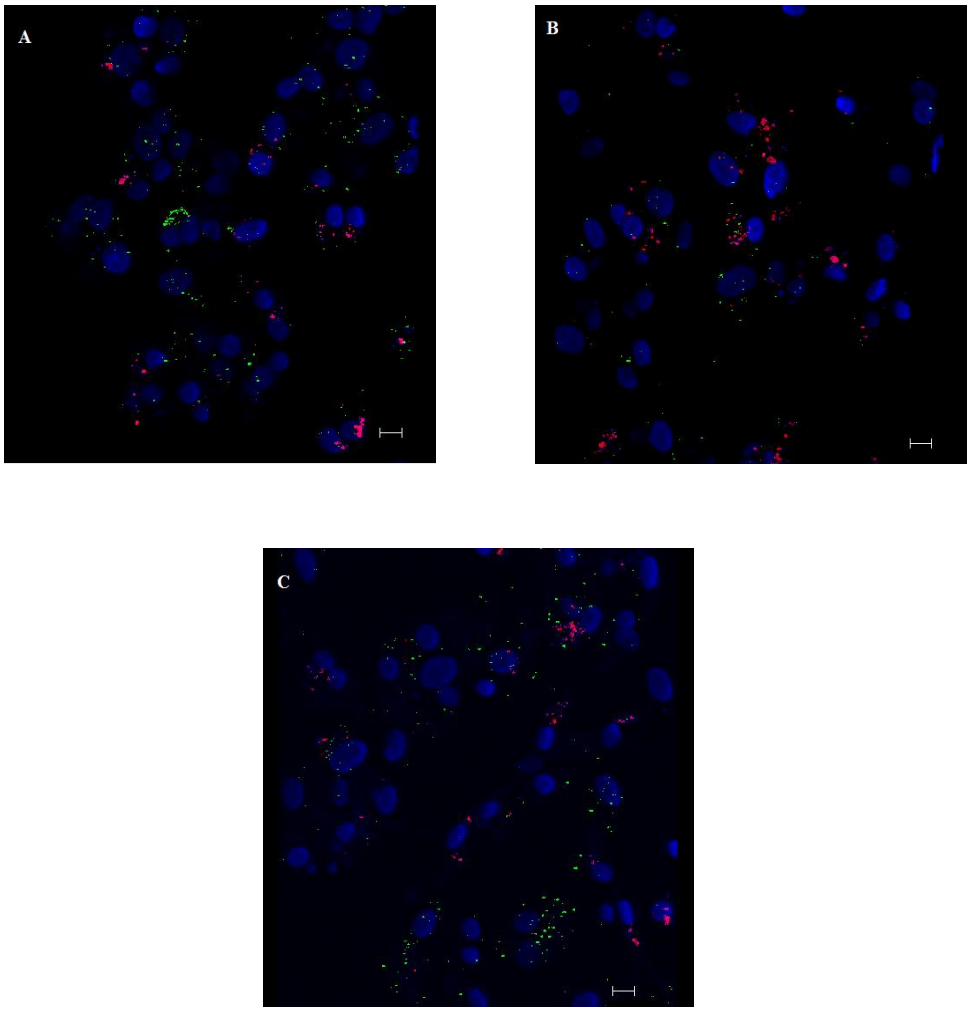

Confocal images of primary human macrophages infected with CFP *M. avium* (red dots) for (A) 4 hours, (B) 24 hours, and (C) 72 hours. The cells were imaged using Zeiss LSM 510 with scan zoom of 0.7 and scale bar=10µm. The LC3 II punctate are represented by green dots and nuclei were stained blue with DRAQ5.

Appendix VI: Optimization of HEK293 reporter cell system

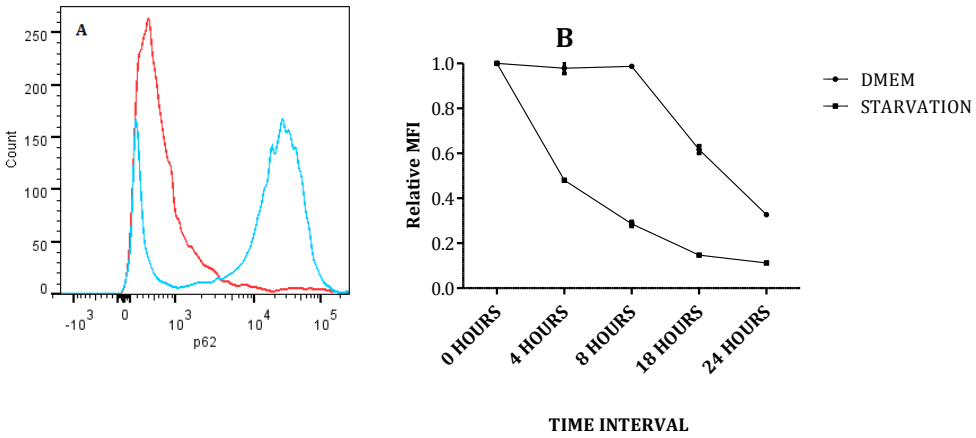

Flow cytometry analysis (A) The differences in green fluorescence intensity between 1ng/ml doxycycline induced (blue line) and uninduced (red line) expression of GFP-p62 on HEK293 GFP-p62 cell lines.(B) After the induction of GFP-p62 for 24 hours, inducer were removed by washing cells with warm PBS twice. The cells were then either incubated in normal DMEM medium with 10% FCS or amino acid free medium (Hanks Balanced salt solution) for indicated time point and then analyzed by flow cytometry. The mean fluorescence intensity of cells after 24 hours of induction was set to one and relative loss in mean intensity in 10,000 cells at different time point was calculated. The data are represented as mean ± SEM and data are representative of at least three independent experiments.

Appendix VII: Immunofluorescence staining for LC3 II in HEK293 cells

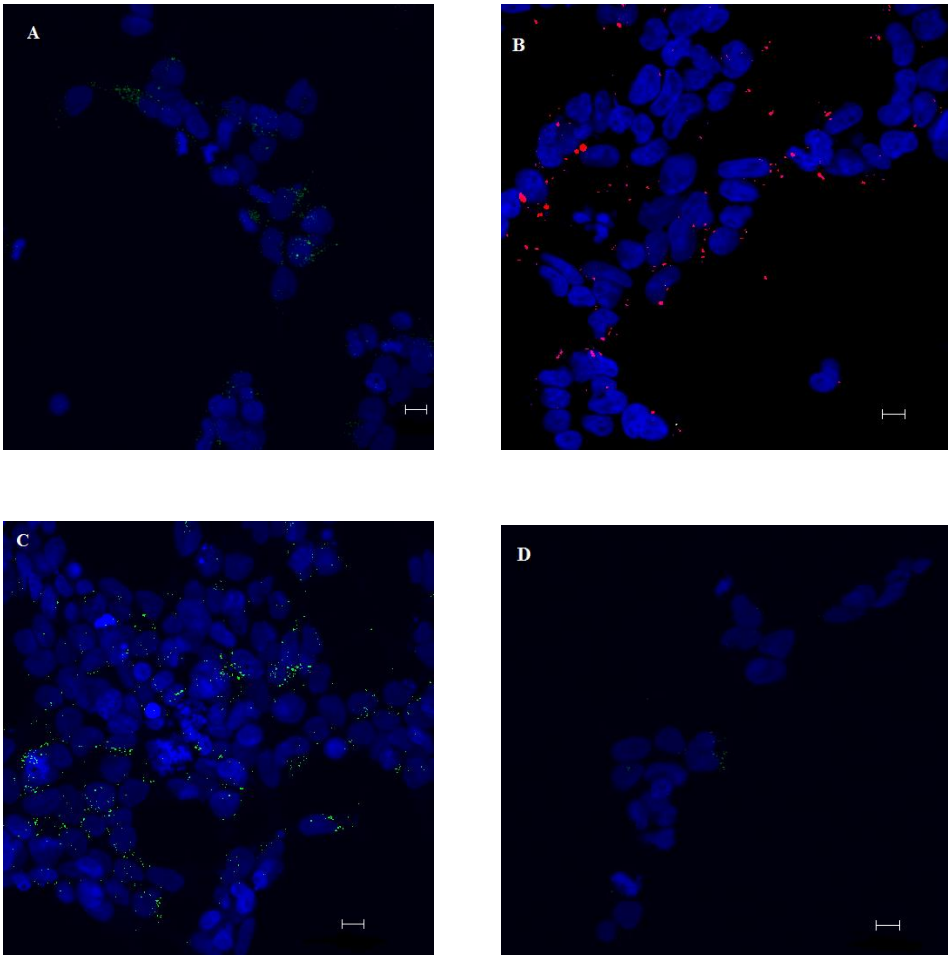

Confocal images of (A) untreated HEK 293 cells, (B) HEK 293 cells infected with CFP-*M. avium* for 4 hours, (C) HEK 293 cells amino acid starved for 2 hours, (D) HEK 293 cells amino acid starved in presence of 3 MA. The LC3 II punctate are represented by green dots, CFP *M. avium* by red dots and nuclei were stained blue with DRAQ5.

Appendix VIII: Lipomannan induces autophagy

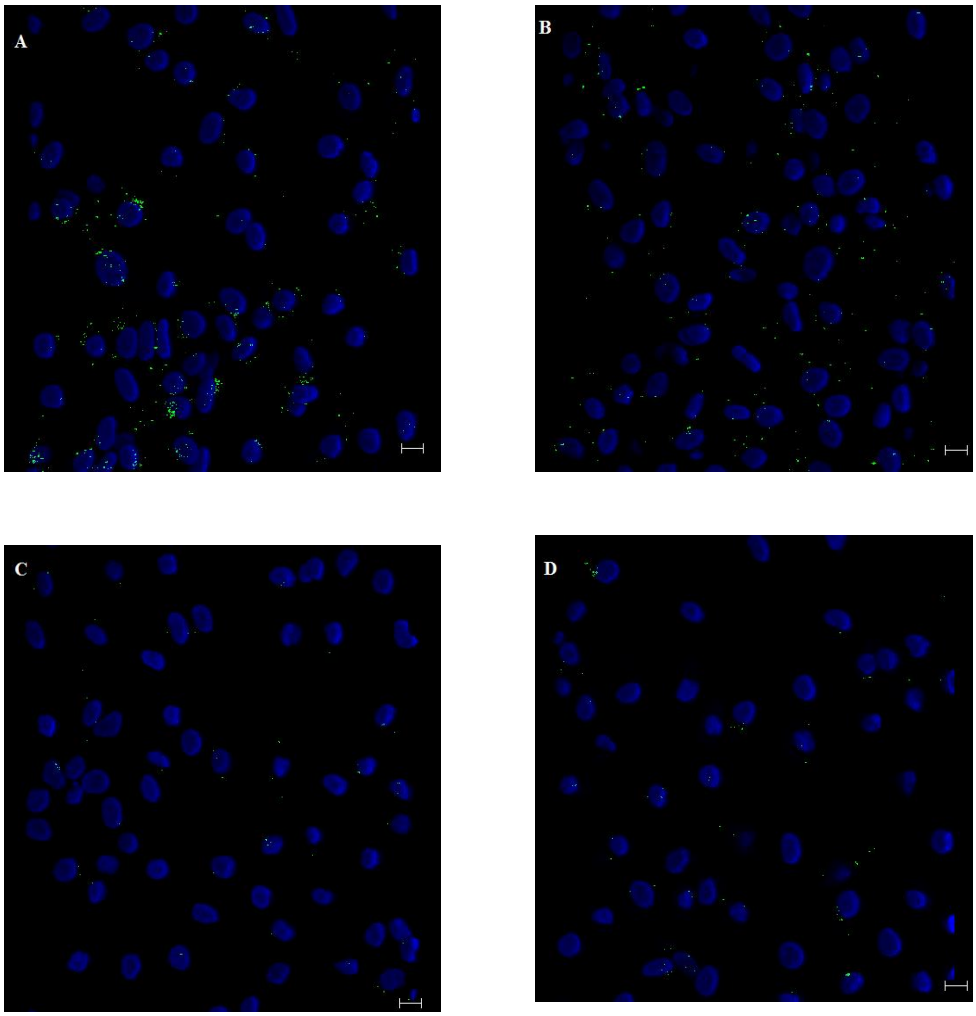

Confocal image of primary macrophages stimulated with 100ng/ml lipomannan for (A) 4 hours, (B) 24 hours. Macrophages without any stimulation at (C) 4 hours and (D) 24 hours time point. The cells were imaged using Zeiss LSM 510 live with scan zoom of 0.7 and scale bar=10µm. The LC3 II punctate are represented by green dots and nuclei were stained with DRAQ5.

Appendix IX: Neutralization of TLR2 with anti-TLR2 antibody reduces autophagy induced via lipomannan stimulation.

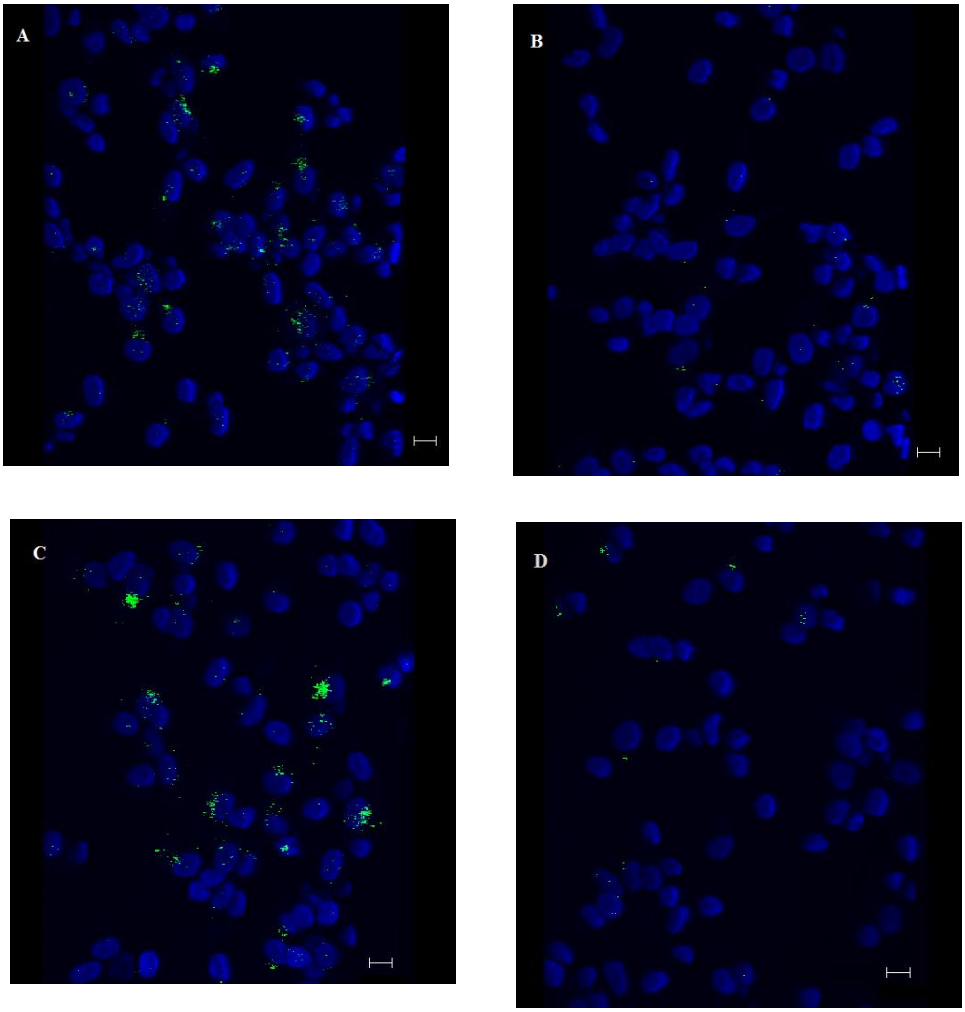

Confocal images of primary human macrophages, pretreated with monoclonal isotype antibody followed by stimulation with 100 ng/ml lipomannan for (A) 4 hours and (C) 24 hours. Macrophages pretreated with anti-TLR2 receptor monoclonal antibody followed by stimulation with 100 ng/ml lipomannan for (B) 4 hours and (D) 24 hours. The cells were imaged using Zeiss LSM 510 with scan zoom of 0.7 and scale bar=10µm. The LC3 II punctate are represented by green dots and nuclei were stained blue with DRAQ5.

Appendix X: CpG ODN does not induce autophagy in primary human macrophages.

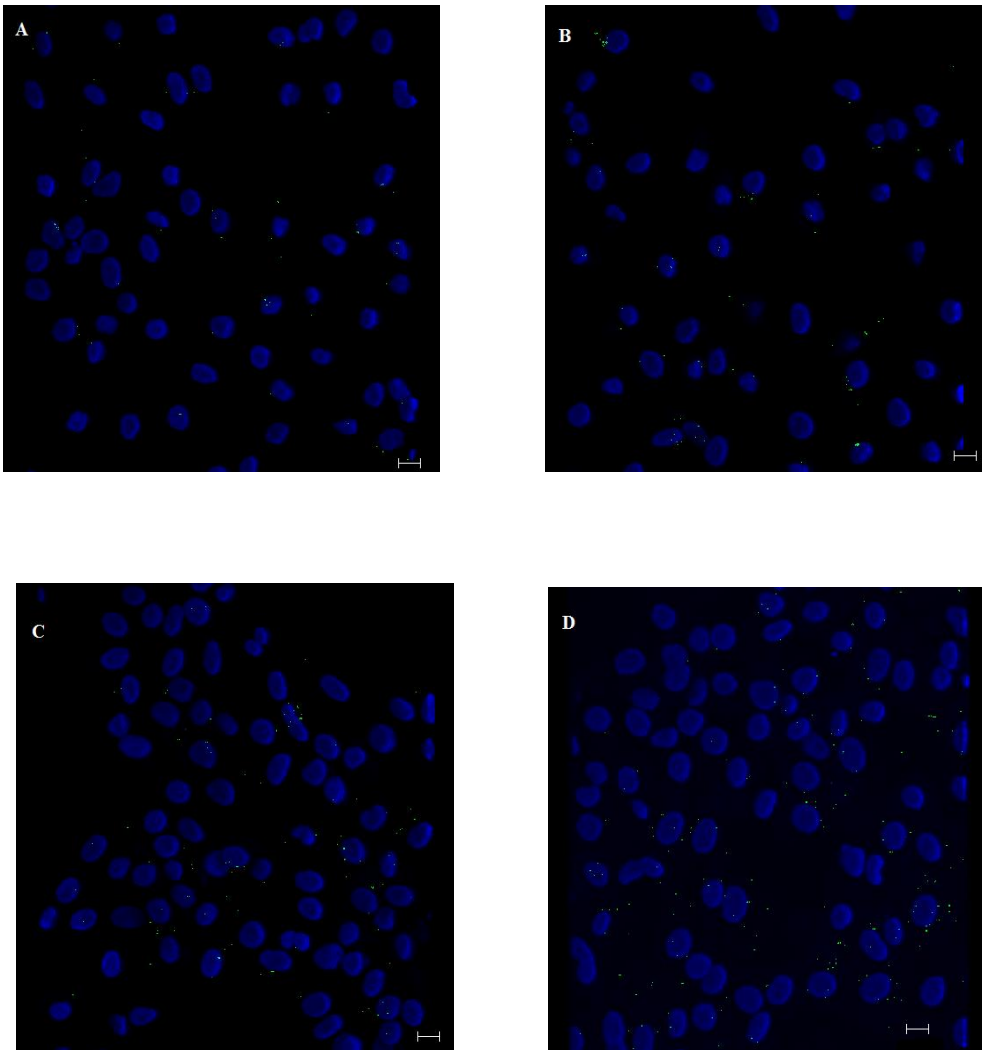

Confocal images of primary human macrophages without any stimulation for (A) 4 hours and (B) 24 hours time point. Macrophages stimulated with 3µM CpG ODN for (C) 4 hours and (D) 24 hours. The cells were imaged using Zeiss LSM 510 with scan zoom of 0.7 and scale bar=10µm. The LC3 II punctate are represented by green dots and nuclei are stained blue with DRAQ5.

Appendix XI: Neutralization of TLR2 by anti-TLR2 monoclonal antibody reduced *M. avium* induced autophagy.

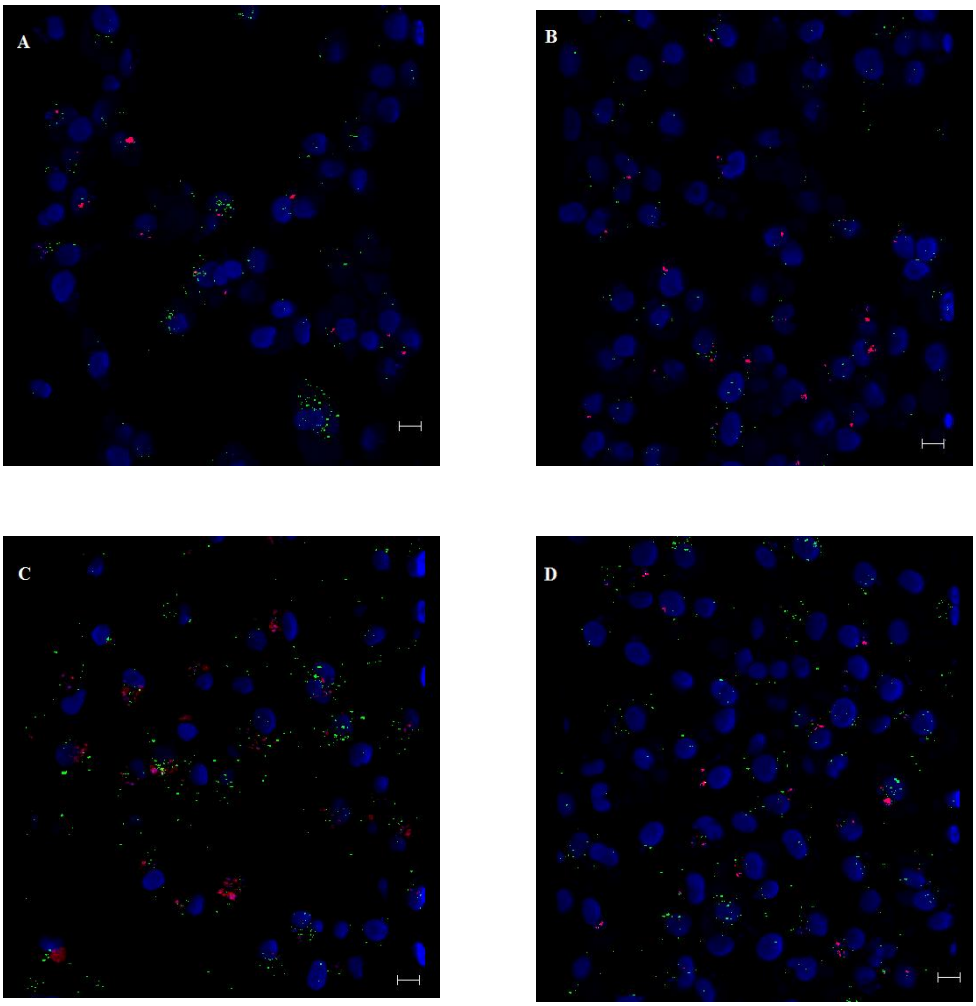

Confocal images of primary human macrophages pretreated with monoclonal isotype antibody followed by infection with CFP *M. avium* for (A) 4 hours and (C) 24 hours. Macrophages pretreated with TLR2 monoclonal antibody followed by infection with CFP *M. avium* for (B) 4 hours and (D) 24 hours infection. The cells were imaged using Zeiss LSM 510 with scan zoom of 0.7 and scale bar=10µm. The LC3 II punctate are represented by green dots, CFP *M. avium* by red dots and nuclei were stained blue with DRAQ5.

Appendix XII: siRNA mediated knockdown of TLR2 reduces *M. avium* induce autophagy but knockdown of TLR9 and STING do not.

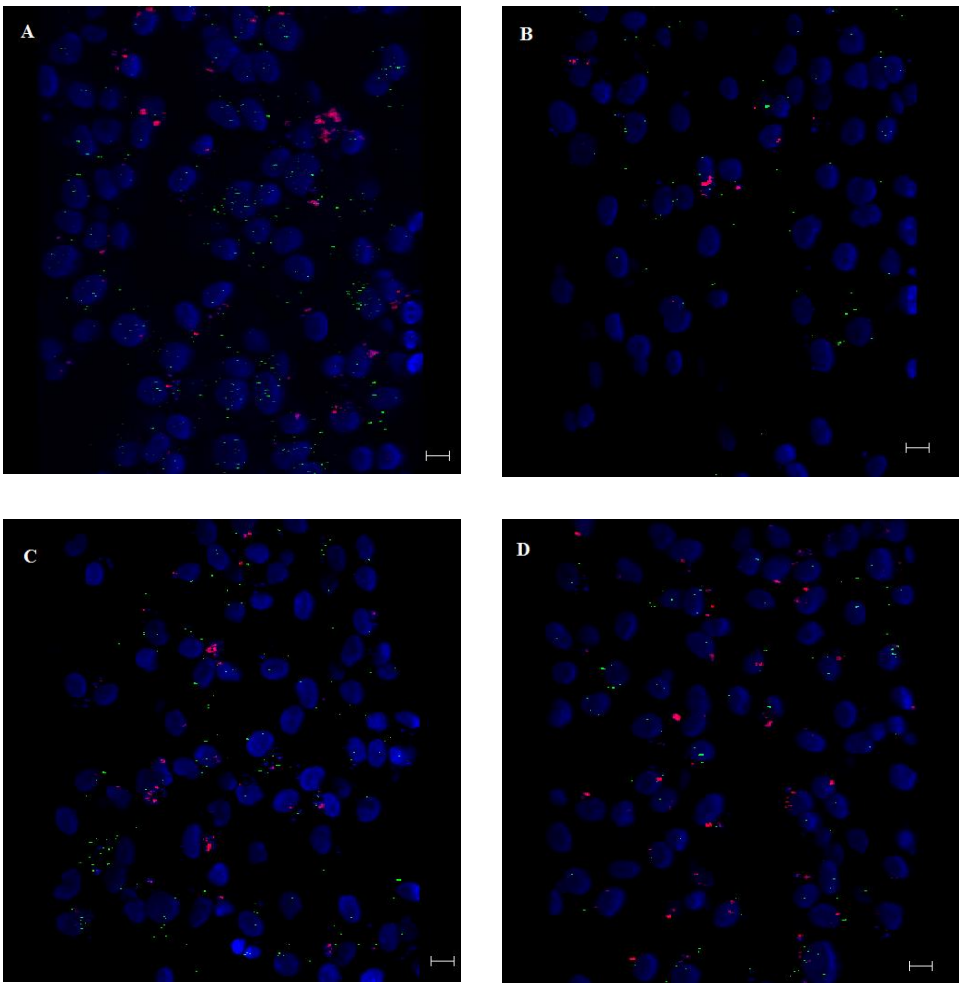

Confocal images of primary human macrophages pretreated with (A) AllStars siRNA as negative control, (B) TLR2 siRNA, (C) STING siRNA, (D) TLR9 siRNA followed by CFP *M. avium* infection for 4 hours. The cells were imaged using Zeiss LSM 510 with scan zoom of 0.7 and scale bar=10µm. The LC3 II punctate are represented by green dots, CFP *M. avium* by red dots and nuclei were stained blue with DRAQ5.

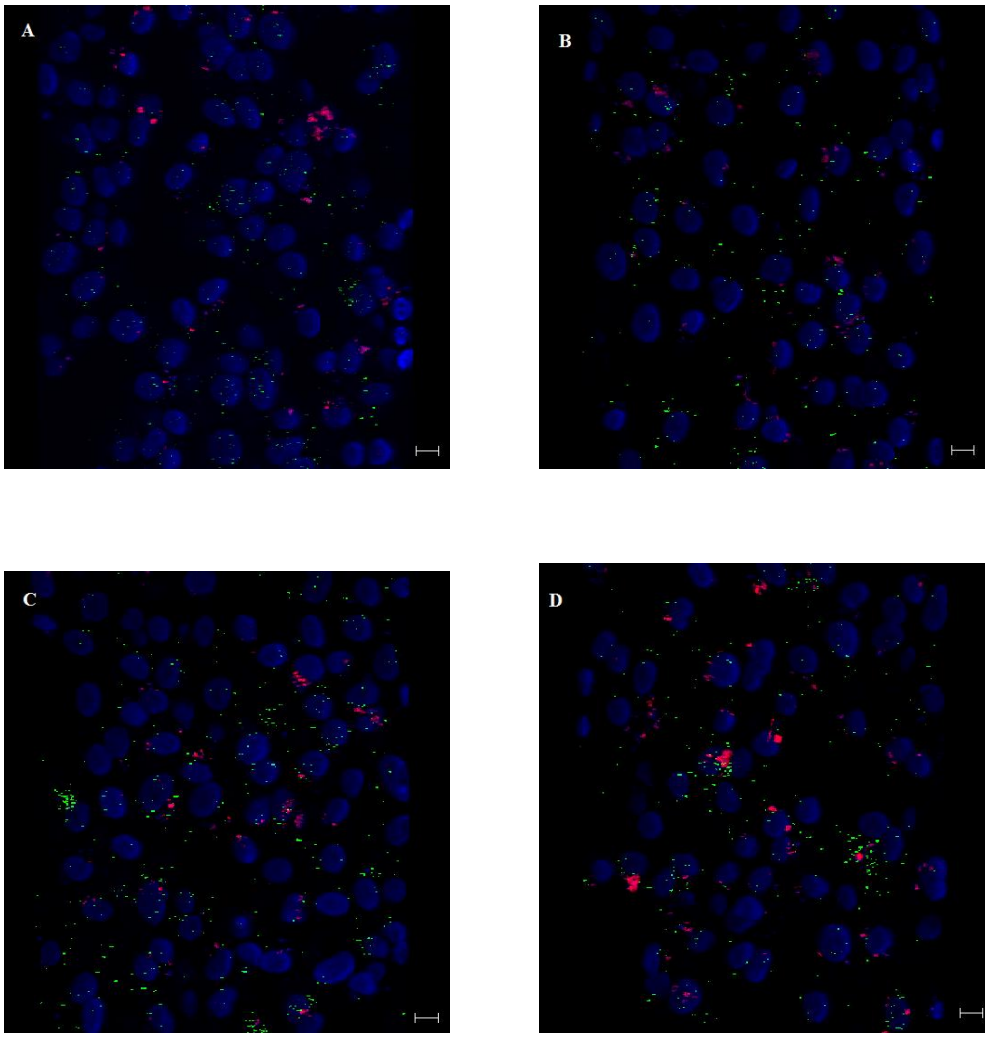

Confocal images of primary human macrophages pretreated with (A) AllStars siRNA as negative control, (B) TLR2 siRNA, (C) STING siRNA, (D) TLR9 siRNA followed by CFP *M. avium* infection for 24 hours. The cells were imaged using Zeiss LSM 510 with scan zoom of 0.7 and scale bar=10µm. The LC3 II punctate are represented by green dots, CFP *M. avium* by red dots and nuclei were stained blue with DRAQ5.

Appendix XIII: Stimulation of primary human macrophages with cyclic-di-GMP induces autophagy.

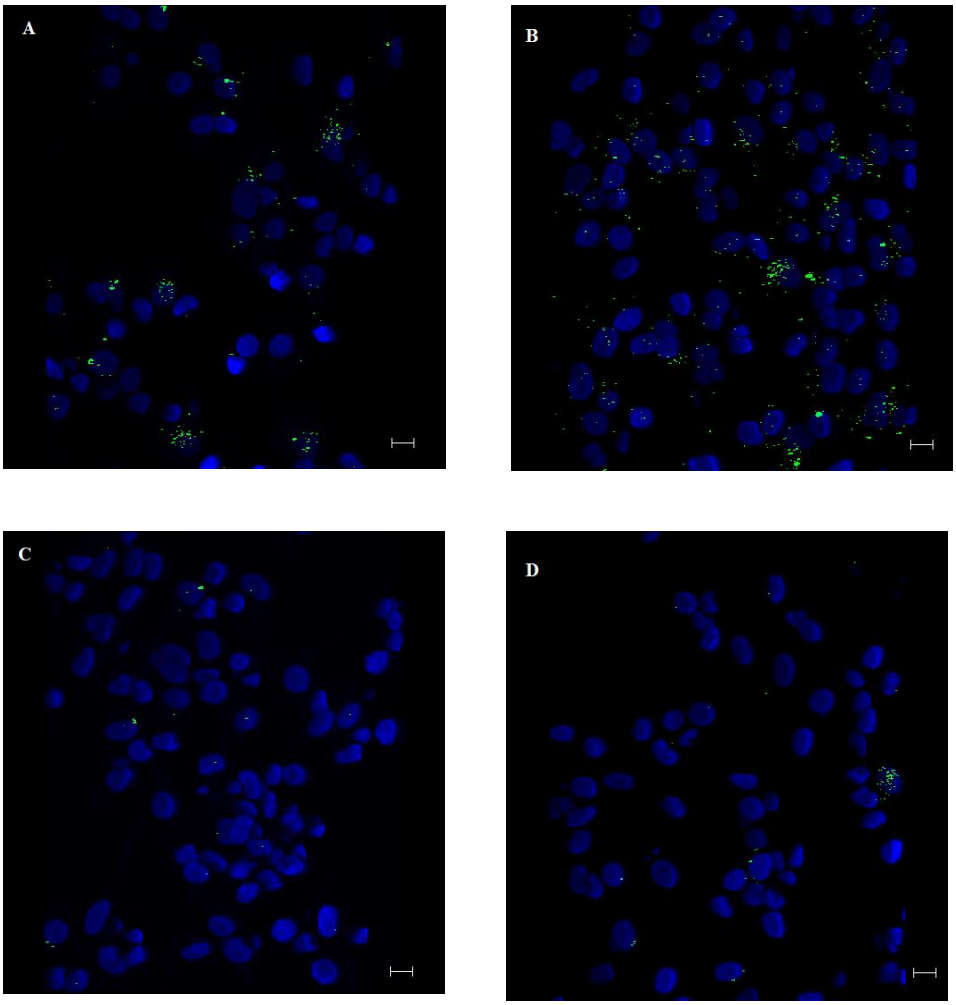

Confocal images of primary human macrophages stimulated with 8µg/ml cyclic-di-GMP for (A) 4 hours and (B) 24 hours. Macrophages stimulated with lipofectamine as negative control for (A) 4 and (B) 24 hours. The cells were imaged using Zeiss LSM 510 with scan zoom of 0.7 and scale bar=10µm. The LC3 II punctate are represented by green dots and nuclei were stained blue with DRAQ5.

Appendix XII: siRNA mediated knockdown of STING reduces autophagy induced via cyclic-di-GMP stimulation.

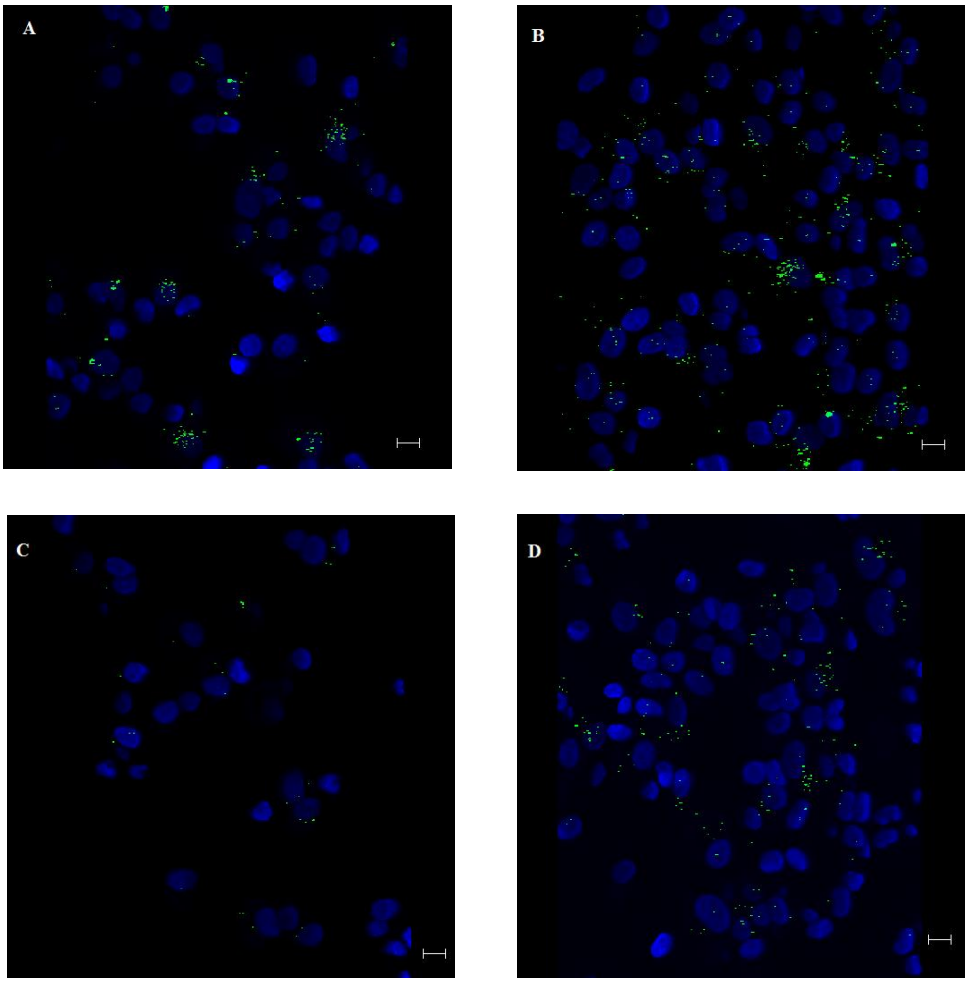

Confocal images of primary human macrophages pretreated with all-star siRNA as negative control followed by stimulation with cyclic-di-GMP for (A) 4 hours and (B) 24 hours .Macrophages were also pretreated with STING siRNA followed by cyclic di-GMP stimulation for (C) 4 hours and (D) for 24 hours. The cells were imaged using Zeiss LSM 510 with scan zoom of 0.7 and scale bar=10µm. The LC3 punctate are represented by green dots and nuclei were stained blue with DRAQ5.

Appendix XIV: Keap1 might negatively regulate *M. avium* induce autophagy but does not have any regulatory effect on basal autophagy.

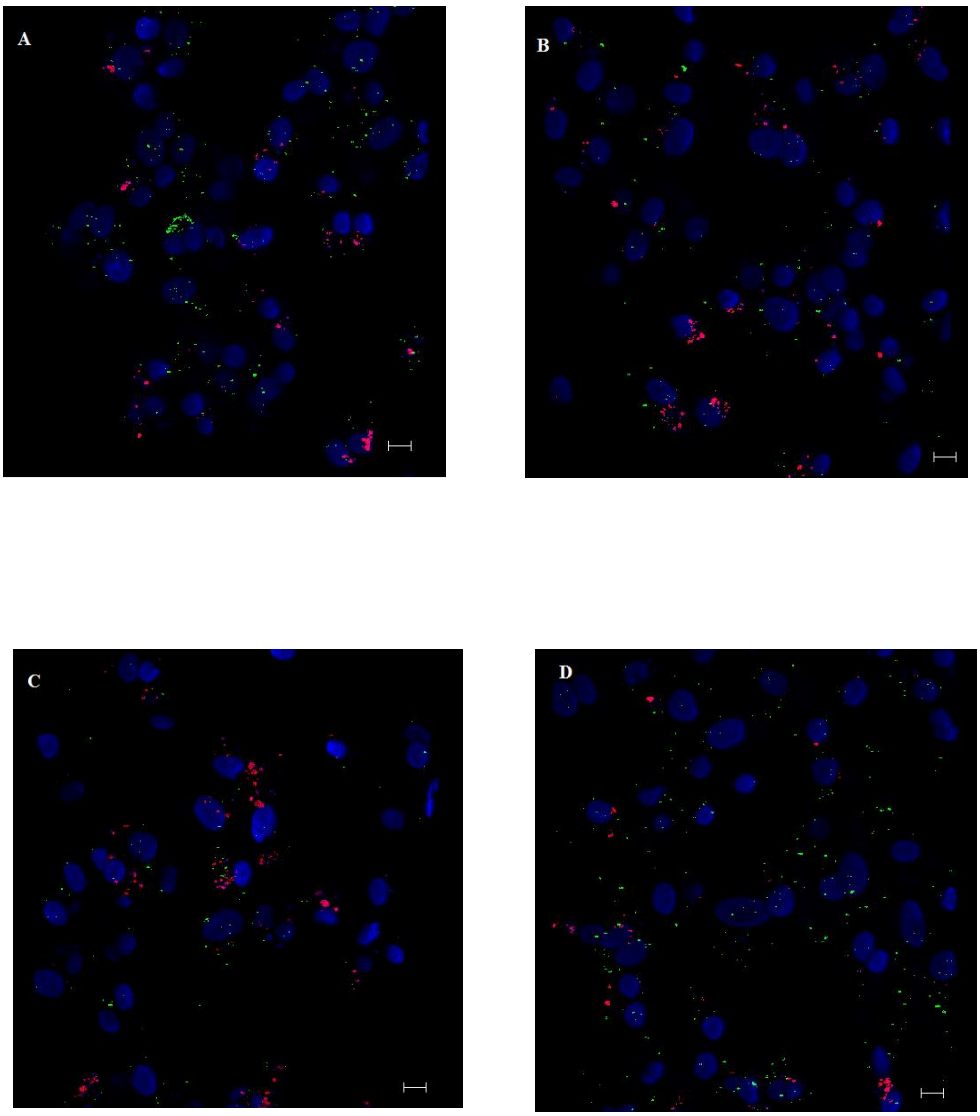

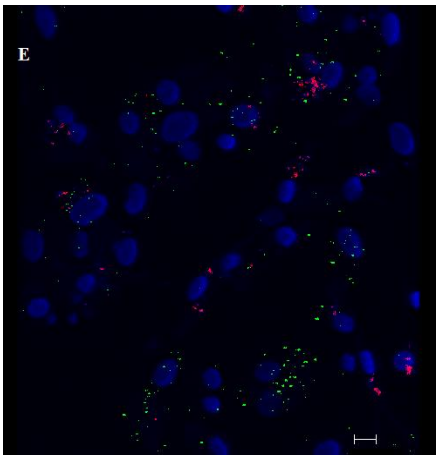

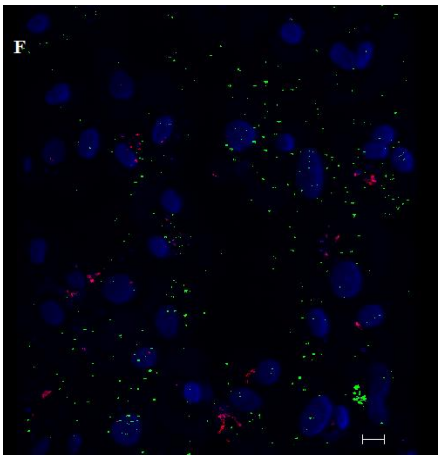

Confocal images of primary human macrophages pretreated with AllStars siRNA as negative control followed by CFP *M. avium* infection for (A) 4 hours, (C) 24 hours and (E) 72 hours. Macrophages were pretreated with Keap1 siRNA followed by CFP *M. avium* infection for (B) 4 hours, (D) 24 hours and (F) 72 hours. The cells were imaged using Zeiss LSM 510 with scan zoom of 0.7 and scale bar=10µm. The LC3 punctate are represented by green dots, CFP *M. avium* by red dots and nuclei were stained blue with DRAQ5.

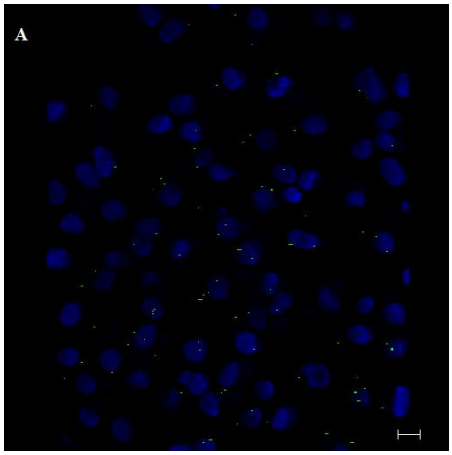

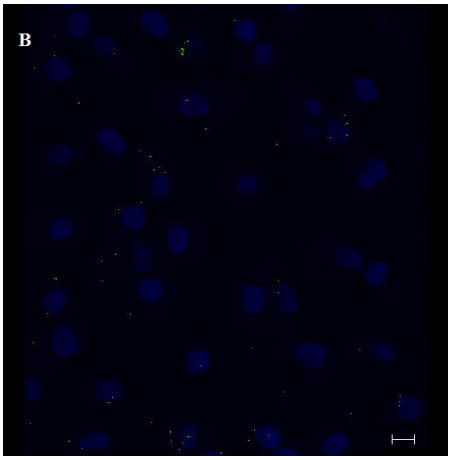

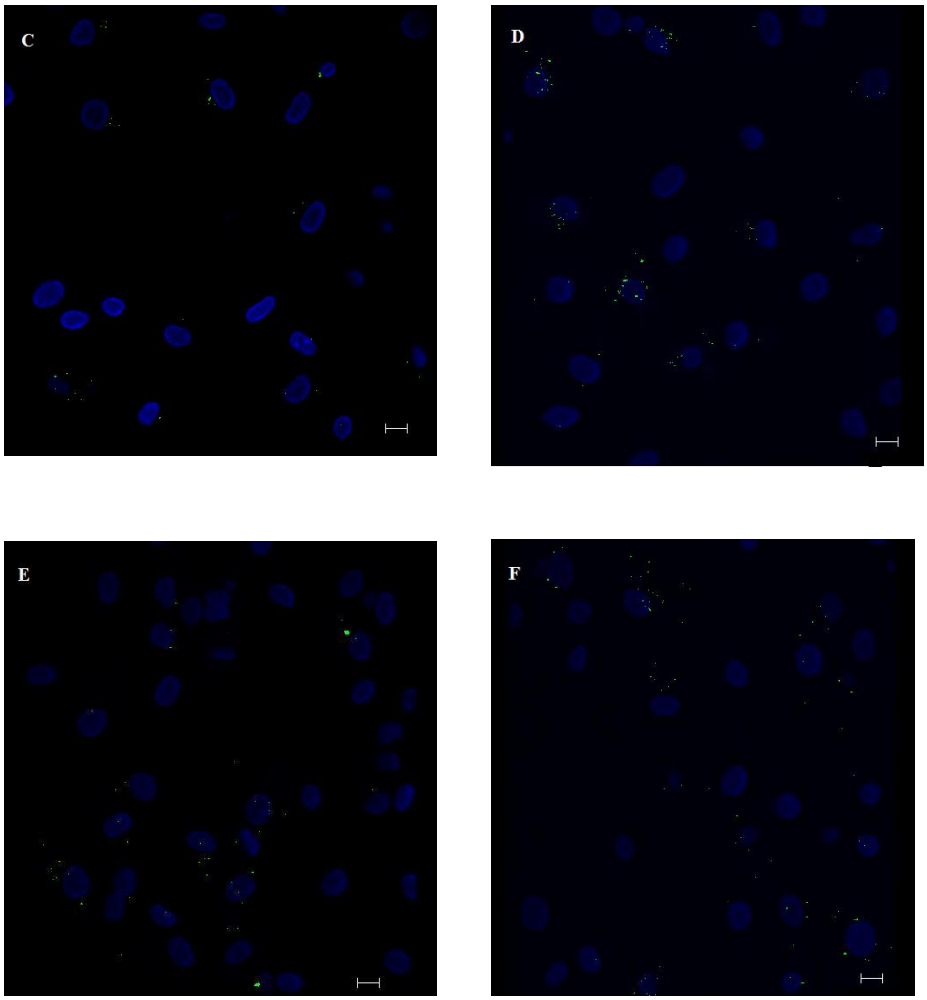

Confocal images of primary human macrophages pretreated with AllStars siRNA as negative control followed by observation of autophagy after (A) 4 hours, (C) 24 hours and (E) 72 hours. Macrophages were pretreated with Keap1 siNRNA followed by measurement of autophagy after (B) 4 hours, (D) 24 hours and (F) 72 hours. The cells were imaged using Zeiss LSM 510 with scan zoom of 0.7 and scale bar=10µm. The LC3 punctate are represented by green dots and nuclei were stained blue with DRAQ5.